Cover Page

Universiteit Leiden

Leiden University
Repository

Muscle MRI in Duchenne
and Becker muscular dystrophy

Beatrijs Wokke

Muscle MRI in Duchenne and Becker muscular dystrophy

Proefschrift

ter verkrijging van
de graad van Doctor aan de Universiteit Leiden,
op gezag van Rector Magnificus prof.mr. C.J.J.M. Stolker,
volgens besluit van het College voor Promoties
te verdedigen op woensdag 9 september 2015
klokke 16.15 uur

door Beatrijs Henriëtte Aleid Wokke
geboren te Haarlem in 1983

Lasciate ogne speranze, voi ch'intrate
Divine Comedy, Dante Alighieri (1265-1321)

CONTENTS

Chapter

1

General introduction

DUCHENNE AND BECKER MUSCULAR DYSTROPHY: HISTORICAL ASPECTS

In 1851 Edward Meryon published the first paper in which Duchenne muscular dystrophy (DMD) was reported as a disease entity. He described eight patients from three families with progressive muscle weakness and wasting, onset in early childhood and death in their late teens. He believed the disease to be hereditary and to have a predilection for males. By studying muscle tissue obtained post-mortem he observed that muscle tissue appeared to be primarily affected while the nervous system was still intact. He also described that the sarcolemma of the 'elementary fibre' was broken down and destroyed and that muscle fibres were converted into 'granular and fatty matter' [1, 2]. Several years later Guillaume Benjamin Amand Duchenne further studied patients with the same symptoms, describing progressive muscle weakness, initially affecting the lower limbs and eventually the upper limbs as well. He also observed a gradual increase in size of the affected muscles. He reported a gradual increase in interstitial connective tissue of affected muscles with age in muscle biopsies, with abundant fibrous and adipose tissue in later stages of the disease [3, 4]. In 1879, Gowers described the well-known Gowers' sign, that refers to the difficulty for patients to rise from the floor, due to hip and knee extensor weakness, and the compensatory use of arms to 'climb up their body' [5].

Several decades later, in the mid-1950s, Becker and Kiener described a 'new X-chromosomal muscular dystrophy' [6]. They observed that these patients had a similar pattern of muscle involvement as DMD patients but a much slower rate of disease progression. This disease entity came to be known as Becker muscular dystrophy (BMD). As the disease phenotype of these patients was so similar to DMD patients, Becker and Kiener thought it likely that DMD and BMD were linked to the same gene. This was confirmed a few decades later, when DMD was mapped to the short arm of the X-chromosome and DMD and BMD were shown to be allelic [7-9]. In the late 1980s the product of the *DMD* gene, dystrophin, was shown to be associated with the muscle sarcolemma and lack of dystrophin was identified to be the primary biochemical defect in DMD patients [9-12].

CLINICAL PHENOTYPE

DMD

DMD has an incidence of 1 in 4700 male live births and prevalence of 2.5 in 100.000 [13, 14]. Patients generally present between the ages of two and four years with symptoms such as difficulty walking stairs, falling, a waddling gait, a tendency to walk

on tip-toe and difficulties rising from the floor [15-17]. Many patients have muscle enlargement, most notably of the calf muscles. Approximately 50% of DMD patients have some delay in motor milestones in terms of the age of walking and most patients are never able to run properly [17]. Muscle weakness is progressive with age, resulting in wheelchair dependency in patients' early teens, loss of upper extremity function and frequent scoliosis [15, 18]. The respiratory muscles become progressively affected and respiratory failure is the main cause of death, although life expectancy has increased over the last decades with the accessibility of mechanical ventilation [19-21]. With age, cardiac muscle also becomes affected, mainly resulting in a dilated cardiomyopathy [22]. Smooth muscle tissue can be involved as well, presenting as gastro-intestinal tract and bladder problems. Some patients have a delay in intellectual milestones and speech development and the intelligence quotient has been found to be one standard deviation below average compared to the general population [23-25]. Patients usually die in their mid-thirties following respiratory or cardiac failure [26].

BMD

The incidence of BMD is around 1 in 18.450 males and the prevalence 2.4 in 100.000 [13, 27]. Overall BMD patients are less severely affected than DMD patients but show great variability in the severity of their clinical symptoms and rate of disease progression. While some patients lose mobility in their teens others experience only mildly progressive weakness during their adult life. Initial clinical presentation is usually in patients' early teens, although some patients present many decades later, with the most common presenting symptoms being cramping muscle pains, falling, problems walking stairs and a waddling gait [28-30]. Frequently there is involvement of the cardiac muscle, which increases with age and is the cause of death in about half of patients [31, 32].

MUSCLE ANATOMY

The skeletal muscle is surrounded by connective tissue called the epimysium and consists of muscle fascicles (encased with perimysium) build up from some or many muscle fibres or myocytes sheated by the endomysium. The myocytes are covered by the sarcolemma (inner plasma membrane) and outer basement membrane (Figure 1). The sarcoplasm is the cytoplasm of the muscle fibre and is composed of myofibrils and mitochondria and ribosomes. In the myofibril, protein filaments (myofilaments) are organized in repeating units named sarcomeres. These filaments include actin (thin filament) and myosin (thick filament), which are contracting proteins in the sarcomere.
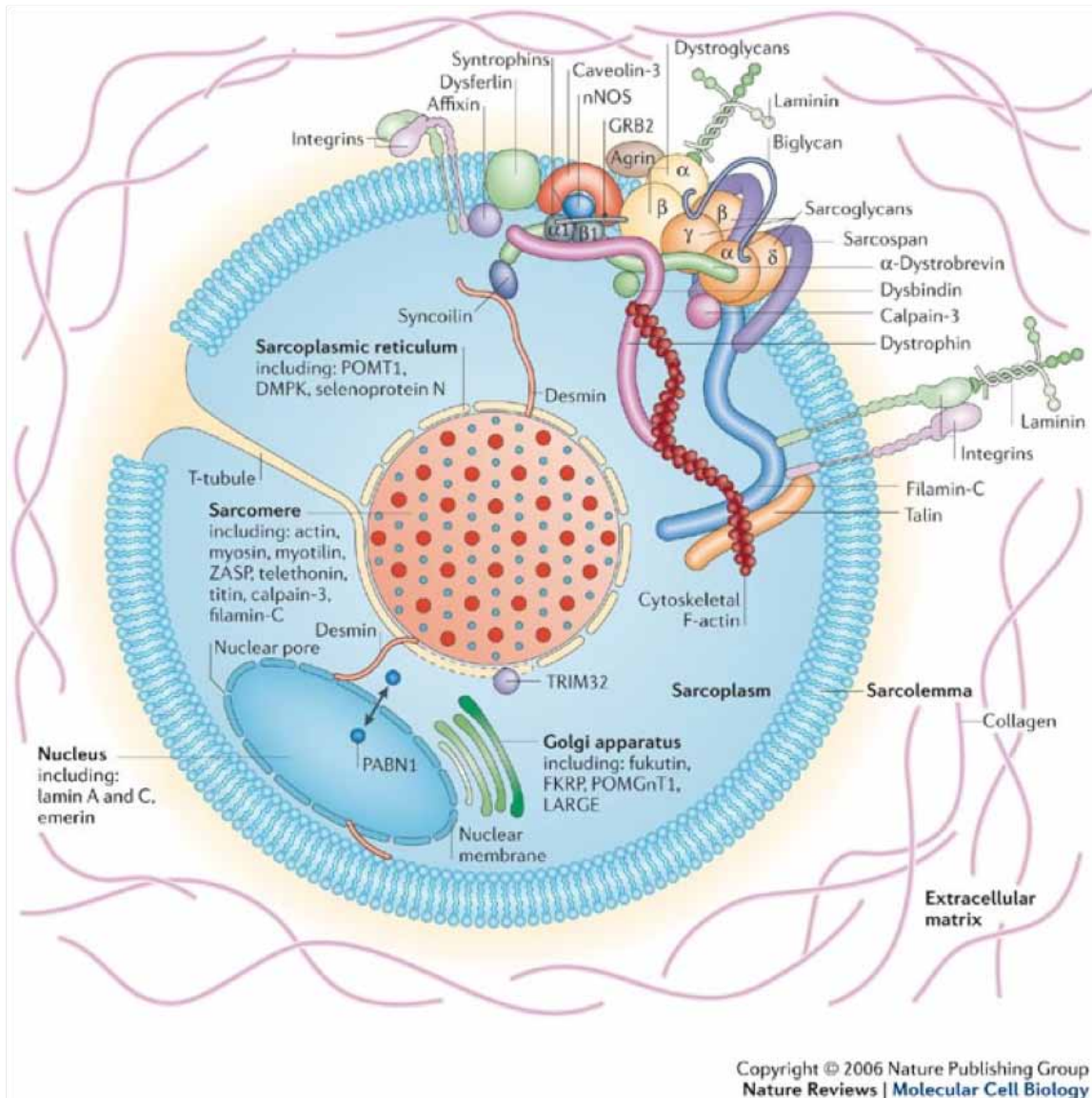
Figure 1. Skeletal muscle fibre showing dystrophin as part of the dystrophin-glycoprotein complex. *(Reprinted by permission from Macmillan Publishers LTD: Natures Reviews Molecular Cell Biology, Copyright 2006).*

PATHOPHYSIOLOGY

Mechanical factors

There are several hypotheses about the pathogenic mechanisms to the progressive muscle damage in DMD and BMD patients (Figure 2). A key causative factor is thought to be mechanical. Dystrophin is part of the multimeric dystrophin-glycoprotein complex (DGC) containing dystrobrevins, syntrophins, sarcoglycans and dystroglycans (Figure 1). The DGC mechanically links the extracellular matrix surrounding the muscle fibre to the sarcomere, providing structural stabilization of the muscle sarcolemma and is also involved in cell signalling [33-36]. The DGCs are localized at the sarcolemma

in rib-like lattices named costameres which help transmit forces laterally to the basal lamina [35]. Dystrophin deficiency disrupts the costameric lattice, which increases susceptibility to contraction-induced injury [35, 37, 38]. In DMD patients dystrophin is absent as a mutation in the *DMD* gene disrupts the translational reading frame or introduces a premature stopcodon. In contrast, in most BMD patients mutations (generally deletions) maintain the translational reading frame and as such a shorter and internally deleted, partly functional, dystrophin protein can be produced [12, 39]. The difference between complete absence and partial absence of dystrophin function is likely to affect the amount of disruption in the structural integrity of the muscle. This could explain some of the variability between the two disease entities.
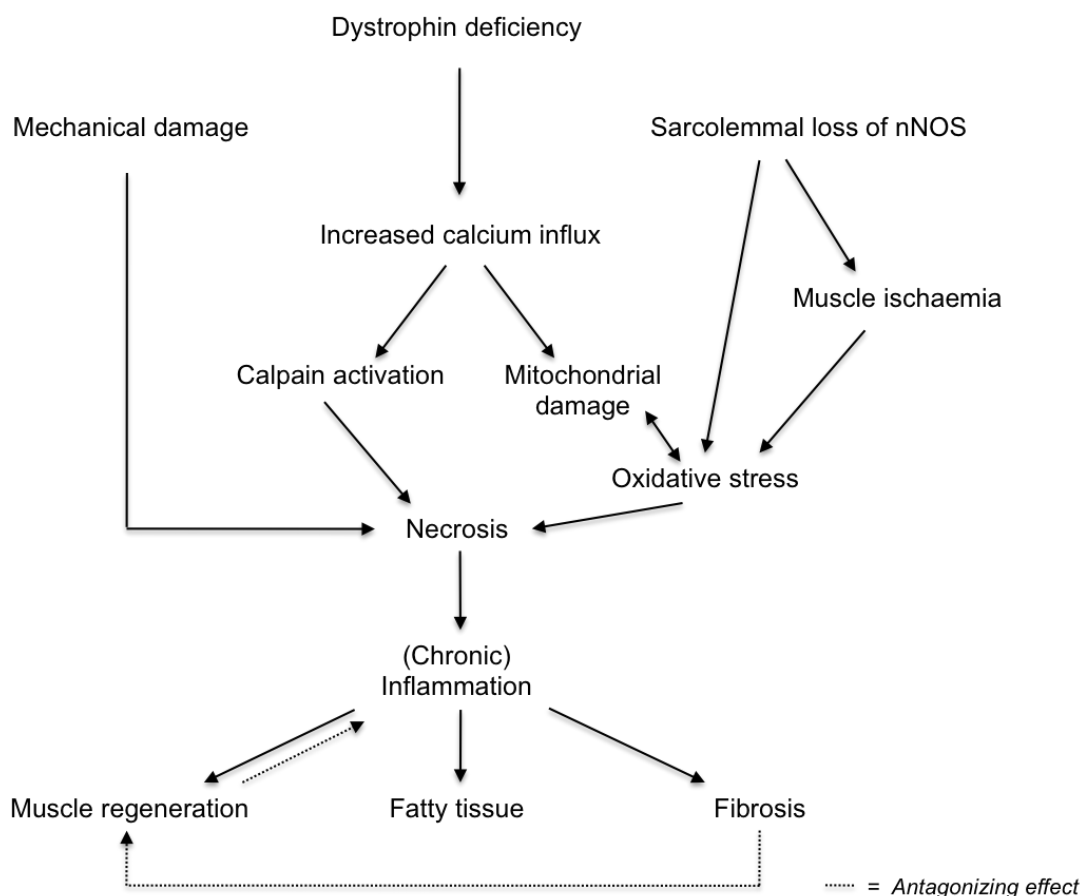
Figure 2. Diagram showing various contributing factors to muscle damage in DMD and BMD patients

Calcium related damage

Another potential mechanism contributing to (secondary) muscle damage is an increase in intracellular calcium. It has been hypothesized that stretch induced muscle damage induces increased intracellular calcium levels, however the exact underlying mechanism is unknown [40]. Increased intracellular calcium levels decrease the ability of the muscle to maintain physiological calcium levels and activate calcium-dependent

proteases like calpain, which contribute to degradation of muscle membrane proteins and cause myonecrosis [41, 42]. Additionally, increased calpain levels may also cause abnormal mitochondrial function, resulting in cell death [43].

Vascular factors

Neuronal nitric oxide synthase (nNOS) is a dystrophin-associated protein and interacts with spectrin-like repeats 16 and 17 within the rod-terminal of dystrophin and is recruited to the sarcolemma via α-syntrophin [44, 45]. nNOS produces nitric oxide (NO), which is an important factor in the reduction of sympathetic vasoconstriction in contracting muscle [46]. Dystrophin deficiency results in nNOS displacement from the sarcolemma to the myofiber cytosol and a reduction in its enzymatic activity [44, 47, 48]. The loss of sarcolemmal nNOS renders the muscle prone to muscle ischemia during muscle contraction following failure of 'normal' NO-mediated vasodilatation [49, 50]. nNOS deficiency also results in NO-related pathology in terms of free radical production and oxidative stress, leading to further mitochondrial damage [51-53].

Inflammatory factors

Various studies have shown that there is inflammation in muscle tissue of both DMD and BMD patients [44, 54, 55]. However, whether the inflammatory reaction is primary or secondary and to what extent inflammation results in additional damage of the muscle fibres still remains debated [56-60]. While some have suggested that inflammation is a result of non-specific inflammatory cell recruitment to sites of muscle fibre destruction [55, 59], others proposed that mechanisms such as a toll-like receptor mediated reaction, a specific cellular auto-immune response or involvement of mast cells could also contribute to the observed inflammation [55, 61-63].

Fatty infiltration and fibrosis

As a result of the ongoing muscle cell damage satellite cells become activated producing precursor cells, which differentiate into myoblasts contributing to the regeneration of the injured myofibers. There is also an influx of inflammatory cells that can phagocytose the degenerated fibres. The capacity of the satellite cells to compensate the ongoing muscle damage progressively fails, also as consequence of the chronic inflammation. As a result muscle fibres are increasingly replaced by adipose and connective tissue (Figure 3) [64, 65]. Although there are some signs of ongoing tissue damage in very young patients before onset of clinical weakness, the signs of muscle damage become progressively clearer with age [54, 55, 58, 62].
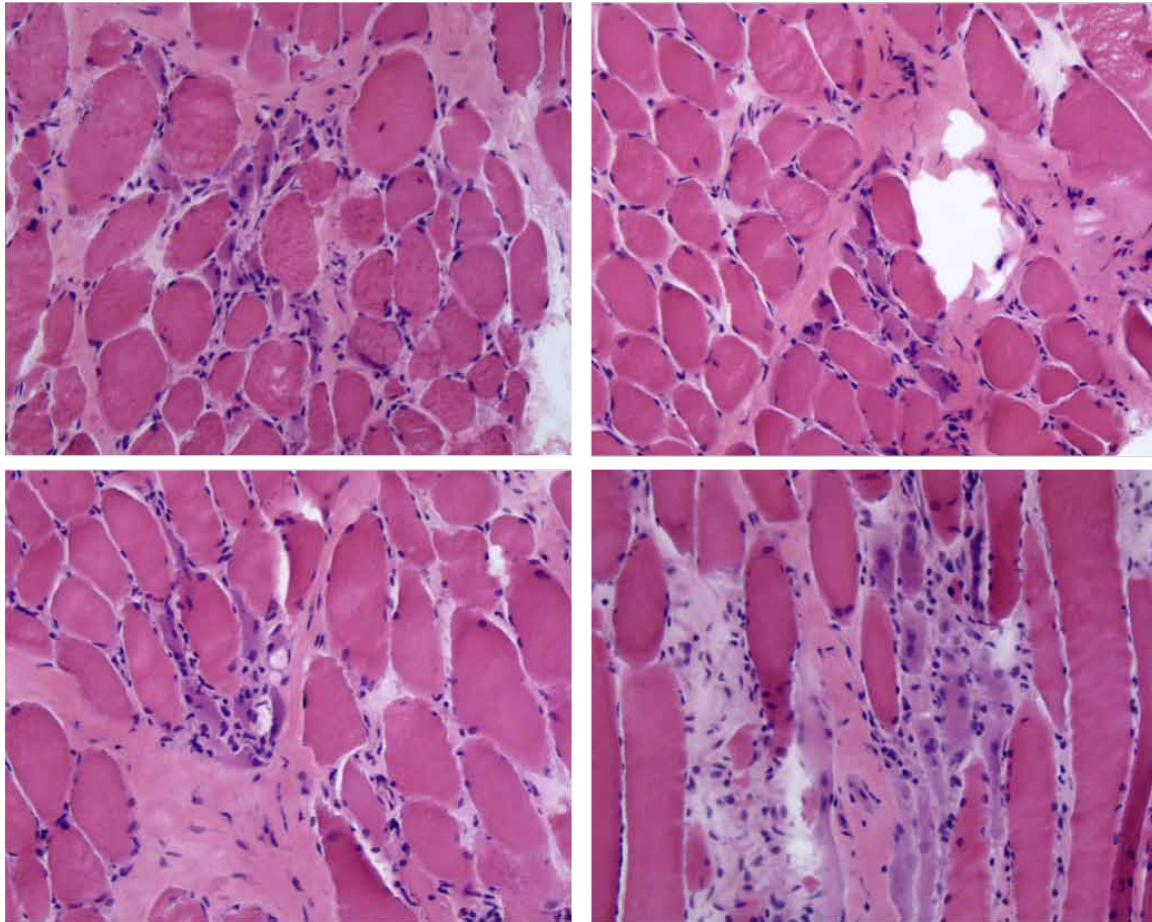
Figure 3. Muscle biopsies of DMD patient showing dystrophic features including fat replacement of muscle, fibrosis and fibre size variability (*courtesy of S.G. van Duinen, Department of Pathology LUMC*).

THERAPY

Since the discovery of the *DMD* gene there have been many studies looking for treatments for DMD patients. Corticosteroids have been shown to increase muscle strength, delay loss of ambulation and appear to affect the progression of cardiac and respiratory function in DMD patients [66-71]. The underlying mechanism of this effect remains largely unknown and the side effects are considerable [72]. Other therapies include supportive therapies such as cardiac, respiratory management and rehabilitation [73, 74]. Although no curative therapies are yet available, disease-modulating approaches including Idebenone, which aims to protect against mitochondrial dysfunction, and Myostatin antibodies aiming to increase muscle mass are currently being investigated. Translarna (Ataluren) interacts with the ribosome and allows the cell to ignore premature stop codons and produce functional proteins and has recently received conditional marketing approval and as such will become available to patients in the near future. Also, several ongoing studies focus on restoring expression of modified dystrophin [70,

75, 76]. These include exon skipping strategies, which use antisense oligonuceotides and aim to ameliorate the DMD into the BMD phenotype [77-79]. Although for BMD patients no disease modifying drugs are available, there are some, albeit less than in DMD, clinical trials for these patients. In BMD patients Tadalafil, a Phosphordiesterase (PDE) 5A inhibitor boosting NO, was shown to alleviate functional muscle ischaemia and restore blood flow in BMD patients [50]. However, recently the results of another study aiming to restore the effects of nNOS using a PDE 5 inhibitor (Sildenafil) were published and found no positive effects muscle blood flow or muscle performance [80]. Studies currently undertaken in BMD patients include the Follistatin gene, aiming to increase muscle fibre size and strength.

MAGNETIC RESONANCE IMAGING IN DMD AND BMD

The first muscle imaging studies in DMD and BMD patients were ultrasound and computed tomography (CT) studies in the early eighties and nineties [81-86]. The initial magnetic resonance imaging (MRI) studies of muscles of DMD patients were published some years later. In these MRI studies a decrease in the muscle T1 relaxation time was described and believed to result from (progressive) fat replacement in the muscles. The changes were found to increase with age, to correlate well with the clinical staging and to be neither uniform in all muscles nor within one muscle [87, 88]. Consequently, it was suggested that MRI could be of potential value in the diagnosis of DMD and staging of the disease. Additionally, as MRI provided multiplanar, high-resolution images with good contrast between soft tissues without the use of ionizing radiation it was felt that MRI could be a preferable imaging method to CT [89].

As MRI is relatively easily accessible and non-invasive it was proposed as a promising method to assess disease progression and the efficacy of future therapeutic interventions in DMD patients [90, 91]. In the same period several magnetic resonance spectroscopy (MRS) studies were performed in DMD and BMD patients [92-97]. MRS can be used to assess muscle metabolites such as intra- and extramyocellular lipids, choline and creatine using proton (^{1}H) -MRS and muscle energy dynamics using phosphorus (^{31}P) MRS. These studies mainly focussed on energy metabolism and the effects of exercise. Although the results of these studies were not fully in agreement, generally there appeared to be alterations in energy metabolism. These alterations included an increase in muscle pH and abnormal recovery of some metabolites after exercise, which was more evident in DMD than BMD patients [92-97].

The interest in imaging in DMD and BMD diminished for some years after these initial studies. The recent development of potential therapies for DMD prompted an increasing number of MR studies. Various MR techniques are thought eligible to identify changes

in the muscle that can be used as markers of disease progression. One of the most striking macroscopic changes in muscles of DMD and BMD patients is the increasing amount of fat replacement of muscle with progression of the disease. Consequently the main focus with regards to MRI in these patients has been on the assessment of the distribution of fatty changes, semi-quantitative and quantitative measurement of the fat and the relation of the remaining viable muscle with muscle function and strength [98-109]. Additionally, some studies have focused on the presence of oedema in the muscles and applied MRS to evaluate the lipid and energy metabolism [103, 108, 110-115].

SCOPE OF THE THESIS

At the start of this thesis there was little imaging data available on quantitative methods that could be used as outcome parameter in dystrophinopathy patients while several promising therapeutic approaches were being developed for these patients. Therefore, the aim of this thesis was to evaluate several MR methods that could serve as potential outcome parameters in the assessment of muscle pathology in DMD and BMD patients. In chapter 2 we compare a visual, semi-quantitative, scoring method to quantitatively score fat fractions in DMD patients and compare different models to account for the multiple peaks in the fat spectrum using the 3-point Dixon technique. In chapter 3 we use the 3-point Dixon technique to differentiate between contractile and non-contractile, fatty infiltrated, muscle in combination with quantitative strength measurements in DMD patients. In chapter 4 we explore the relation between the quality and quantity of dystrophin with the amount of fatty infiltration in the lower leg of BMD patients. In chapter 5 we focus on the muscle T2 relaxation times as indicator of oedema/inflammation in the muscle in DMD and BMD patients and healthy controls. Finally, in chapter 6 we use ^{31}P MRS in BMD patients in combination with Dixon MRI to investigate metabolic changes in lower leg muscles of BMD patients with non-increased and increased levels of fatty infiltration.

Chapter 2

Comparison of Dixon and T1-weighted MR methods to assess the degree of fat infiltration in Duchenne muscular dystrophy patients

B.H. Wokke, C. Bos, M. Reijnierse, C.S. van Rijswijk,
H. Eggers, A.Webb, J.J. Verschuuren, H.E. Kan

ABSTRACT

Purpose

To compare different lipid multi-peak spectral models to the single peak model in Dixon based fat-water separation and to evaluate differences between visually scored MR images and quantitatively assessed fat fractions in muscle of Duchenne muscular dystrophy patients.

Materials and methods

T1-weighted and 3-point Dixon imaging of the upper and lower leg was performed in thirteen Duchenne patients and six healthy controls. Three-, four- and five peak lipid spectrum models were compared to a single peak model and to each other. T1-weighted images were visually scored by two radiologists and quantitative fat fractions were obtained from Dixon images.

Results

Differences between the multiple-peak spectral models were minimal. The three-peak model was used for subsequent comparisons. Although there was high correlation between quantitative and visual scores, visual scores were consistently higher than quantitative values of the same muscles.

Conclusion

There are minor differences between the various lipid spectral models in terms of quantifying fat fraction in a large number of skeletal muscles in the legs of Duchenne patients and healthy controls. Quantitative 3-point Dixon MRI is more precise and reliable than visual radiological methods for evaluation of fat fractions for potential longitudinal follow-up or therapy evaluation of Duchenne patients.

INTRODUCTION

Muscle MRI is increasingly being used in the evaluation of disease severity in neuro-muscular diseases such as Duchenne muscular dystrophy (DMD) [98, 99, 109, 116]. DMD is a progressive muscle disease affecting young males and results in a severely reduced life expectancy of ~30 years. Skeletal muscles of DMD patients show hypertrophy, inflammation, progressive fatty infiltration and fibrosis. The level of fatty infiltration is considered to be a useful parameter to quantify the effect of new therapeutic interventions, and can potentially be measured accurately using non-invasive MRI protocols [77, 78, 117].

Chemical shift based water-fat separation methods such as the Dixon method use the phase difference between water and fat to separate these two components. As such, they can give a quantitative measure of the signal fraction of both water and fat. The first goal of our study was to compare the performance of different lipid spectrum models (three-, four- and five- peaks) to the single peak model of the lipid spectrum in fatty infiltrated muscles of DMD patients, using images acquired with a three-point Dixon method [98, 118-121]. In its most basic form, processing of the Dixon data models the fat signal as a single spectral peak, although the fat signal in fact contains multiple peaks from different saturated methyl and methylene protons, as well as unsaturated methyne groups. Previous studies have shown both in vitro and in liver, that modelling of the fat signals as multiple peaks significantly improves the fit and performs better in tissue with higher fat fractions [119, 122]. However, it is unknown how the multipeak spectral model behaves in much more spatially inhomogeneous tissues such as fatty infiltrated muscle.

There are various "semi-quantitative" visual-assessment scales available to describe the fatty infiltration in the muscle [101, 123-126]. However, although such scales are very quick to implement for the practicing radiologist, a recent study shows that semi-quantitative assessment of the fat fraction in muscles of patients with diabetes overestimates the fatty infiltration when compared to quantitative MRI methods [127]. Most patients in this previous study had relatively low levels of fatty infiltration and it is currently not known if this overestimation is still present if the muscle fat fraction is very high, as is often observed in DMD patients. Additionally, in patients with increased levels of fatty infiltration in the muscles, visual assessment of the fatty infiltration, especially in intermediate fat ranges, is likely to be less sensitive in detecting small changes [102]. Therefore, these methods could be less suitable for longitudinal follow up or therapy assessment. The second aim of our study was to compare "semi-quantitative" fat fractions obtained with an accepted neurological visual scoring method with those obtained using the quantitative MRI method outlined in the first part of the paper [123].

METHODS

Patients and controls

In total thirteen DMD patients (mean age 10.8 ± 2.0 years; range 8-14 years) and six healthy controls (mean age 11 ± 0.9 years; range 10-12 years) participated in this study. For the reconstruction with a different number of peaks, raw data are needed. As they were not present for all subjects data sets of nine patients (mean age 10.6 years ± 1.9; range 8-14 years) and six healthy controls (mean age 11 years ± 0.9; range 10-12 years) were used for the comparison of single- versus multipeak modelling. For the comparison of the semi-quantitative and quantitative analysis the images of ten patients (mean age 10.3 ± 1.9 years; range 8-13 years) were analysed using the three-peak model [122].

Patients were recruited from the Dutch dystrophinopathy database. Diagnosis of DMD was confirmed by DNA testing or muscle biopsy showing absence of dystrophin. Patients had no history of illness other than DMD. Healthy subjects were recruited from local schools. The local medical ethics committee approved the study and all subjects or their legal representative gave written informed consent.

MRI

MR images were acquired on a 3T scanner (Achieva, Philips Healthcare, Best, The Netherlands) from the left upper and lower leg using a 14-cm diameter two-element receive coil and body coil excitation. The receive coils were positioned on the anterior and posterior side of the leg; directly below the patella for lower leg imaging and directly above the patella for upper leg imaging. The left leg was imaged since this allowed optimal positioning of the coil in all patients, even those with some contractures, with respect to the patient table and the coil. The scanning protocol consisted of a T1-weighted spin echo (SE) sequence (25 five mm slices, 0.5 mm gap, repetition time (TR) 600ms, echo time (TE) 16ms) and a 3-point gradient echo Dixon sequence of the same region of interest (25 five mm slices identical to the T1- weighted slices, 0.5 mm gap, TR 400 ms, first TE 4.41 ms, echo spacing 0.71 ms, flip angle 8°). The TR of 400 ms and low flip angle of 8° were chosen to produce minimal T1 weighting. The total scanning protocol, including positioning of the patients, was performed in 20 minutes.

Quantitative analysis

The 3-point Dixon images were reconstructed with the lipid spectrum modelled as a single peak or multiple peaks using three different lipid spectrum models. The first model was a three peak model with frequencies $f_{p=}$[94, -318, -420] Hz and amplitudes $A_{p=}$[0.08, 0.15, 0.78] and was based on the model proposed by Yu et al. [122]. The four peak model resolves the peak from the terminal CH3 group from the large

aliphatic peak with $f_{p=}$[94, -318, -418, -470] Hz and $A_{p=}$[0.08, 0.15, 0.72, 0.04], and it was obtained by a weighted average of the signals at -300 and -325 Hz from the five peak model. Finally, a five peak model with $f_{p=}$[94, -300, -325, -418, -470] Hz and $A_{p=}$[0.08, 0.05, 0.1, 0.72, 0.04] was implemented [128]. The five peak model separates the α-methylene protons of the COO and C=C bonds into two separate signals. To obtain fat fractions per muscle, regions of interest (ROIs) were manually drawn using Medical Image Processing, Analysis and Visualization software package (www.mipav. cit.nih.gov) on co-registered T1 images on every other slice provided that the muscle was clearly identifiable. The fat fraction was modelled as $SI_{fat}/(SI_{fat}+cSI_{water})$, with SI representing the signal intensity and the factor c (1.41) correcting for differences in the proton densities of water and fat, as well as the differences in the T2 values of water (38 ms) and fat (150 ms). In order to obtain realistic proton density and T2 values, these were measured in one healthy control. T2 values were measured by using a single slice multi-echo experiment. The proton densities were estimated using a single slice spin echo sequence with TR/TE 5000 ms/6 ms, and then back-calculating the signal intensity for a virtual echo time of 0 ms using the T2 values measured previously.

Visual scoring

T1-weighted images of the left upper and lower leg of ten patients (mean age 10.3 years ± 1.9; range 8-13) were scored in consensus by two experienced musculoskeletal radiologists. For the scoring the available slices within the entire field-of-view, which was identical to the Dixon images, were used. A visual 4-point scale classified muscle as: 1-normal muscle, 2-mild changes of less than 30% estimated fatty infiltration, 3-moderate changes of 30-60% estimated fatty infiltration, and 4-severe changes of more than an estimated 60% showing an increased signal intensity [123]. The following muscles were scored in the upper leg: rectus femoris, vastus lateralis, vastus intermedius, vastus medialis, short head of the biceps femoris, long head of the biceps femoris, semitendinosus, semimembranosus, adductor longus, adductor magnus, gracilis and sartorius, and in the lower leg: medial and lateral head of the gastrocnemius, soleus, flexor digitorum longus, flexor hallucis longus, posterior tibialis, extensor hallucis longus, peroneus, anterior tibialis and extensor digitorum longus.

Statistical analysis

The SPSS statistical package Version 17.0 for Windows (SPSS Inc., Chicago, IL) was used for all analyses. A box plot was used to visualize differences between the visual and quantitative scoring methods and a Spearman correlation was used to compare the two methods. To evaluate differences between the different multipeak models a Bland-Altman plot was used. Statistical significance was set at $p<0.05$. Values are shown as mean ± one standard deviation (SD).

RESULTS

Single versus multipeak analysis

Figure 1 shows the comparison of the three different multipeak models to the single peak model. In the range of 0-70% fatty infiltration the multipeak models consistently show higher fat fractions than the single peak model. The difference between the models is most prominent in the range of 20-50% fatty infiltration and negligible in the very high ranges. Subtracted images of the single peak and the three peak model (Figure 2a.) show a clear difference between these two models, which is much less evident between the three- and the five peak model (Figure 2b), showing predominantly noise.
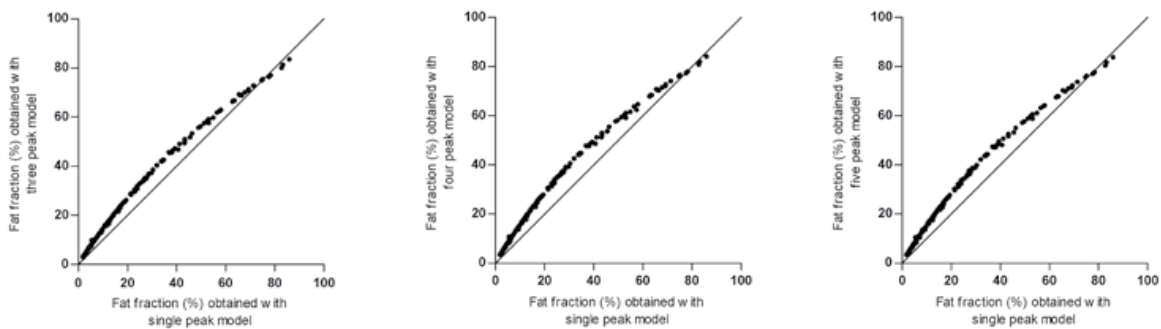
Figure 1. Single peak model versus three peak, four peak and five peak spectral model.
The four peak model deviates most from the single peak model. For all three models the differences are most apparent in the mid-range of the fat fraction.
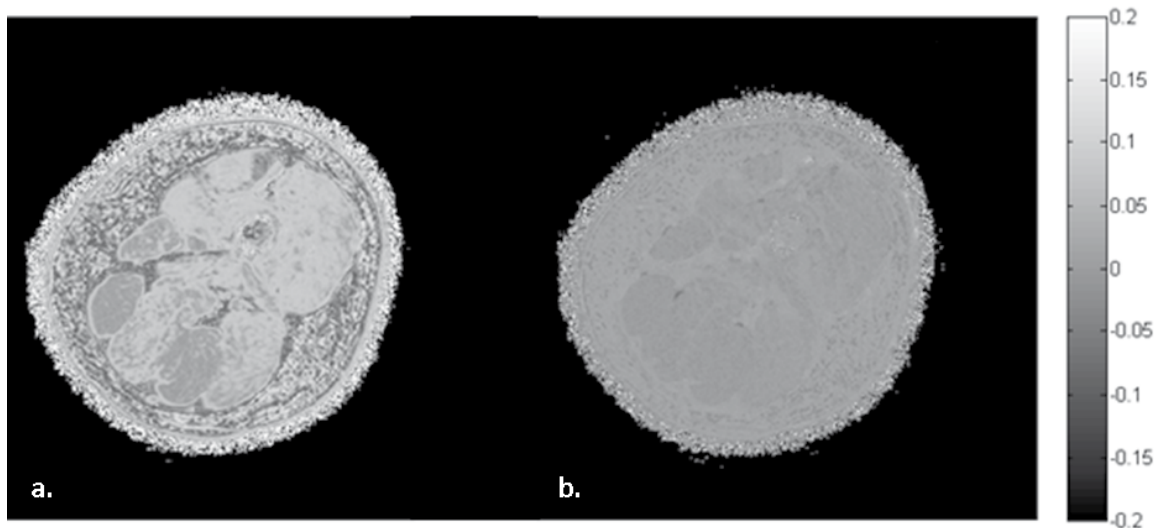
Figure 2. Subtracted images of the different spectral peak models.
The three peak minus the single peak model (a) shows a clear difference between the fat fractions of the two models. The five peak minus the three peak model (b) shows much smaller differences and mainly noise.

Figure 3 shows the difference between the four and the five peak model as compared to the three peak model. Both the four and the five peak model show very slightly higher fat fractions than the three peak model, with the four peak model showing less variability in the data. Nevertheless, the differences between the models were so small that in the subsequent comparisons the three peak model was used.
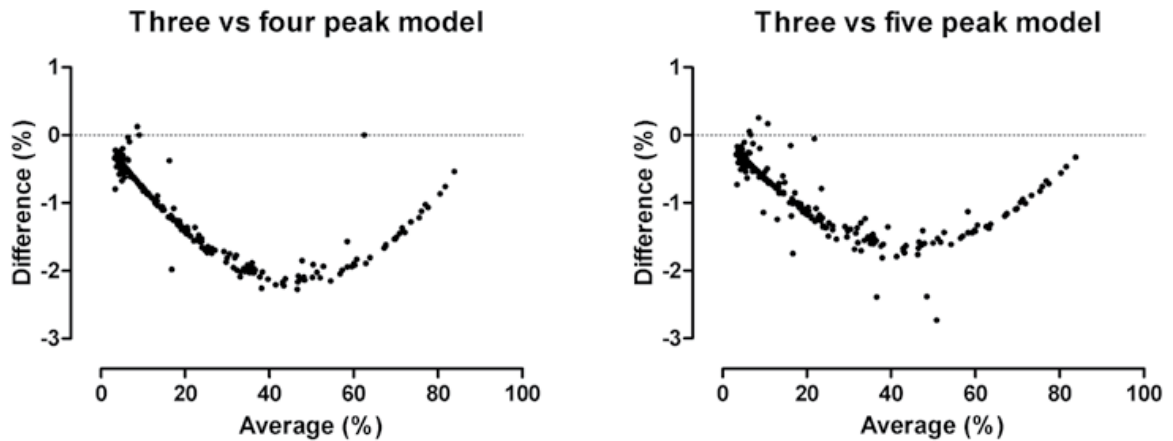
Figure 3. Bland-Altman plot showing the differences between the four and five peak model compared to the three peak model for the average fat fraction.
The four peak model shows less variation in the values which would make the model more precise than the five peak model.
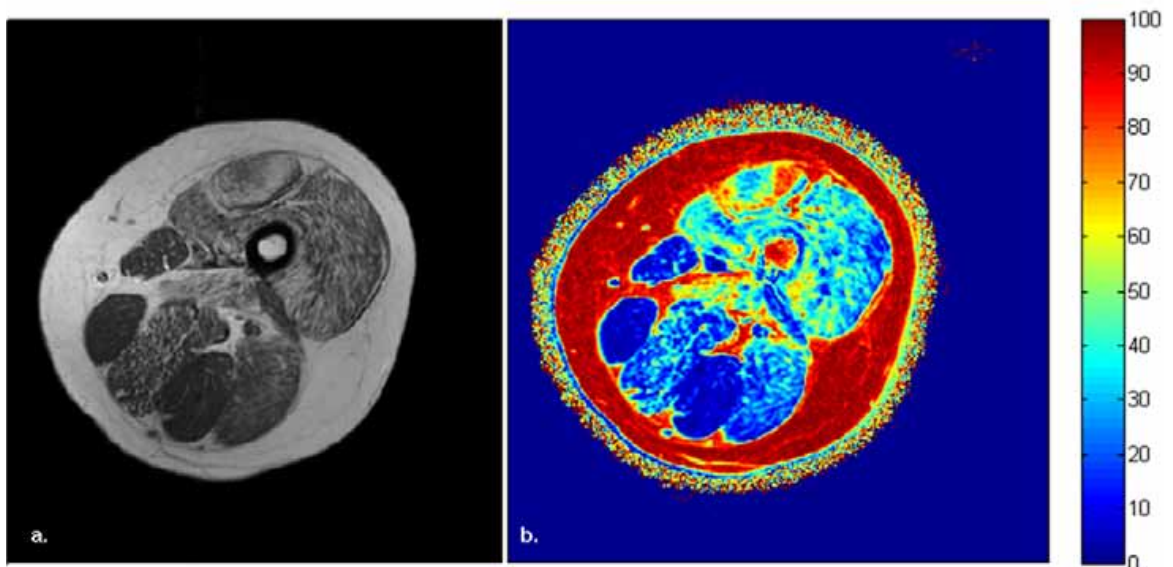
Figure 4. Upper leg of DMD patient showing the T1 weighted image (a) and a color representation of the fat fraction in the Dixon image (b).

Visual scoring and quantitative analysis

In ten patients fat fractions from a total of 201 muscles were scored on the 4-point scale. Of these, 17 (8.5%) were scored as normal, 62 (30.8%) as mildly affected, 34 (16.9%) as moderately affected and 88 (43.8%) as severely affected. The same muscles were analysed using the data from the 3-point Dixon scans (Figure 4).

There was a significant correlation between the two scoring methods, Spearman r=0.89, p<0.0001. Figure 5 shows how the quantitative Dixon values relate to the visual scores. Two main differences were noted. First, the visually scored fat fractions were higher than their quantitative equivalents, except for normal appearing muscle (Figures 5 and 6). Second, the variation in the values of the quantitative fat fraction scores was higher with increasing visually scored values. The variation was most evident in the visually scored group of severely affected muscles, defined as more than 60% fatty infiltration. Quantitative fat values in this group ranged from a minimum of 16% up to a maximum of 86%. Overall, in healthy controls the mean quantitative fat fraction was $5.3 \pm 0.98\%$ ranging from 3 to 10%. The mean quantitative fat fraction in the patients was $29.7 \pm 13.2\%$ ranging from 5 to 86%.
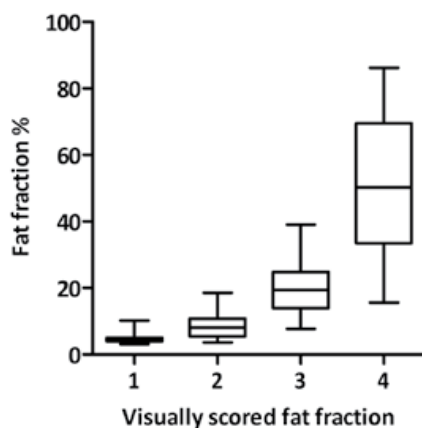
Figure 5. Visually scored versus quantitative fat fractions.
With visually scored fat scores as 1: normal appearing muscle, 2: mildly affected muscle (<30%), 3: moderately affected muscle (30-60%) and 4: severely affected muscle (>60%). Especially in the third and the fourth group of the semi-quantitative values there is large variation of the quantitative values.

DISCUSSION

The first aim of our study was to evaluate the performance of the multipeak models of the lipid spectrum in chemical shift-based water-fat separation over the entire range of healthy to severely affected muscles. Several previous in vitro and in vivo liver studies have shown that accounting for multiple peaks (up to six) of the lipid spectrum

results in a more accurate measurement of the fat fraction. In this paper we have shown that in muscle of healthy controls and DMD patients with varying disease severity multipeak models shows consistently higher fat fractions in the range of 0-70% fatty infiltration. Compared to the multipeak models, single peak modeling underestimates the fat fraction in the range of these values, and this underestimation is a non-linear function of fat fraction. Overall there were very minor differences in the estimate of fat fraction using a three-, four- or five peak model. The difference between these results, and those acquired in phantoms and in liver, could be that the lipid spectrum depends significantly upon muscle fiber orientation. This results in a shift of the lipid peaks and consequently increases the sensitivity of the model to the specific frequency of the spectral peaks [129], whereas there is no such variation in either homogenous phantoms or liver tissue.
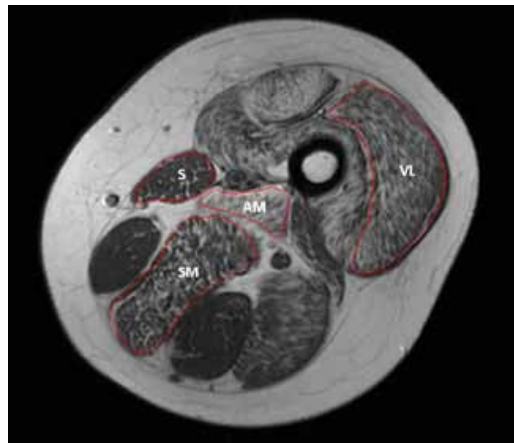
Figure 6. T1 weighted image of upper leg of DMD patient comparing visually scored and quantitative values.
The vastus lateralis visual score was 4 (severely affected) with a quantitative fat fraction of 33%. The adductor magnus (AM) visual score 4 with fat fraction 47%, sartorius (S) visual score 2 (mild changes) and fat fraction 10% and for the semimembranosus (SM) the visual score was 4 with a fat fraction of 24%.

Accurate fat quantification in chemical shift-based water-fat separation can also be influenced by other factors such as the difference in T1 values between fat and water (which itself is dependent upon the fat/water fraction in a particular voxel) if the images are T1-weighted [122, 129-131]. By choosing a low flip angle and a long TR in this study T1 effects were minimized [130]. Additionally, as mentioned above, the lipid spectrum depends significantly upon muscle fiber orientation and this could also affect its quantification. However, as in multi echo acquisitions with a low number of echoes and a short range of echo times the influence of these shifts on the resulting signal is relatively small [129].

The second aim of our study was to compare a radiological visual scoring method of the fat fraction with quantitative MRI values in both healthy and fatty infiltrated muscles. The mean quantitative fat fraction in our healthy volunteers was in agreement with a recent study [132]. In muscle of healthy controls and DMD patients with relatively low fat fractions, the visual scores were highly correlated with the quantitatively obtained fat fractions. However, the visual scores for the fat fractions in the muscle were generally higher than their corresponding quantitative values. This finding implies that the visual scoring measurements overestimate the fat fraction in affected muscles. Alizai et al. showed a similar finding in the muscle of diabetes patients: in this study most patients were only relatively mildly affected [127]. Our data shows large variation between the visually scored and quantitative values, specifically in the severely affected muscles. The large variability of the visually-scored method illustrates that these methods are less sensitive for the recognition of subtle changes, as could be present in longitudinal follow up of DMD patients or in therapy evaluation [133]. The overestimation and possibly also the variation of the fat fraction with the visually scored methods could partly be explained by the difficulty in visually differentiating between a moderate and severely fatty infiltrated voxel, which has also been suggested by Alizai [127]. Secondly it might be difficult to consistently estimate the amount of muscle left in a diffusely fatty infiltrated muscle as frequently observed in the DMD patients. In the radiological literature the Goutallier classification is commonly used, (normal muscle, fatty streaks, less fat than muscle, as much fat as muscle and more fat than muscle) [125]. This might be easier to use in scoring fatty infiltration of muscle by the human eye. However, the largest differences are seen in the most severely fatty infiltrated muscles. Both the overestimation of the fat fraction and the large variability in visually scored DMD muscle can influence the assessment of possible changes in the muscles in longitudinal follow up of or in the evaluation of therapy effects. Therefore, in these situations quantitative evaluation of the fat fraction seems more precise and reliable than visual radiological methods.

There were also some limitations to our study; most importantly no validation of the data with histology was made. A previous study has shown that values obtained with chemical shift-based water-fat separation methods are generally in accordance with data obtained from muscle biopsy [134]. The multipeak approach has previously been validated with in vitro measurements and MR spectroscopy and we therefore assume that any of our multipeak models are more representative of the actual fat fraction than a single peak model [119, 122, 135]. Another limitation of our study could be that a relatively low number of subjects were included. However, as a total of 201 different muscles were scored, the number of data points used for the comparison was very high.

In conclusion our results show that visually scored assessment of the fat fraction generally correlates with quantitative values, but overestimates the fat fraction and shows

higher variability. Quantitative MRI methods such as chemical shift-based water-fat separation produce a more accurate estimation of the fat fraction, especially in the more severely affected muscle. Correcting for the multiple peaks of the lipid spectrum contributes to obtaining more precise fat fractions. These findings further stress the importance of quantitative evaluation of the fat fraction to accurately demonstrate changes in the muscle.

Chapter 2

Chapter 3

Quantitative MRI and strength measurements in the assessment of muscle quality in Duchenne muscular dystrophy

B.H. Wokke, J.C. van den Bergen, M.J. Versluis, E.H. Niks, J.Milles, A.G. Webb, E.W. van Zwet, A. Aartsma-Rus, J.J. Verschuuren, H.E. Kan

ABSTRACT

The purpose of this study was to assess leg muscle quality and give a detailed description of leg muscle involvement in Duchenne muscular dystrophy patients using quantitative MRI and strength measurements. Fatty infiltration as well as the total and contractile (not fatty infiltrated) cross sectional areas of various leg muscles were determined in 16 Duchenne patients and 11 controls (aged 8 to 15). To determine specific muscle strength, four leg muscle groups (quadriceps femoris, hamstrings, anterior tibialis and triceps surae) were measured and related to the amount of contractile tissue. In patients, the quadriceps femoris showed a decreased total and contractile cross sectional area, attributable to muscle atrophy. The total, but not the contractile, cross sectional area of the triceps surae was increased in patients, corresponding to hypertrophy. Specific strength decreased in all four muscle groups of Duchenne patients, indicating reduced muscle quality. This suggests that muscle hypertrophy and fatty infiltration are two distinct pathological processes, differing between muscle groups. Additionally, the quality of remaining muscle fibers is severely reduced in the legs of Duchenne patients. The combination of quantitative MRI and quantitative muscle testing could be a valuable outcome parameter in longitudinal studies and in the follow-up of therapeutic effects.

INTRODUCTION

Duchenne muscular dystrophy (DMD) is an X-linked muscle disease affecting approximately 1 in 3500 male newborns. Patients develop progressive muscle weakness and become wheelchair-dependent around the age of twelve. They have a severely reduced life expectancy due to cardiac and respiratory problems [136]. DMD is caused by the absence of functional dystrophin, due to mutations in the *DMD* gene. This causes inflammation, muscle fiber necrosis and replacement of fibers by connective and fatty tissue [10, 38, 54].

Several promising therapies for DMD are currently being tested in clinical trials [77, 137-139]. Histological analysis of a muscle biopsy is an important outcome parameter for the evaluation of therapeutic effects. However, this procedure is invasive and provides only local information on a single muscle, whereas it is known that muscles are not affected equally and a distribution of pathological changes can occur even within a single muscle.

Quantitative non-invasive magnetic resonance imaging (MRI) of muscle is increasingly being used to assess disease-related parameters in DMD patients [98, 99, 103-107, 109, 111, 116, 140]. A commonly used parameter is fatty infiltration, which has been shown to correlate with age and muscle function in the upper leg [91, 98, 101, 106, 140]. With MRI, fatty infiltration can be quantified using several approaches, including methods based on signal intensity differences, which rely on thresholding bright fat pixels and lower intensity water pixels, chemical shift based approaches which rely on the difference in chemical shift between water and fat, and T2 maps which rely on the difference in T2 relaxation time between water and fat. Signal intensity approaches can be biased by partial volume effects (i.e. a voxel seldom solely consist of either fat or water) resulting in an inaccurate assessment of the fat fraction and T2 based methods can be significantly influenced by B1 inhomogeneities. In contrast, chemical shift based fat-water separation methods such as the 3-point Dixon technique are less biased by partial volume effects compared to thresholding approaches and are less influenced by B0 and B1 magnetic field inhomogeneities. Additionally, fat fractions obtained by this method have been shown to correlate well with histology and magnetic resonance spectroscopy (MRS) [105, 134].

The functional consequences of fatty infiltration i.e. a decrease in the amount of contractile tissue have recently been described for the quadriceps femoris, but not for other muscle groups in the upper and lower leg [140]. However, it is known that in DMD patients different muscles become affected at different stages of the disease and hence some muscles remain preserved longer than others [91, 113, 141]. In the lower leg, hypertrophy of the calf muscles has frequently been noted, but its effect on muscle function and the relation with fatty infiltration and age has not been described in detail.

35

In order to address the issues of limited volumetric coverage of only a few muscle groups from previous publications, here we studied fatty infiltration and muscle volume in four different muscle groups in the upper and lower leg of DMD patients using quantitative MRI with the 3-point Dixon technique [118, 142]. An additional aim of our study was to obtain a measure for muscle quality for each of these muscle groups by comparing the MR parameters to muscle strength. A non-invasive description of muscle quality would be very valuable to increase our knowledge of the pathophysiology of DMD and could be used as an outcome parameter for longitudinal follow-up studies.

METHODS

Patients and controls

Sixteen DMD patients (mean age 11.4 ± 2.2 years, range 8-14 years) and eleven healthy male controls (mean age 10.7 ± 2.1 years, range 8-15 years) participated in the study. Patients were recruited from the Dutch dystrophinopathy database. Diagnosis had been confirmed by DNA or muscle biopsy in all patients. Healthy subjects in the same age range were recruited from local schools and sports clubs. Exclusion criteria were the presence of contra-indications for the MRI and inability to lie supine for 30 minutes. The local medical ethics committee approved the study. Written informed consent was obtained from subjects and parents before inclusion.

MRI

MR images from the left upper and lower leg were acquired on a 3T scanner (Achieva, Philips Healthcare, Best, The Netherlands) using one 14-cm two-element receive coil with body coil excitation for both the upper and lower leg. The receive coil elements were positioned on the anterior and posterior side of the leg; directly below the patella for lower leg imaging and directly above the patella for upper leg imaging. The scanning protocol consisted of a survey scan for positioning, a T1-weighted turbo spin echo (TSE) sequence (twenty-five slices of five mm thickness, 0.5 mm gap, repetition time (TR) 600 ms, echo time (TE) 16ms, field of view (FOV) 180x180x137 mm, voxel size 0.9x0.9 mm, TSE factor 5) and a 3-point gradient echo Dixon sequence (twenty-five slices of five mm thickness, 0.5 mm gap, TR 400 ms, first TE 4.41 ms, echo spacing 0.76 ms, flip angle 8°, FOV 180x180x137 mm, voxel size 0.6x0.6 mm) of the upper and lower leg. The T1 and Dixon scans were planned using the survey scan, so that the central slice would be at the part of the lower leg with the largest diameter, and cover a significant part of quadriceps in the upper leg. The total scanning protocol, including positioning of the patients, could be completed in 25 minutes.

Data analysis

The 3-point Dixon images were reconstructed with multipeak correction as proposed by Yu et al. with frequencies $f_{p=}$[94, -318, -420] Hz and amplitudes $A_{p=}$[0.08, 0.15, 0.78], to account for the multiple peaks of the fat spectrum [122, 143].

Regions of interest (ROIs) were drawn manually using Medical Image Processing, Analysis and Visualization software package (http://mipav.cit.nih.gov) on T1-weighted images in the following muscles of the upper leg: rectus femoris, vastus lateralis, vastus intermedius, vastus medialis, short head of the biceps femoris, long head of the biceps femoris, semitendinosus, semimembranosus, adductor longus, adductor magnus, gracilis and sartorius. In the lower leg the muscle groups were: medial head of the gastrocnemius, lateral head of the gastrocnemius, soleus, flexor digitorum longus, flexor hallucis longus, posterior tibialis, extensor hallucis longus, peroneus, anterior tibialis and extensor digitorum longus. ROIs were drawn on every other slice, provided that the muscles were clearly identifiable in the slices.

The average fat fraction per muscle was computed using the co-registered contours from the T1w images on the Dixon images and calculated by averaging all pixels assigned to that muscle. The fat fraction was modelled as $SI_{fat}/(SI_{fat}+cSI_{water})$, with SI = signal intensity and the factor c (1.41) correcting for differences in proton density and T2 relaxation times between water and fat. We used T2 instead of T2* in our correction as we used a three echo method and therefore could not reliably determine T2* [144]. Proton density and T2 relaxation times of water and fat were measured in the muscle and subcutaneous fat of one healthy volunteer using the assumption that T2 values of subcutaneous fat and highly fat infiltrated muscle are similar [143, 145].

To assess total cross sectional area (CSA) in the upper leg the most proximal slice in which the short-head of the biceps femoris could be identified was used, as described by Akima et al. [140]. For the lower leg the total CSA was determined separately for the anterior tibialis and the triceps surae in the slice or slices with the largest CSA of the muscles on the axial images [100]. For the contributing muscles for knee extension (quadriceps femoris; i.e. rectus femoris, vastus lateralis, vastus medialis, vastus intermedius), knee flexion (hamstrings; i.e. biceps femoris long and short head, semimembranosus, semitendinosus), ankle dorsiflexion (anterior tibialis) and ankle plantar flexion (triceps surae; i.e. gastrocnemius medial and lateral head, soleus), the relation between the contractile CSA and strength was assessed. Contractile CSA was calculated from the mean fat fraction and the total cross sectional area (i.e. the cross sectional area including fat and muscle tissue) of these muscles (contractile CSA= total CSA x (100-mean fat percentage in entire muscle volume)/100). As a measure for muscle quality, the specific strength i.e. peak muscle strength per mm^2 of contractile tissue) was determined.

Clinical measurements

A quantitative muscle assessment (QMA) system (www.qmasystem.com) was used to assess knee flexion, knee extension, and ankle plantar- and dorsiflexion in both patients and controls. Maximal voluntary isometric contraction was obtained using a fixed myometer. For knee flexion and knee extension patients were tested in sitting position, with hip and knee at 90° flexion with the strap attached around their ankle. Ankle plantar- and dorsiflexion were assessed in a supine position with the hip at full extension; heel slightly raised with the calf on a cushion and strap around the metatarsals [146]. The highest value of three consecutive measurements was used as the maximum strength. If a measurement differed more than 10% from previous measurements, it was discarded and an extra measurement was performed. Measurements were performed after the MRI.

Statistical analysis

To assess differences between patients and controls in total CSA, contractile CSA, peak muscle strength and specific strength (strength per mm^2 of contractile tissue), general linear models were used with Duchenne status as a fixed factor and normalized age (i.e. age – average) as a covariate. Bonferoni-Holms correction was used to correct for the multiple comparisons in this analysis. A student's t-test was used to test for differences in patients' age, height and weight. Pearson correlation analysis was performed to assess the relation between peak muscle strength (kg) and contractile CSA (mm^2). The SPSS statistical package Version 20.0 for Windows (SPSS Inc., Chicago, IL) was used for the analysis. The level of statistical significance was set at $p<0.05$.

RESULTS

Patient characteristics are shown in Table 1. All healthy controls completed the MRI protocol, but in two DMD patients only the lower leg was scanned. One patient was unable to lie on his back for more than 15 minutes and one patient wore braces, which prevented accurate positioning in the scanner for upper leg scanning. There were no significant differences in age, weight and height between patients and controls (Table 1). Twelve patients were on corticosteroids during the study (one patient used deflazacort, eleven used prednisone). Of the four patients not on steroids, two 13-year old boys had been on steroids for several years up to one year prior to the study. Two DMD boys (8 and 13 yrs) had never used corticosteroids.

Table 1. Patient demographics.

	Patients	**Controls**	**P value**
Age (years)	11.4 ± 2.2	10.7 ± 2.0	0.40
Height (m)	1.48 ± 0.1	1.54 ± 0.1	0.38
Weight (kg)	48.6 ± 12.5	41.9 ± 12.1	0.17
Corticosteroid use	12/16	0/11	
Mobility			
- Fully ambulant	7/16	11/11	
- Wheelchair user	2/16	0/11	
- Wheelchair dependent	7/16	0/11	

Fatty infiltration

To evaluate the disease severity and the pattern of muscle involvement fat fractions were calculated for all muscles. The mean fat fraction in patients in the leg muscles was 28.8 ± 22.8% (range 2-86%). In controls the value was 5.3 ± 1.5% (range 3-10%). Compared to controls all patients showed increased fat fractions (i.e. higher than the mean plus two times the SD of the control values of that muscle) in at least one muscle of the upper leg and lower leg (Figures 1 and 2). The flexor digitorum longus and extensor hallucis longus could not be identified in all patients and/or in all slices because of a limited field-of-view in the cranial-caudal direction.
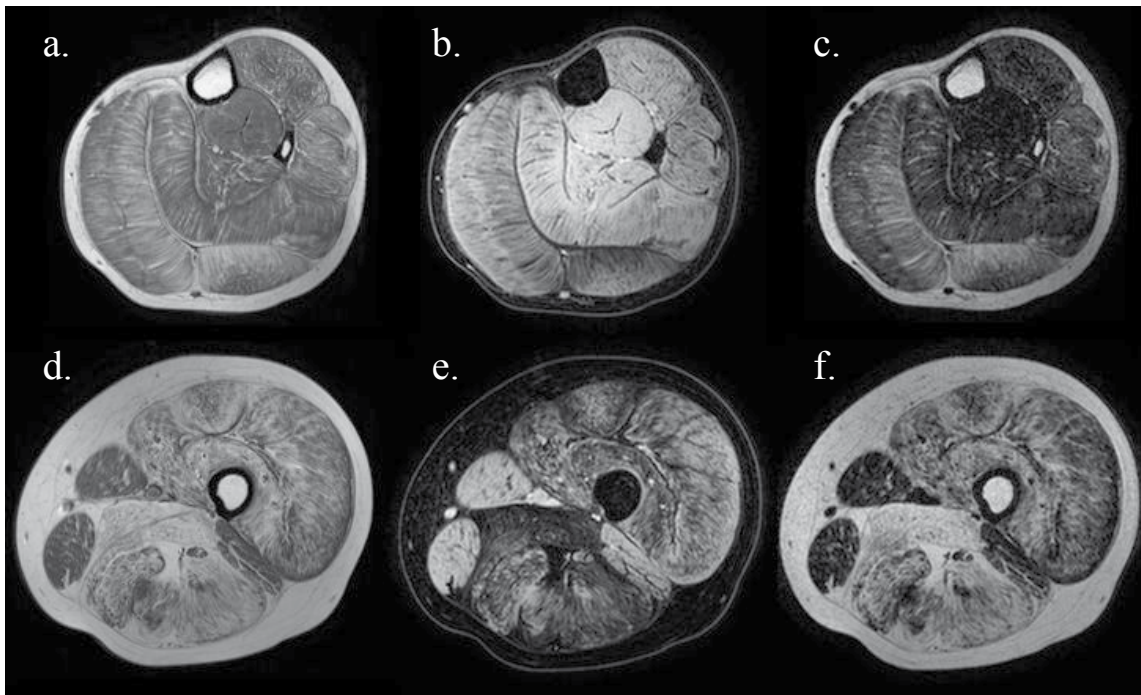
Figure 1. T1 weighted and Dixon MR image of upper and lower leg.
T1-weighted (a,d), Dixon fat (b,e) and Dixon water (c,f) image of lower and upper leg of a eleven year old DMD patient.
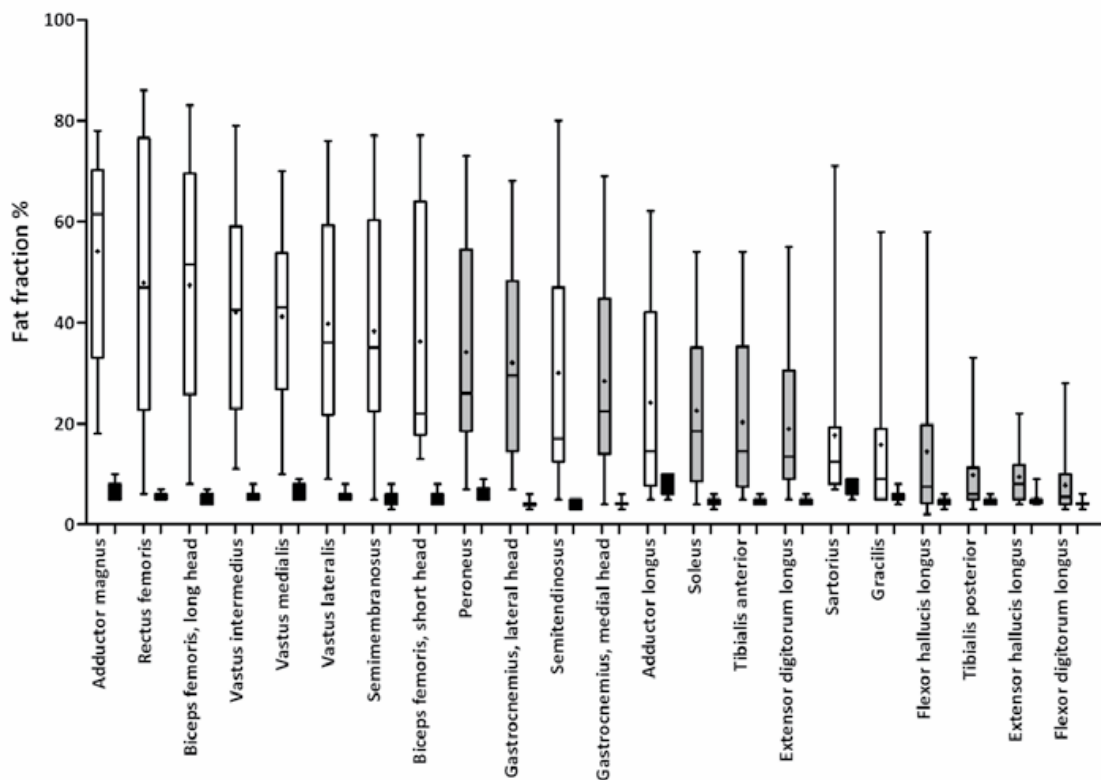
Figure 2. Box and whisker plot of the average fat fraction per muscle in upper and lower leg of DMD patients and healthy controls.

Fat fractions shown for all patients in all muscles of the upper leg (white) and lower leg (grey) and for all healthy controls (black). The upper leg is more affected compared to the lower leg muscles. Values shown as median ± maximum and minimum and are ordered by the mean fat fraction ($^+$).

Total and contractile cross sectional area

The total CSA of the quadriceps femoris muscles was smaller in patients than in healthy controls (Table 2). For the hamstrings and anterior tibialis there were no significant differences in the total CSA between the groups. In the triceps surae the total CSA in patients was significantly larger than in healthy controls. In controls total CSA increased significantly with age in all muscle groups ($p < 0.03$) (Figure 3a-d). In patients, however, no significant correlation between total CSA with age was found.

The contractile CSA in the quadriceps femoris and hamstrings was smaller in patients than in healthy controls (Table 2). For the other two muscle groups there were no significant differences in contractile CSA between patients and controls. In healthy controls contractile CSA increased significantly with age ($p < 0.02$), but no such relation was observed in the patients.

Table 2. Muscle characteristics in patients and controls.

		Patients	Controls	P value
Total CSA (mm^2)	Quadriceps femoris	2889 ± 974	4203 ± 1203	<0.001
	Hamstrings	2071 ± 580	1753 ± 630	0.33
	Anterior tibialis	475 ± 115	439 ± 142	0.87
	Triceps surae	4671 ± 1373	3081 ± 960	0.016
Contractile CSA (mm^2)	Quadriceps femoris	1527 ± 509	3955 ± 1098	<0.001
	Hamstrings	1255 ± 531	1669 ± 591	0.02
	Anterior tibialis	377 ± 114	421 ± 135	0. 22
	Triceps surae	3454 ± 1159	2875 ± 953	0.27
Peak muscle strength (kg)	Quadriceps femoris	5.9 ± 3	27.0 ± 10	<0.001
	Hamstrings	6.8 ± 3	19.4 ± 7	<0.001
	Anterior tibialis	7.4 ± 4	18.5 ± 7	<0.001
	Triceps surae	12.0 ± 8	25.7 ± 8	<0.001
Specific strength (kg/mm^2)	Quadriceps femoris	3.9 ± 1.6	6.7 ± 0.8	<0.001
	Hamstrings	5.8 ± 2.4	11.6 ± 1.8	<0.001
	Anterior tibialis	18.7 ± 9.2	43.4 ± 7.9	<0.001
	Triceps surae	3.6 ± 2.1	9.1 ± 1.3	<0.001

Muscle strength

Peak muscle strength was significantly lower in patients than in healthy controls for all four muscle groups (Table 2). In controls, muscle strength increased significantly with age in all muscle groups (p<0.001). In patients only the strength of the anterior tibialis and the triceps surae increased with age (p=0.035 and p=0.003 respectively). Significant positive correlations between peak muscle strength and contractile CSA were found for all muscle groups in controls. In patients there was a significant correlation in the quadriceps, hamstrings and anterior tibialis, but no significant relation in the triceps surae (Figure 4). To assess muscle quality, we compared the specific strength between patients and controls. In DMD patients this was significantly lower in all muscle groups compared to controls (Table 2). In controls specific strength did not increase with age, while in patients an increase of specific strength with age was seen in the triceps surae (p< 0.001) and the tibialis anterior (p= 0.03).

Total cross sectional area (mm^2)

Fat percentage

A Quadriceps femoris

E Quadriceps femoris

B Hamstrings

F Hamstrings

C Anterior tibialis

G Anterior tibialis

D Triceps surae

H Triceps surae
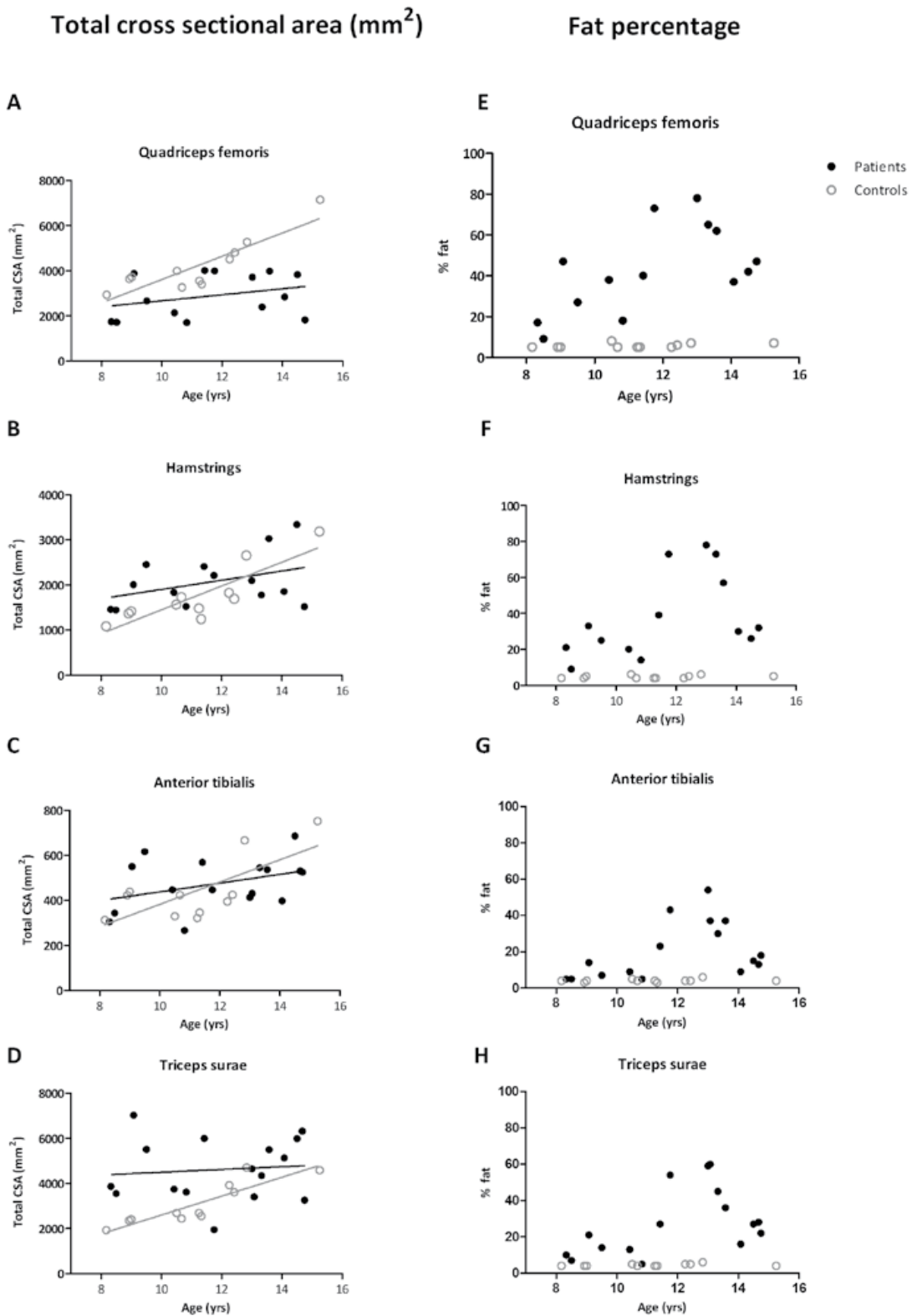
Figure 3. Plots of total contractile area and fat percentage.
In patients no significant increase in total cross sectional area (CSA) was found with age, whereas in controls a significant relation was found in three muscle groups (a-d). In all four muscles in patients the fat percentage increases with age, but it starts later the lower leg compared to the upper leg (e-h).
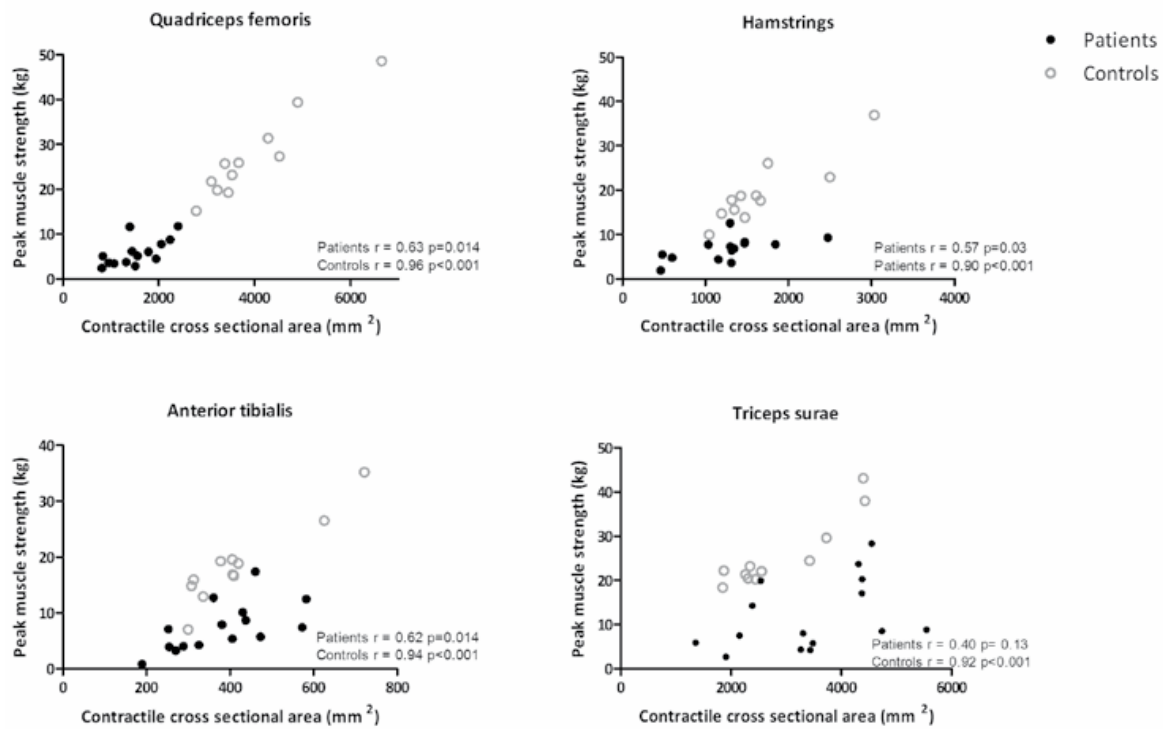
Figure 4. Relation between peak muscle strength and contractile cross sectional area.
Correlation between contractile cross-sectional area (CSA) and peak muscle strength in patients and controls in four different muscle groups.

DISCUSSION

Our data show that the absence of dystrophin elicits significantly different responses in the four main muscle groups of the leg in terms of muscle volume and fatty infiltration. The quadriceps and triceps surae represent two ends of the spectrum, while the hamstrings and anterior tibialis have an intermediate phenotype. In addition, the specific strength of the muscles was significantly lower for all four muscle groups compared with healthy controls confirming a reduction in muscle quality.

The most severely fatty infiltrated muscle in patients was the adductor magnus, followed by the individual muscles of the quadriceps femoris and the biceps femoris longus, which is in accordance with previous studies [106, 109, 113, 141]. Overall, the lower leg was affected later in the disease, with the lateral and medial head of the gastrocnemius and the peroneus being most severely affected [111].

In patients, the total CSA of the triceps surae was significantly larger compared to healthy controls, while the contractile CSA (i.e. the area of the muscle that consists of muscle tissue with no fat) was similar to controls. An increased total CSA was already present in our youngest patients but did not increase further with age, suggesting early

hypertrophy. Clinical hypertrophy of the triceps surae is well known in DMD patients and has been reported at a very young age. Hypertrophic fibres have been observed in muscle biopsies of DMD patients from 4 years and older [147]. In contrast, both the total CSA and the contractile CSA of the quadriceps femoris were smaller compared to healthy controls. The reduction in total CSA was already present in the youngest patients and remained stable with age, suggesting relative atrophy at a young age, which is in accordance with a previous muscle biopsy study [147]. The hamstrings and tibialis anterior showed no significant differences in total CSA compared to healthy controls but also showed no increase with age. The tendency towards a larger total CSA at younger age there indicates hypertrophy in these muscle groups as well. Taken together, our results suggest that the quadriceps femoris shows no or a mild hypertrophic response in young patients, the triceps surae shows hypertrophy and the hamstrings and anterior tibialis show an intermediate response.

Interestingly, the extent of the hypertrophic response does not seem to predict the extent of the fatty infiltration. The quadriceps femoris showed no clear hypertrophy, but did have severe fatty infiltration, which can be interpreted as a hallmark of an early and severely dystrophic muscle. On the other hand, the hamstrings showed a mild hypertrophic response, but also showed severe fatty infiltration [106]. In the lower leg, the triceps surae showed the greatest degree of hypertrophy, but the amount of fatty infiltration was similar to the tibialis anterior muscle, which only had a moderate hypertrophic response. Thus, the onset and progression of changes in muscle volume and fatty infiltration appear to be two distinct, independent pathological processes that differ in rate of progression between muscle groups.

In controls, muscle strength increased with age and with the amount of contractile tissue. The cross-sectional data from our patients showed no significant increase in muscle strength with age in the upper legs, but there was an increase in the lower legs. Additionally, DMD patients showed an overall reduction in the specific muscle strength. The availability of both quantitative MRI data and quantitative muscle strength measurements allowed us to calculate this parameter, which is an indication of the strength per muscle fiber, excluding the fatty infiltrated part of the muscle. The significantly lower specific strength in patients compared to controls for all four muscle groups indicates an overall reduction in muscle quality. This could be due to several factors, including limited capacity of the diseased muscle fibers to contract, reduced efficacy of force transduction to the connective tissue and tendons and increased muscle stiffness due to increased levels of fibrosis or as a result of disorganization and inefficient alignment of muscle fibers [148]. A similar observation has been made both in the quadriceps muscle of DMD patients and in *mdx* mice [140, 149]. In these mice isometric forces produced by soleus muscles from young mice were weaker than in wild type mice, when force was normalized for cross-sectional area. Surprisingly,

there appeared to be an increase in both strength and specific strength in the lower leg muscle groups with age in patients, while this increase was absent in controls. This could suggest that in patients, there is a selection of high quality muscle fibers, which might also have the ability to increase their capacity to generate force.

The current study has some limitations. The percentage of fatty infiltration (Figure 3) was relatively low in the 14 year old patients in our study compared to the other patients. This finding emphasizes that in DMD patients there is variability between how severely patients are affected. Nevertheless, these patients also show lower specific strength of the remaining muscle tissue compared to healthy controls, indicating that despite the relatively high amount of contractile tissue, there is a reduction in muscle quality in all muscle groups. Although we obtained a good match with healthy controls regarding age and height, a limitation of our study was the absence of longitudinal data. We compensated for this by analysing our data with age as a covariate, but true longitudinal data where muscle MRI and strength tests are combined might prove very fruitful in analysing the differences between dystrophic muscles [106]. We determined contractile CSA using the largest total CSA and the mean fat fraction for each muscle group. In DMD muscle, significant amounts of fat infiltration are present, and this fat will likely contribute only minimally to the force of that muscle. Fatty infiltration could be distributed inhomogenously across the muscle of DMD patients, and it is unclear how this could affect the muscle strength. As the whole muscle contributes to delivering force, taking into account only the fat percentage of one slice could bias the results. Therefore, we felt that using the mean fat fraction of a number of slices instead of the fat fraction from the slice used for determination of maximal CSA would provide a more realistic value of the contractile abilities of the muscle. Finally, we did not incorporate fitting of the T2* decay into our model of fat quantification, which could have led to a slight overestimation of the fat levels in our study.

In summary, progressive fatty infiltration is seen with a decrease in total volume in some muscles, but with muscle hypertrophy in others, which suggests that these are two distinct pathological processes, which differ over time between muscle groups. Quantitative MRI enabled us to calculate the fatty infiltration and thus contractile cross-sectional area, and this showed a reduction in muscle quality in DMD patients. This could yield valuable insight in the pathophysiology of dystrophic muscle and form an outcome parameter in longitudinal follow-up and therapeutic trials.

Chapter

4

Dystrophin levels and clinical
severity in Becker muscular
dystrophy patients

J.C. van den Bergen, B.H. Wokke, A.A. Janson,
S.G. van Duinen, M.A. Hulsker, H.B. Ginjaar,
J.C. van Deutekom, A. Aartsma-Rus, H.E. Kan,
J.J. Verschuuren

ABSTRACT

Objective

Becker muscular dystrophy (BMD) is characterized by broad clinical variability. Ongoing studies exploring dystrophin restoration in Duchenne muscular dystrophy ask for better understanding of the relation between dystrophin levels and disease severity. We studied this relation in BMD patients with varying mutations, including a large subset with an exon 45-47 deletion.

Methods

Dystrophin was quantified by Western blot analyses in a fresh muscle biopsy of the anterior tibial muscle. Disease severity was assessed using quantitative muscle strength measurements and functional disability scoring. MRI of the leg was performed in a subgroup to detect fatty infiltration.

Results

Thirty-three BMD patients participated. No linear relation was found between dystrophin levels (range 3-78%) and muscle strength or age at different disease milestones, in both the whole group and the subgroup of exon 45-47 deleted patients. However, patients with less than 10% dystrophin all showed a severe disease course. No relation was found between disease severity and age when analysing the whole group. By contrast, in the exon 45-47 deleted subgroup muscle strength and levels of fatty infiltration were significantly correlated with patients' age.

Conclusion

Our study shows that dystrophin levels appear not to be a major determinant of disease severity in BMD, as long as it is above approximately 10%. A significant relation between age and disease course was only found in the exon 45-47 deletion subgroup. This suggests that at higher dystrophin levels the disease course depends more on the mutation site, than on the amount of the dystrophin protein produced.

INTRODUCTION

Becker and Duchenne muscular dystrophies (BMD and DMD) are caused by mutations in the *DMD* gene encoding the dystrophin protein. Absence of dystrophin, as in DMD patients, or reduced levels of a semi-functionial dystrophin, as in BMD patients, leads to progressive muscle weakness due to continuous muscle fibre damage. While DMD is characterized by a relatively uniform disease course, disease progression in BMD is more variable [20, 150-153]. The mechanisms underlying this variability are not fully understood. Factors believed to be involved include the regenerative capacity of muscle tissue, inflammation as well as quantity and quality of the dystrophin protein [154-157]. Qualitatively, dystrophin has multiple functions that depend on the presence of functional domains within the protein, most importantly the N-terminal actin-binding and the C-terminal beta-dystroglycan-binding domains. While the connecting 'central rod domain' appears to be largely dispensable, the way in which remaining spectrin-like repeats are phased likely impacts dystrophin functionality [158]. An important role for dystrophin quantity has been suggested by previous reports, although there is still uncertainty about the nature of this relationship as both linear relations and a threshold effect have been suggested [150, 153-155, 159-164]. The interest in this possible relation increased with the development of the exon skipping technology in DMD [165, 166]. Clinical trials testing systemic delivery of antisense oligonucleotides (AONs) targeting exon 51 have shown restoration of dystrophin levels of up to 18% [77, 79].

In the present study we investigate the relation between dystrophin levels quantified from a freshly obtained muscle biopsy and disease severity in 33 BMD patients, including 13 patients with an exon 45-47 deletion.

MATERIAL AND METHODS

Patients

Adult BMD patients registered in the Dutch Dystrophinopathy Database were eligible to participate when complying with the following inclusion criteria: (1) in frame mutation in the *DMD* gene OR (2) any other mutation in the *DMD* gene AND a mild disease course, defined by age at wheelchair dependence after the age of 16 OR (3) no known mutation in the *DMD* gene AND reduced dystrophin staining in muscle biopsy. Patients using mechanical ventilation were excluded. During a one-day visit quantitative muscle testing of several muscle groups in upper and lower extremity and (optionally) a muscle biopsy of the anterior tibialis (TA) muscle was obtained from the study participants. The TA was chosen because it usually contains an adequate amount

of muscle tissue for dystrophin analysis in BMD patients with a wide range of disease severity, and since this muscle has also been used in several DMD exon skip trials [77, 78]. Additionally, a quantitative MRI of the lower leg was obtained from the subgroup of participants with an exon 45 to 47 deletion who did not have a pacemaker or ICD, or severe contractures.

The local medical ethics committee approved the study and written informed consent was obtained from all subjects.

Strength measurements

Quantitative muscle testing (QMT) was used to assess the maximal voluntary isometric contraction (MVIC). Measurements of the following muscle groups were obtained: elbow flexion and extension, handgrip and knee and hip flexion and extension. Ankle dorsiflexion was not included, as measurement of this muscle group has been shown to be unreliable [146]. Measurements were performed as described by Hogrel et al. [146]. Wheelchair dependent participants unable to make the transfer to the research bench were examined in their wheelchair. The mean of the bilaterally-tested muscle groups was calculated. To minimize the possible confounding effect of age and weight on the analyses, a z-score for muscle strength of the individual muscle groups was also calculated, taking these factors into account [146]. QMT was also performed in twenty male age-matched healthy volunteers.

Disease milestones

Disease milestones were used to compare disease severity between BMD patients, and thus to partially correct for the wide range of ages. A structured natural history was obtained from the 89 BMD patients with a genetically confirmed in-frame deletion in the Dutch Dystrophinopathy Database, including our participants. The data were used to determine the median ages as well as the 33rd and 66th percentile at which the following disease milestones were reached: first motor symptoms, difficulty walking stairs, use of walking aids (braces, cane, walker or wheelchair) and wheelchair dependence.

Western blot analysis

The muscle biopsy from the TA was processed as previously described by Van Deutekom et al. [78]. Protein lysates were generated from muscle biopsies and Western blotting were performed according to previously described methods [78]. Monoclonal NCL-DYS1 (dilution 1:100, Novacastra, UK) or polyclonal ab15277 (dilution 1: 200 Abcam, UK) were used to detect dystrophin. Rabbit polyclonal antibody to sarcomeric alpha-actinin (ACTN2) ab72592 (dilution 1: 500 Abcam, UK) was used as a loading control. Blots were visualized and quantified with the Odyssey system and software (Li-Cor, USA) as described previously [78]. Samples obtained from the TA and medial

and vastus lateralis muscles of five healthy males were used as reference samples. For each patient sample at least 2 technical replicates were performed.

Immunohistochemistry

Sections of 10 μm were cut from the TA biopsies using a Shandon Cryotome (Thermo Fisher Scientific Co., Pittsburgh, PA, USA). Sections were fixed for 1 min with ice-cold acetone. Goat polyclonal dystrophin diluted 1:50 (SC-7461, Santa Cruz Biotechnology, USA) was used to detect dystrophin. Alexa-fluor 488 donkey-anti goat IgG (A11055, Invitrogen, the Netherlands) diluted 1:1000 was used as a secondary antibody. Slides were analysed using a fluorescence microscope (DM RA2; Leica Microsystems Wetzlar, Germany), and digital images were taken using a CCD camera (CTR MIC; Leica Microsystems).

Muscle MRI

In BMD patients with an exon 45-47 deletion MR Images were acquired on a 3T scanner (Achieva, Philips Healthcare, Best, The Netherlands) from the left lower leg using a 14-cm diameter two-element receive coil and body coil excitation. The scanning protocol consisted of a T1-weighted sequence (25 five mm slices, 0.5 mm gap, repetition time (TR) 600 ms, echo time (TE) 16 ms) and a 3-point Dixon sequence (25 five mm slices, 0.5 mm gap, TR 400 ms, first TE 4.41, echo spacing 0.76 ms, flip angle 8°) with multipeak analysis [122]. The mean fat fraction per muscle was calculated from regions of interest (ROIs) using Medical Image Processing, Analysis and Visualization (MIPAV) software. The medial and lateral head of the gastrocnemius, soleus, flexor digitorum longus, flexor hallucis longus, posterior tibialis, extensor hallucis longus, peroneus, tibialis anterior and extensor digitorum longus were analysed.

Statistics

Pearson's correlation test was used to analyse the relation between dystrophin expression, MVIC score and the mean fat fraction of the muscles. Dystrophin expression levels for the groups based on disease milestones were compared using an independent-samples Student's t-test. Differences between participants and non-participants as well as differences in disease milestones were analysed by Kaplan-Meier survival analysis, using the Log Rank test. SPSS version 16 for Windows (SPSS Inc., Chicago IL) was used. The level of significance was set at $p < 0.05$. Values are shown as mean ± SD.

RESULTS

Patients

We approached 60 adult Becker patients to participate in the study of whom 33 consented to participate (Table 1). Reasons not to participate included the physical burden, inability to attend due to work and travel distance to the Leiden University Medical Center. Participants did not differ significantly from non-participants in terms of age or age at reaching disease milestones (Table 2). Mean age of participants was 40 years (± 13, range 19-66 years) versus 44 years (± 13, range 19-65 years) in the non-participating patients.

Table 1. Included BMD participants

	DMD phenotype (loss of ambulation <12 years)	Intermediate phenotype (loss of ambulation 13-16 years)	BMD phenotype (loss of ambulation >16 years)
In frame deletion	1	-	29
Out of frame deletion or point mutation	-	-	2
Unknown mutation, reduced dystrophin staining	-	-	1

The study population represented a wide clinical variety (Supplementary Table 1), ranging from a patient of 26 years who only noticed mild impairment while walking upstairs carrying heavy tools to a patient with a DMD-like phenotype (wheelchair-dependence at the age of 10), but with an in frame deletion in the *DMD* gene and dystrophin expression as assessed by Western blot (see below).

Table 2. Characteristics of participating and non-participating BMD patients.

	Study participants n=33		Non participants n=27		p-value
	Events	Estimated mean	Events	Estimated mean	
Age		40 (± 13)		44 (± 13)	0.27
First symptoms	31	12 (± 1.6)	26	11 (± 2.1)	0·41
Walking stairs	26	30 (± 3.0)	25	24 (± 2.7)	0.16
Walking aid	19	41 (± 3.6)	20	36 (± 3.4)	0.49
Wheelchair dependence	8	54 (± 3.2)	11	49 (± 3.4)	0.33

Dystrophin quantification

Fresh muscle biopsies were obtained from 27 patients. Six patients refused a biopsy because of previous negative experiences. Dystrophin expression as assessed by Western blot (Figure 1 and Supplementary Figure 1) ranged from 4% to 71% of normal human skeletal muscle as detected by the rod-domain antibody (NCL-DYS1) and from 3% to 78% using the C-terminus antibody (AB15277). The mutation of one patient (exon 29;c.3940C>T,p.Arg1314X) resulted in the deletion of exon 29 on RNA transcript level, which encodes the epitope of the rod-domain antibody and was therefore only recognized by the C-terminus antibody. As there was a good correlation between the dystrophin levels detected by the two antibodies (R 0·87; p<0·001) further analyses were performed using the C-terminus antibody. Using immune fluorescence analysis we observed homogeneous staining for most patients (16/22), generally at lower intensity than the normal control. For a few patients we observed both dystrophin positive and negative fibres (5/22), while for one patient the biopsy was so fibrotic we did not observe any dystrophin staining (see Supplementary Figure 2 for representative examples).

Strength measurements

QMA testing of elbow flexion and extension, handgrip and hip flexion and extension was performed in all patients. Due to inability to transfer to the research bench testing of knee flexion and extension was not possible in one and four patients respectively. A significant correlation existed between the MVIC-scores of all seven individually tested muscles. The mean MVIC-sum of the five muscle groups tested in all patients was 99 kg (± 59 kg, 15-186 kg). There was no significant relation between the MVIC-sum score and the age of patients at the time of QMA-testing (R -0.15; p=0.41) (Figure 2a). However, when analysing our subgroup of thirteen patients with an exon 45-47
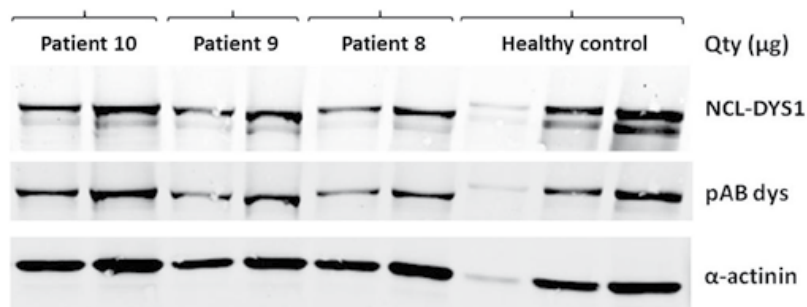
Figure 1. Example of Western blot analysis on total protein extracts from three BMD patients and one healthy control.
The rod-domain antibody (NCL-DYS1), C-terminus antibody (pABdys) and loading control (α-actinin) are shown. As anticipated from the deletions, the proteins in the BMD patients are slightly smaller than those in the healthy control. In the BMD group both patients with uniform and mosaic dystrophin expression were found by immunofluorescent staining.

deletion a significant relation between MVIC-sum score and age was found (R -0.74; p=0.004). The mean MVIC-sum score of age-matched healthy male volunteers (mean age 42 ± 13 years, range 20-62 years) was 182 kg (± 23 kg, 142-220 kg), and showed no significant relation within this age range (R -0·41; p=0·07).
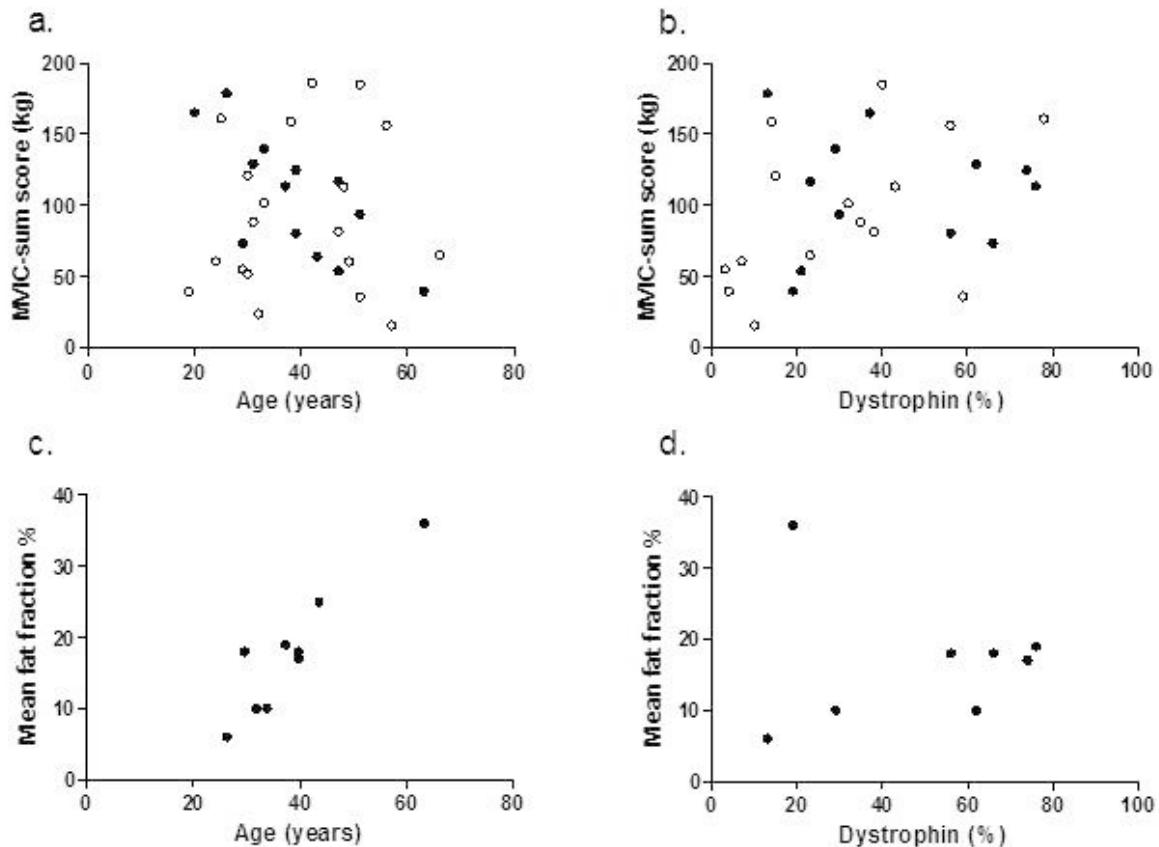
Figure 2. Correlation between age (a. and c.) or dystrophin expression for the C-terminus antibody (b. and d.) with the MVIC-score and the mean fat fraction of the lower leg on MRI.
Data of the subgroup with an exon 45-47 deletion are represented in closed dots, all other mutations in open circles. There is an evident relation for both the MVIC-score (a.) and the mean fat fraction (c.) with age of the patients in the deletion 45-47 subgroup (R -0.74; p 0.004 and R 0.92; p <0.001 respectively). No relation is found between dystrophin expression and MVIC-score (b.) or mean fat fraction on MRI (d.).

No relation was found between dystrophin expression and disease severity, as measured by MVIC-sum score in the whole group (R 0.30; p=0.13) or the exon 45-47 deleted subset (R -0.10; p=0.98) (Figure 2b). This relation was also absent when analysing all muscle groups individually. To decrease the possible confounding effect of age related differences in muscle strength, the analysis was subsequently performed in three subgroups: patients aged 18-30 (n=8), 31-45 (n=8) and 46 and older (n=11). No significant correlation between dystrophin levels and MVIC-sum score was present in

any of these groups (R 0.40; p=0.33, R -0.30; p=0.47 and R 0.46; p=0.16 respectively). Analyses correcting for both age and weight were added using the z-scores calculated using data from Hogrel, showing again no correlation between dystrophin levels and muscle strength for the whole group (R 0.23; p=0.25) as well as the exon 45-47 sub-group (R -0.71; p=0.83) [146].

Disease milestones

The median age of the disease milestones in 89 BMD patients (aged 3-66 years) was 6 years for 'first motor symptoms', 20 years for 'difficulties walking stairs', 28 years for use of a walking aid and 33 years for wheelchair dependency. For each milestone we grouped our patients with known dystrophin levels based on whether that milestone presented before or after the median age of that milestone (Figure 3a). No significant differences were found between dystrophin levels of the two groups for 'first motor symptoms' (p=0.39), 'difficulties walking stairs' (p=0.91) and 'use of a walking aid' (p=0.25). As too few patients were wheelchair dependant, statistical analysis was not possible for this milestone. When this same analysis was repeated using three instead of two groups, with cut-off points based on the 33rd and 66th percentile of age at reaching a certain disease milestones, no significant difference in dystrophin levels was present either (Figure 3b).

When analysing the exon 45-47 deletion subgroup the dystrophin levels were not significantly different for two disease milestones (p=0.94 and p=0.40 for first motor
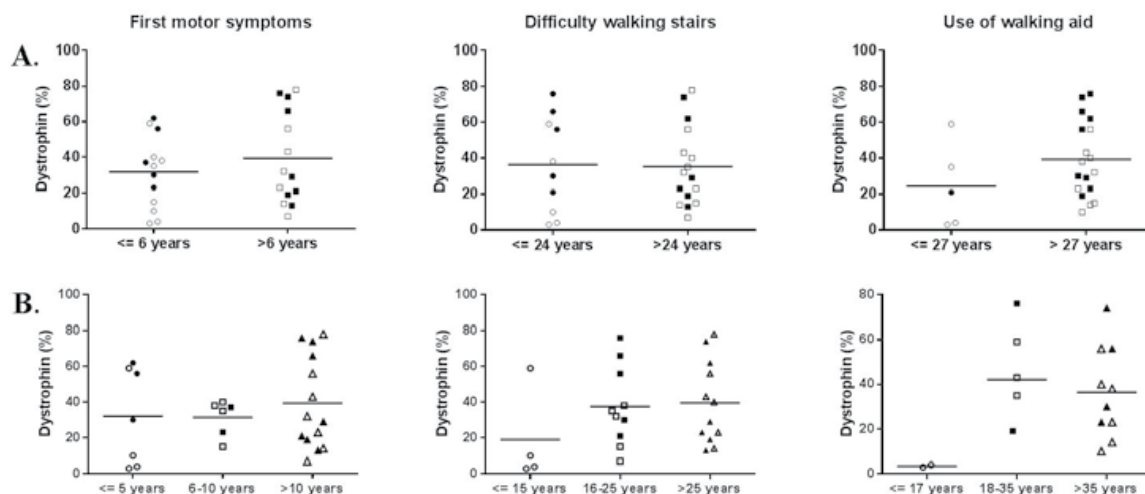
Figure 3. Distribution of dystrophin levels between patients reaching a disease milestone.
A. before or after the median age of that milestone and B. before the 33rd percentile, between the 33rd and 66th and after the 66th percentile of 89 BMD patients for first motor symptoms, difficulty walking stairs and use of a walking aid. The horizontal lines mark the average dystrophin level within the groups. Data for the patients with an exon 45-47 deletion are presented in black dots, data for all other patients in open circles. Note that grouping of a specific patient can be different for different milestones.

symptoms and difficulties walking stairs, respectively). Too few patients had reached the other milestones to include these items in the analysis.

Muscle MRI

An MRI scan was obtained from nine patients with an exon 45-47 deletion. The lower leg showed a distinct pattern of muscle involvement, with the medial head of the gastrocnemius muscle being most severely affected, followed by the lateral head of the gastrocnemius and the peroneus muscle (Figure 4). The TA was relatively spared in all patients, but still showed a significant increase of the fat fraction with age (R 0·94; $p<0.001$). There was no correlation between dystrophin levels and fatty infiltration on MRI (R -0·03; p=0·95) (Figure 2d). There was however a significant correlation between patients' age and mean fat fraction of the lower leg muscles (R 0·92; $p<0·001$) (Figure 2c).
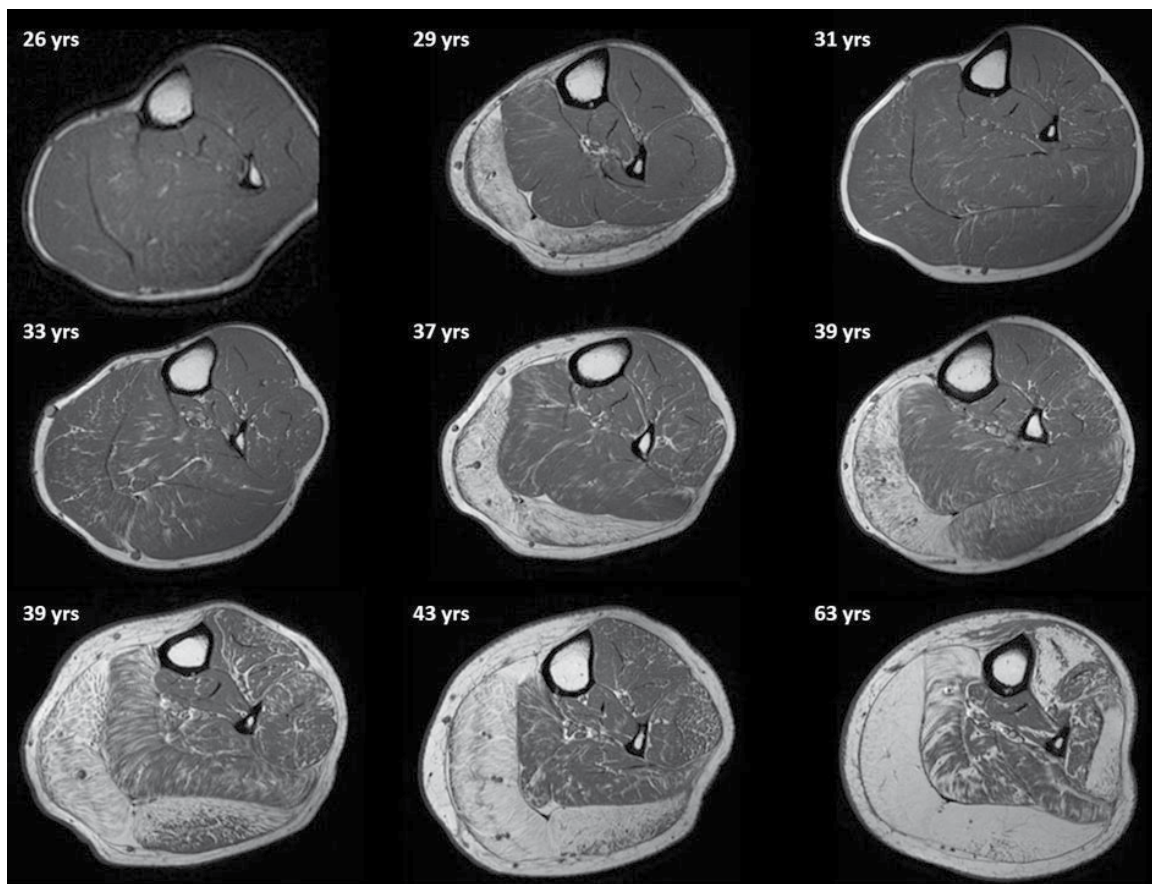
Figure 4. Transversal image of lower leg of BMD patients with an exon 45-47 deletion.
There is an evident increase in the mean fat fraction with age. The changes are most evident for the medial head of the gastrocnemius muscle and in later stages also for the lateral head.

DISCUSSION

We studied a group of BMD patients with a large diversity in disease severity, as well as a wide range of different forms of dystrophin, with 18 different mutations, and assessed dystrophin levels from freshly acquired muscle biopsies, with dystrophin levels ranging from 3 to 78%. In this group of BMD patients there was no linear relation between dystrophin levels and disease severity, defined by quantitatively measured muscle strength, fatty infiltration on MRI or by clinical milestones.

The relation between the variable disease severity observed in BMD patients and dystrophin levels has been of increasing interest with the development of exon skipping therapy for DMD patients. Although a small amount of dystrophin in muscle is better than none, it remains unclear what the relation between dystrophin levels and disease severity entails. Some previous studies found indications that higher dystrophin levels are associated with a milder disease course [150, 153, 154, 159, 161, 163]. Others reported a threshold effect [160, 162, 164]. However, these studies pooled data from patients with different mutations. Becker patients with in-frame deletions on the 5'-end of the *DMD* gene generally have a more severe disease course, including an earlier age of cardiac involvement [159, 160, 167, 168]. Therefore, it is likely that the pooling of different mutations has influenced these results.

A recent study by Anthony et al. focused on a more selected group of patients with a mutation bordering exon 51 or exon 53 and patients with an exon 45-55 deletion, therefore limiting the effect of the location of the mutation on disease progression to some extent [154]. Their results suggested that higher dystrophin levels were associated with a less severe disease course. However, their analysis was performed in asymptomatic and mild patients with relatively high dystrophin levels (all above 50%). Therefore, the results cannot be extrapolated to the entire BMD disease spectrum. In our subgroup of 13 patients with an exon 45-47 deletion no relation between dystrophin levels (varying from 13-76%) and disease severity was found. In contrast, in this subgroup there was an evident relation between disease severity and age of the patients. These findings are supported by the MRI data, showing a progressive increase in fatty infiltration with age. We believe this finding illustrates that the study of subsets of BMD patients with the same mutations can identify relations otherwise obscured.

Although we found no relation between dystrophin levels and disease severity, our four patients with dystrophin levels below 10% showed low MVIC-sum scores and early onset of symptoms (Figure 3 and Supplementary Table 1). This finding implies a threshold effect, which is conform several previous clinical studies suggesting that dystrophin levels below 10% are indicative of a more severe disease course [160, 162, 164]. This could suggest that a relatively small amount of dystrophin is sufficient to result in a disease course that is milder than DMD, but relatively more severe than

'typical BMD'. This is also in accordance with previous reports of several mouse models, showing threshold levels between 15-20%, and with a recent study in mice showing that in a dystrophin and utrophin negative background, very low levels of dystrophin (up to 5%) improved survival, but not histology, levels between 5 and 15% further improved survival and fibrosis and levels of over 15% normalized survival and further improved fibrosis [169-172]. The clinical disease course in patients with an exon 45-47 deletion was quite uniform, but still there was variability, suggesting a role for additional factors such as differences in regenerative capacity, genetic modifiers or inflammation.

Exons 45-47 encode the last half of spectrin-like repeat 17 as well as repeat 18 of the dystrophin protein. It is known that repeat 16 and 17 (encoded by exon 42-45) are involved in nNOS-binding [173, 174]. Anthony et al. and Beggs et al. both have shown a relationship between (properly located) nNOS levels and disease severity [154, 160]. Possibly, differences in nNOS expression could be one of the factors involved in the disease variability of the exon 45-47 deleted group.

As dystrophin plays an important role in muscle fiber membrane stability any change in protein structure could lead to a decreased functioning. The findings that in-frame mutations at the 5'-end of the *DMD* gene lead to a more severe BMD or a DMD phenotype suggest that this domain is less dispensable for protein function. In contrast the central rod domain that connects the N-terminal actin-binding and C-terminal beta-dystroglycan binding domains allows more flexibility, as underlined by the finding that a deletion of >60% of the rod domain (deletion exon 17-48) resulted in a very mild BMD phenotype [175]. Structural changes of the dystrophin protein, caused by a specific mutation, will impair dystrophin function to an extent, characteristic for that mutation.

Our study suggests a direct effect of the exact mutation on the clinical phenotype of BMD patients. This finding has important implications for future BMD studies, where it will be essential to account for different mutations when looking at other possible contributing factors to disease severity. The possible disease modifying effect of dystrophin quality also has implications for exon skipping trials. As this therapy aims to change a DMD phenotype into a BMD phenotype, knowledge of the specific BMD phenotypes is important, as for some mutations ameliorating of the phenotype may be more beneficial than for others.

The suggestion of a threshold effect in this study could benefit therapeutic studies aiming to restore dystrophin in DMD patients. Clinical trials testing systemic delivery of antisense oligonucleotides targeting exon 51 have shown dystrophin levels of up to 18% [77, 79]. If relatively low levels of dystrophin are sufficient to result in a relatively mild BMD phenotype, it may be expected that patients may improve with these therapies.

There are several limitations to our study. Firstly, several other studies used muscle biopsies from the quadriceps muscle, while we chose to biopsy the anterior tibialis muscle, as it contains viable muscle tissue over wider clinical severity. Variation in dystrophin expression between muscles cannot be ruled out, but there are no indications that this could limit the interpretation. A previous immunohistochemical study reported no significant variation in dystrophin levels between various muscles in DMD patients, nor between biceps brachialis and vastus lateralis muscles in a group of BMD patients [159, 176]. Additionally, no significant variation in dystrophin expression was found in different skeletal muscles in mice [177]. Although our study is the largest study in BMD patients comparing disease course and dystrophin levels using fresh biopsies, our study could be underpowered to detect a possible relation between dystrophin levels and disease severity. Larger subgroups of BMD patients with the same mutation would be necessary to study such a relation, which, due to the rareness of BMD, will be challenging. However, in our subgroup of patients with an exon 45-47 deletion we did find a relation with age, but not with dystrophin. Thirdly, although there is no significant difference in disease course between participants and non-participants, a small trend favouring the participation of milder patients appears to be present. This is probably caused by the greater burden on severely affected patients to participate.

In summary, our study shows that there is no linear correlation between dystrophin levels and disease severity in BMD patients and that disease progression is uniform in a subgroup of BMD patients with an exon 45-47 deletion, as demonstrated by the decrease of muscle strength as well as increase of fatty infiltration of muscle. In contrast to the whole BMD group, these phenomena increase with age at a constant pace in the exon 45-47 deletion group, indicating that the mutation is likely an important factor in determining disease severity. Furthermore, there are indications for a threshold rather than a dose-effect relation and the fact that this threshold could likely be around 10% of normal levels (at least for the exon 45-47 deletion) has important implications for therapeutic approaches aiming at dystrophin restoration.

Chapter 4

Supplementary Table 1: Overview of data and clinical characteristics of study participants ([1] brothers).

Patient	Mutation	Age at examina-tion (years)	Biopsy	MRI	QMA sum score (kg)	Dystro-phin (%)	Disease Milestones (years)			
							First Symptoms	Walking Stairs	Walking Aid	Wheelchair Dependence
1	del 45-47	47	Yes	No	117	23	6	38	43	-
2	del 45-47	51	Yes	No	94	30	5	18	51	-
3	del 45-47	26	Yes	Yes	179	13	21	-	-	-
4	del 45-47	63	Yes	Yes	54	19	25	30	35	60
5	del 45-47	47	Yes	No	54	21	17	19	25	37
6	del 45-47	39	Yes	Yes	80	56	5	20	38	-
7[1]	del 45-47	37	Yes	Yes	113	76	16	20	30	-
8	del 45-47	20	Yes	No	165	37	6	-	-	-
9	del 45-47	29	Yes	Yes	73	66	12	20	-	-
10	del 45-47	39	Yes	Yes	125	74	21	35	-	-
11[1]	del 45-47	33	Yes	Yes	140	29	25	28	-	-
12	del 45-47	43	No	Yes	64	NA	6	35	35	-
13	del 45-47	31	Yes	Yes	129	62	2	-	-	-
14	del 03-04	31	Yes	No	88	35	6	25	25	-
15	del 03-05	33	Yes	No	102	32	18	25	-	-
16	del 03-07	57	Yes	No	15	10	4	12	40	45
17	del 05	19	Yes	No	40	4	2	4	4	10
18	del 10-22	47	Yes	No	82	38	6	20	37	-
19	del 10-30	30	No	No	52	NA	4	4	20	-
20	dup 14-42	66	Yes	No	65	23	18	60	65	-
21	Exon 19: c.2380+3A>C	29	Yes	No	55	3	2	4	9	25
22	Exon 26: c.3515G>A; p.Trp1172X	30	Yes	No	121	15	6	25	-	-
23	Exon 29: c.3940C>T;p. Arg1314X	38	Yes	No	159	14	-	-	-	-
24	del 45-55	51	Yes	No	185	40	6	-	-	-
25	del 45-49	32	No	No	24	NA	8	18	20	27
26	del 48-49	42	No	No	186	NA	11	-	-	-
27	del 30-44	24	Yes	No	61	7	12	21	-	-
28	del 45-48	49	No	No	60	NA	12	30	25	-
29	del 45-48	48	Yes	No	113	43	15	30	35	49
30	del 45-48	51	Yes	No	36	59	4	13	25	39
31	del 48-49	25	Yes	No	161	78	-	-	-	-
32	Unknown	56	Yes	No	156	56	18	50	-	-
33	del 45-55	63	No	No	124	NA	6	43	63	-

(NA: data not available, hyphen in section: patient has not reached the specific milestone).
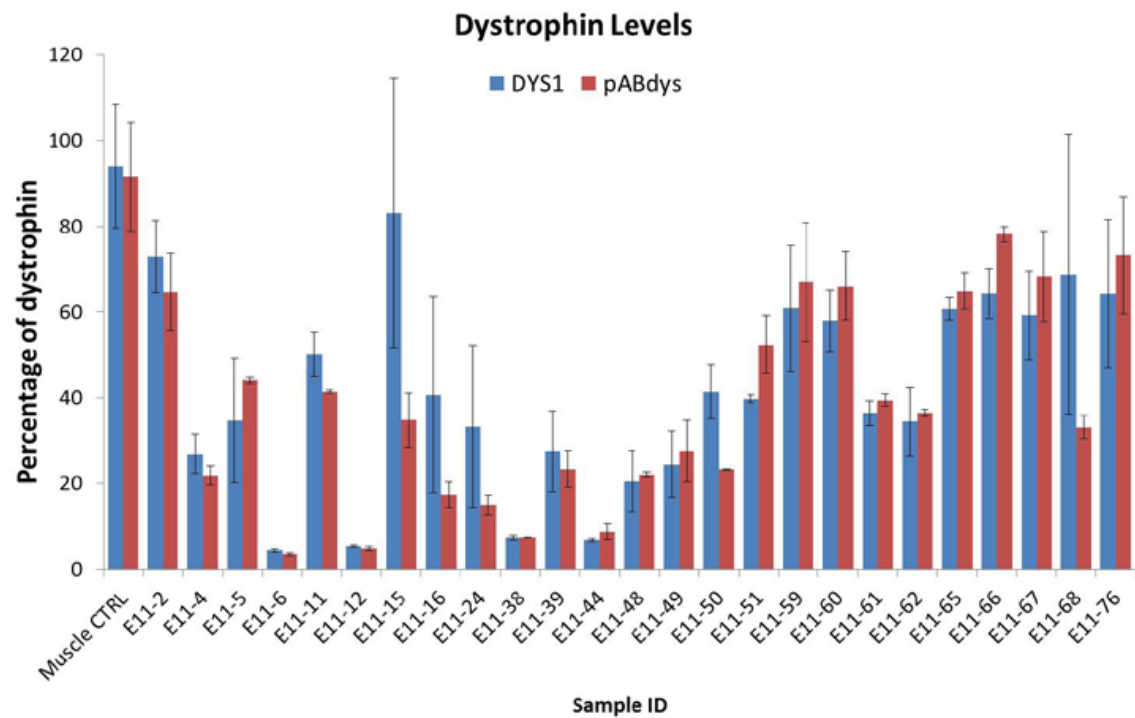
Supplementary Figure 1. Average dystrophin levels assessed by Western blot for BMD patients. Protein was isolated from muscle biopsies and dystrophin levels were quantified by quantitative Western blotting using the Odyssey system setting dystrophin levels observed in healthy muscles to 100% and using alpha-actinin to correct for equal loading. Each sample was measured at least two times with monoclonal (DYS1) and polyclonal (pABdys) antibody. Average dystrophin levels are shown. Error bars show standard deviation.
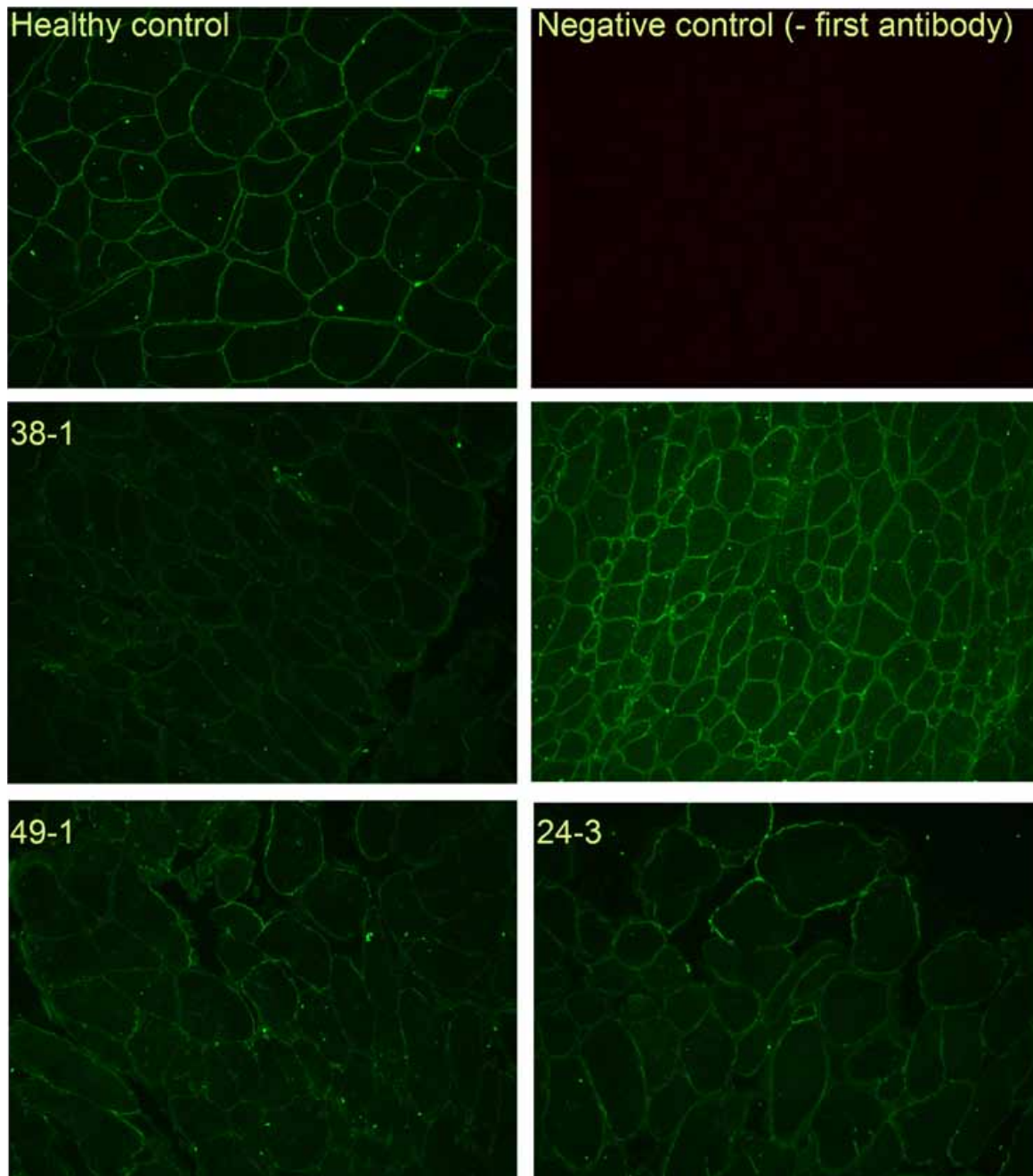
Supplementary Figure 2. Immunofluorescent staining for dystrophin.
Dystrophin staining is continuous and bright for the healthy control (top left panel). Representative images of cross sections from BMD patiens are shown, showing either continuous staining at a lesser intensity (middle panels) or a mosaic pattern (bottom panels).

Chapter 5

T2 relaxation times are increased in skeletal muscle of DMD but not BMD patients

B.H. Wokke, J.C. van den Bergen, M.H. Hooijmans,
A.G. Webb, J.J. Verschuuren, E.H. Niks, H.E. Kan

ABSTRACT

Introduction

Exon-skipping drugs in Duchenne muscular dystrophy (DMD) aim to restore truncated dystrophin expression, which is present in the milder Becker muscular dystrophy (BMD). MRI skeletal muscle T2 relaxation times as a representation of oedema/inflammation could be quantitative outcome parameter for such trials.

Methods

We studied T2 relaxation times, adjusted for muscle fat fraction using Dixon MRI, in lower leg muscles of DMD and BMD patients and healthy controls.

Results

T2 relaxation times correlated significantly with fat fractions in patients only ($p<0.001$). After adjusting for muscle fat, T2 relaxation times were significantly increased in 6 muscles of DMD patients ($p<0.01$), except for the extensor digitorum longus. In BMD, T2 relaxation times were unchanged.

Discussion

T2 relaxation times could be a useful outcome parameter in exon-skipping trials in DMD but are influenced by fat despite fat suppression. This should be accounted for when using quantitative T2 mapping to investigate oedema/inflammation.

INTRODUCTION

Duchenne muscular dystrophy (DMD) and Becker muscular dystrophy (BMD) are X-linked muscle diseases caused by a mutation in the dystrophin encoding *DMD* gene [10]. As a result there is generally no functional dystrophin in DMD patients and shortened, partially functional dystrophin in BMD patients. Initially muscle fibers undergo processes of degeneration and regeneration accompanied by inflammation in the muscle. As the regenerating capacity of the muscle progressively disappears, muscle fibers are increasingly replaced by adipose and fibrotic tissue [38, 54, 113]. However, the exact pathophysiological process underlying the progressive muscle damage is not understood fully [65, 178]. Clinically, both DMD and BMD patients have progressive muscle weakness, predominantly in proximal limbs in early stages of the disease, with more generalized weakness later on. DMD patients become wheelchair-bound in their early teens and die prematurely due to cardiac or respiratory failure, whereas BMD patients have a more variable and usually less severe disease course [136].

Although there is no curative therapy available for DMD, several clinical trials aim to restore expression of truncated dystrophin using antisense oligonucleotide-mediated exon skipping [77, 78, 117]. This would potentially change the DMD patients into a milder phenotype similar to BMD patients. As a result, there is interest in objective and reliable tools to assess outcome measures for patients of different ages and at different disease stages. Quantitative magnetic resonance imaging (MRI) could be such a tool, as it is non-invasive, has good spatial resolution over a large imaging plane, can be applied repetitively, and has shown promise in monitoring disease progression in DMD [103-106, 108, 113, 114, 179, 180]. Inflammation is present in both DMD and to a lesser extent in BMD from early disease stages when muscle damage is less extensive and is considered potentially reversible in contrast with fatty infiltration [17, 181]. As such, assessment of inflammation could be a valuable outcome parameter, especially as therapies would preferably start in young patients who have minimal irreversible structural changes [108].

In MRI, the proton transverse relaxation time (T2) depends on the presence of oedema/inflammation as well as the level of fatty infiltration in muscle. T2 relaxation times in inflamed muscle are longer than relaxation times of normal muscle tissue and the T2 relaxation times in muscles with fatty infiltration are even longer [90, 103, 182]. Therefore, especially in fat infiltrated muscle, it is essential that the fat is taken into account in the analysis, as otherwise it is unknown to what extent longer T2 relaxation times are a result of increased fat fractions or due to oedema/inflammation [183]. Several studies have quantitatively measured the T2 relaxation times in DMD patients and found it to be increased [90, 109, 114]. However, without fat suppression it is unknown to what extent the observed longer T2 relaxation times result from increased

fat fractions or oedema/inflammation [183]. Two recent studies sought to circumvent this problem by applying fat suppression in quantitative T2 images in a subset of their DMD patients [103, 108]. Unfortunately, fat suppression does not always suppress the entire fat signal present in skeletal muscle, and hence the results could still have been influenced by increased fat fractions [183]. Similar MRI studies assessing oedema/inflammation have not been done in BMD patients. To evaluate if the T2 relaxation time could be a possible outcome parameter in clinical trials, a better understanding of how changes in muscle of DMD patients relate to BMD patients is needed. Therefore, the aim of our study was to compare T2 relaxation times in lower leg muscles of DMD and BMD patients and healthy controls, while taking the increased fat levels into account.

METHODS

Subjects

DMD and BMD patients were recruited from the Dutch dystrophinopathy database. The diagnosis of DMD or BMD had been confirmed by genetic testing for mutations in the *DMD* gene or from a muscle biopsy. Healthy age-matched controls were recruited from local schools and from the Leiden University Medical Center Radiology database for healthy controls. The local medical ethics committee approved the study, and informed consent was obtained from all subjects. For participants under age 18, informed consent was obtained from both the subjects and their parents.

MRI

MR images were acquired on a 3T Philips Achieva Scanner (Philips Healthcare, Best, The Netherlands) from the left lower leg using a 14-cm 2-element receive coil with body coil excitation. The receive coil was positioned directly distal to the patella on the anterior and posterior sides of the leg. The scanning protocol consisted of a T1-weighted turbo spin echo (TSE) sequence [25 slices, 5 mm thickness, 0.5 mm gap, repetition time (TR) 600 ms, initial echo time (TE) 16ms, TSE factor 5], a 3-point gradient echo Dixon sequence (25 slices, 5 mm thickness, 0.5 mm gap, TR 400 ms, TE 4.41 ms, echo spacing 0.71 ms, flip angle 8°) and a multi-echo sequence with fat suppression for quantitative T2 mapping [5 slices, 5 mm thickness, 22.5 mm gap, TR 2500 ms, 7 echo times (13, 26, 39, 52, 65, 78 and 91 ms), flip angle 90°, spectral presaturation with inversion recovery (SPAIR) fat suppression] using a mono-exponential fit and maximum likelihood estimation [118, 122]. The total scanning protocol, including positioning of the patients, could be completed in 20 minutes.

Data analysis

T2 values were calculated using a maximum likelihood estimation algorithm supplied by the scanner manufacturer. Regions of interest were drawn using Medical Image Processing, Analysis and Visualization software (www.mipav.cit.nih.gov) on the second, third, and fourth slices of the shortest echo image and superimposed on the calculated T2 maps to obtain the mean T2 values of the following muscles: medial and lateral head of gastrocnemius muscle (GCM and GCL), soleus (SOL), posterior tibialis (TP),
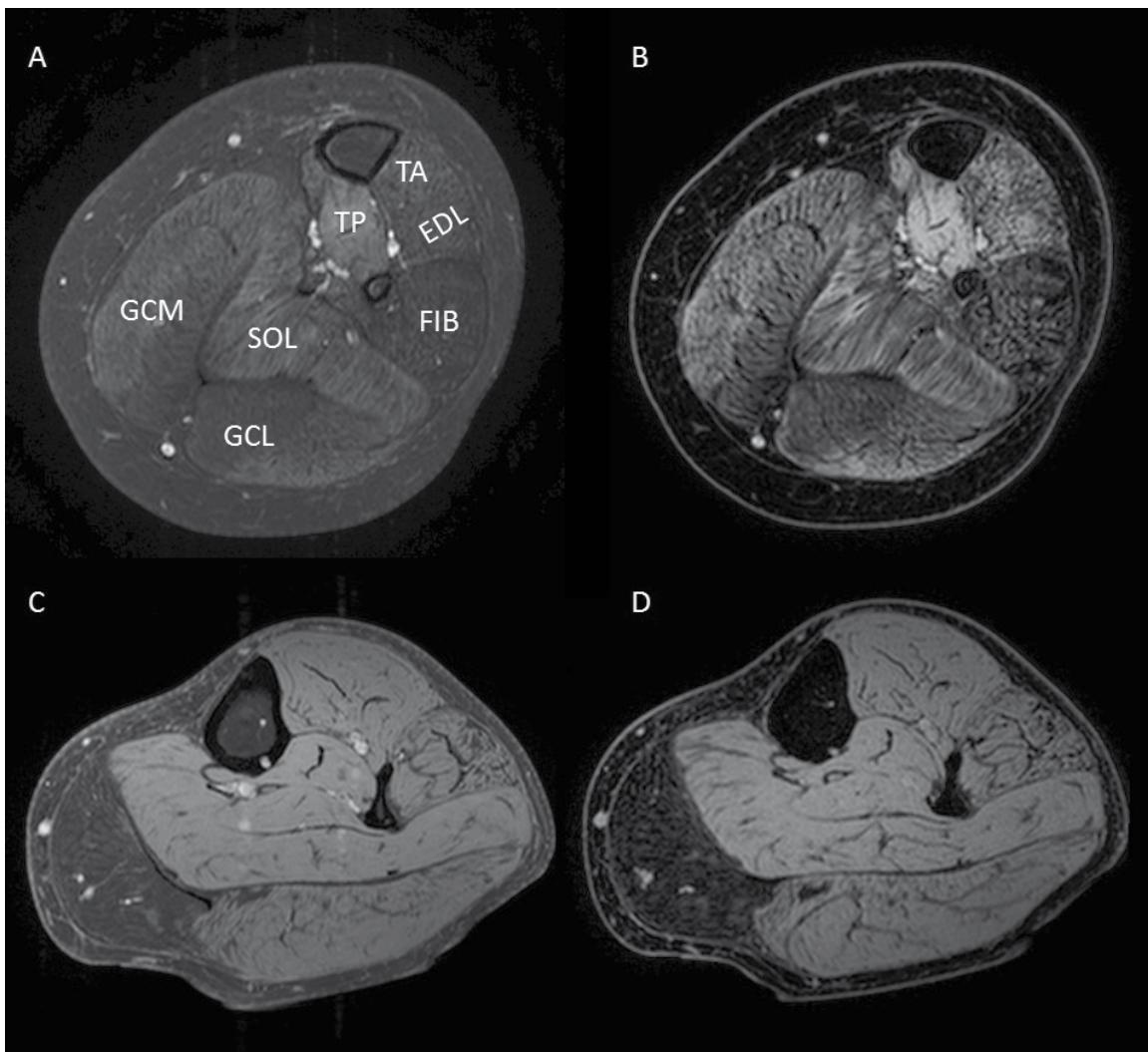
Figure 1. Axial image of lower leg showing the first echo time of the quantitative T2 image of a 12 year-old DMD patient (a), a 63 year-old BMD patient, and (c) a Dixon water image of the DMD patient (b), and the BMD patient (d).

The Dixon image clearly shows diffuse fatty infiltration in virtually all muscles in the DMD patient, whereas in the BMD patient the medial gastrocnemius is most severely affected while the other muscles are still relatively spared.

Muscles shown are medial gastrocnemic muscle (GCM), lateral gastrocnemic muscle (GCL), soleus muscle (SOL) posterior tibialis muscle (TP), anterior tibialis muscle (TA), extensor digitorum longus muscle (EDL) and fibularis muscle (FIB).

fibularis (FIB), anterior tibialis (TA), and extensor digitorum longus (EDL) (Figure 1). Dixon images were co-registered to T1 images, on which regions of interest in every other slice were drawn for the previously mentioned muscles. The middle 11 slices were used to cover the same FOV from which the T2 relaxation times were calculated. Fat and water images were generated using multipeak fitting, and fat fractions were calculated as described previously [143].

Statistical analysis

One-way between-groups analysis of covariance (ANCOVA) was conducted to compare the T2 values in patients and controls. Disease status was used as fixed factor, and fat percentage and age were used as covariates. By including the muscle fat fraction as a covariate the T2 relaxation times adjusted for fat fractions could be calculated and were subsequently incorporated in the analysis. A Bonferroni-Holm model was used to correct for multiple comparisons. A Pearson correlation was performed to test the relationship between fatty infiltration and T2 relaxation time in DMD and BMD patients and in healthy controls. SPSS statistical package Version 20.0 for Windows (SPSS Inc., Chicago, IL) was used for the analysis. The level of significance was set at $p < 0.05$.

RESULTS

Patient characteristics

Nineteen DMD patients (age 10.5 ± 2.7, range 6-14 years), 11 healthy boys (age 10.7 ± 2.1, range 8-15 years), 7 BMD patients (age 39.6 ± 11.7, range 26-63 years), and 8 healthy male adults (age 34.4 ± 12.6, range 24-62 years) participated in the study, and all completed the protocol. Of the DMD patients, 10 were fully ambulant, 2 used a wheelchair intermittently, and 7 were completely wheelchair dependent. All but 3 DMD patients used corticosteroids: an 8-year old boy who was still completely mobile and had never used steroids and 2 13-year old boys who were both wheelchair dependent and had been on steroids for approximately 5 years, but had stopped 1 and 2 years, respectively, prior to this study. Of the BMD group, 2 men (aged 26 and 38) experienced no problems or weakness in their daily activities. Three patients (aged 63, 39, and 31) reported muscle weakness when carrying out daily activities such as climbing stairs, but none required a walking aid. Two patients (aged 37 and 43) were completely wheelchair-dependent. All BMD patients experienced occasional muscle cramps.

Fatty infiltration

To adjust for potential effects of fatty infiltration on the T2 values, the fat fractions for the analysed muscles were calculated using Dixon MRI. The mean fat fraction of all analysed muscles was 20.7±7.0% for DMD patients, 5.6±0.9% for paediatric controls, 15.3±11.8% for BMD patients, and 4.4±0.5% for adult controls. Of the analysed muscles, the GCL had the highest mean fat fraction in DMD patients (28.4%), and the TP had the lowest (8.2%). In the BMD patients, the GCM had the highest mean fat fraction (31.8%), and the TA had the lowest (2.2%).

T2 relaxation times

There was a significant correlation between unadjusted T2 values and fatty infiltration in the DMD and BMD patients (R=0.70, p<0.001), but not for healthy controls (R=1.13, p=0.15) (Figure 2). Uncorrected average T2 relaxation times in DMD patients were 43±2.4 ms, 42±4.2 ms in BMD patients, 36±1.4 ms in paediatric controls, and 38±1.8 ms in adult controls. After adjusting for the fat percentage the average T2 relaxation times were 42.2±2.2 ms in DMD patients, 39.1±3.3 ms in BMD patients, 37.3±1.4 ms in paediatric controls, and 39.8±2.6 ms in adult controls. The adjusted T2 relaxation times were significantly higher in DMD patients compared to controls for the GCM, GCL, SOL, and TP (all p<0.001), TA (p=0.005) and FIB (p=0.002), but not for the EDL (p=0.96) (Figure 3). There were no significant differences between BMD patients and controls after adjusting for the fatty infiltration in any of the investigated muscles (Figure 3).
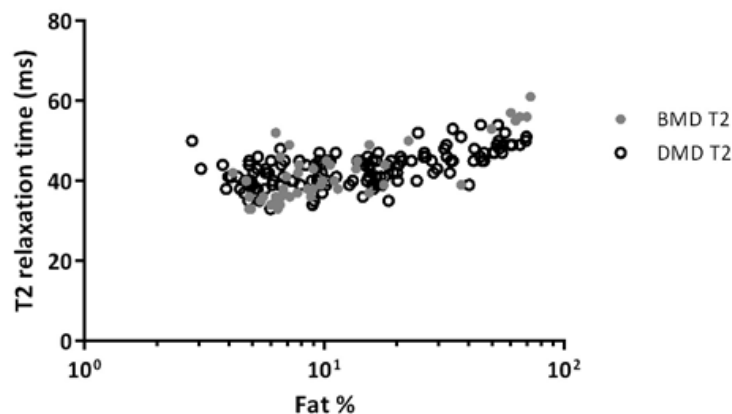
Figure 2. Correlation between fatty infiltration and fat suppressed T2 values in DMD patients (open circles) and BMD patients (grey dots).
Although fat suppression was applied, there remains a significant influence of the fatty infiltration on the T2 values, increasingly towards the higher fat fractions.
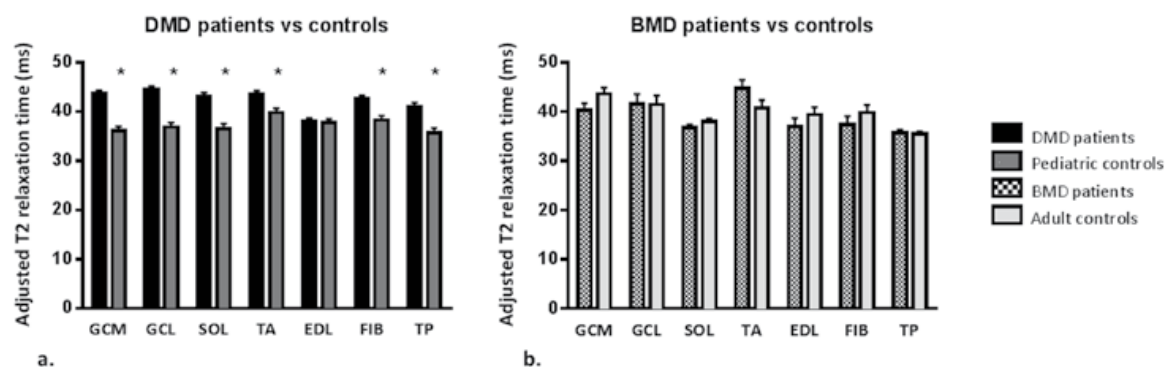
Figure 3. Mean adjusted T2 relaxation times ±SD of DMD patients (black) versus controls (dark grey) (a) and BMD patients (checked) versus controls (light grey) (b) of the investigated muscles [medial and lateral heads of gastrocnemius (GCM, GCL), soleus (SOL), anterior tibialis (TA), extensor digitorum longus (EDL), fibularis (FIB) and posterior tibialis (TP)). Muscles with significantly different T2 values are shown with an asterisk (*).

DISCUSSION

In this study we show that in DMD patients the T2 relaxation times, with adjustment for the increased fat percentage, are significantly increased compared to healthy boys in all analysed muscles except the extensor digitorum longus. In contrast, BMD patients did not show significant increases in adjusted T2 values compared to healthy controls. This suggests that the T2 relaxation time could be a useful outcome parameter in DMD trials that aim to restore truncated dystrophin expression, which is typically expressed in BMD patients.

Increased T2 relaxation times in skeletal muscle can originate from a number of factors, including inflammation, necrosis, or moderate-severe exercise [183]. The T2 relaxation time has also been shown to increase with age [184]. In muscle tissue of DMD and BMD patients mononuclear cell infiltrates predominantly consist of T-lymphocytes and macrophages [54-56, 181, 185]. Several mechanisms have been hypothesized to contribute to the inflammation. It has been suggested that inflammation is a non-specific event, which could be triggered by surrounding necrotic muscle fibers [55, 59]. Activation of an immune response via toll-like receptors triggered by myofiber damage before more structural changes are present is believed to be another explanation [55, 62]. A specific cellular autoimmune response to an unknown antigen has also been suggested [61]. The various components involved in the inflammatory response are thought to contribute directly to some of the muscle damage [56, 62, 63, 185, 186]. In addition to the potential effects of inflammation, a recent sodium MR study demonstrated oedema-like changes in muscle of DMD patients and suggested that increased intracellular sodium might also play a direct role in the pathogenesis of

progressive muscle degeneration[187]. These mechanisms could all contribute to an increase in the T2 relaxation time, as observed in our DMD patients

In contrast to DMD patients, there are no specific anatomical pathology studies describing to what extent inflammatory processes contribute to muscle degeneration in BMD patients. As BMD patients have some, albeit not full-length, dystrophin it could be that the mechanism(s) causing inflammation are less prominent compared to DMD patients. This is supported by the observation that inflammation is less in muscle biopsies of BMD patients than in DMD patients [17, 181]. This could explain why no significant increase in adjusted T2 relaxation time was seen in our BMD patients.

While several studies have quantitatively measured the T2 relaxation times in DMD patients and found it to be increased [90, 109, 114], only two recent studies described increased T2 relaxation times in lower leg muscles of DMD patients using fat suppression[103, 108]. Our results show that even though fat is suppressed using SPAIR, the T2 values and level of fatty infiltration were correlated in many of the investigated muscles. Therefore, an influence of the lipid signal on the T2 values in previous studies cannot be ruled out. Recently, it was shown that suppressing fat with just SPAIR aimed at the aliphatic fat region around 2.6 parts per million is not sufficient to eliminate the entire fat signal[188]. This could be solved by using additional methods to suppress the olefinic fat signal [188, 189]. Alternatively, applying proton MR spectroscopy and separately assessing the T2 relaxation time of water and fat can circumvent this problem. However, this will only yield results over a small volume of interest and is too time consuming to perform for a large number of muscles. Thirdly, a chemical shift method can be employed in which water and fat images are obtained at multiple echo times, but unfortunately this sequence is not currently available on all commercial MR scanners [190]. Finally, water and fat can be separated in post-processing, as proposed by several authors [145, 183, 191-193], or by adjusting for the fat by statistical analysis, as we have done here.

Several previous studies have suggested the use of the fatty infiltration in DMD patients as a measure of disease progression and potential outcome parameter [103, 104, 106, 194]. In the dystrophic process, oedema/inflammation is thought to occur prior to fatty infiltration and could therefore be used as an earlier marker of therapy effectiveness compared to changes in levels of fatty infiltration. In addition, it is questionable if severely fatty infiltrated muscles can still be rescued, and as such fatty infiltration in these patients might be irreversible. Alternatively oedema/inflammation is potentially more likely to be reversible and could therefore be of value as an outcome parameter in assessment of future therapies, especially in early disease stages when effect of the lipid signal on the T2 relaxation times is minimal.

Recently it has been suggested that T2 relaxation times in DMD patients are reduced as a function of age [115, 195, 196]. However there remains some discussion as to these

findings, since some authors report a decrease and others report an increase [103, 108]. The cause for this potential decrease is still uncertain and could be due to technical reasons or pathophysiology, i.e. a decrease in oedema or an increase in fibrosis. So far the available data imply that if the T2 relaxation times decrease, they do not normalize to the levels of healthy controls, and they have only been described for older DMD patients. Therefore, even if such an effect were to be present, the T2 relaxation time remains a potential valuable parameter in the follow-up of younger patients.

This study has some limitations; firstly, the group of BMD patients participating in the study was relatively small. However, as we obtained data from several muscles ranging from patients with very few clinical symptoms to wheelchair-dependent patients we felt that our findings are likely to be representative of the whole spectrum of the disease. Secondly, 3 of our DMD patients did not use corticosteroids. Although a previous study showed no significant effect on the T2 relaxation time in DMD patients before and after steroid treatment, a recent report suggested that corticosteroids do in fact result in a decrease of the T2 relaxation time [114, 197]. However, a reduction of the T2 relaxation time as an effect of steroids would decrease possible differences between patients and controls. As the number of steroid-free patients in our cohort was very small, it is unlikely that the patients not on steroids represented the sole contribution to the significant difference between patients and controls. Thirdly, a TR of 2500ms was used to avoid very long acquisition times, which result in partial saturation effects due to the long T1 of water. Finally, we only assessed the lower leg in our study, as the B1 field in this region is much more homogeneous compared to the upper leg. However, the upper legs are known to be involved earlier in both DMD and BMD patients. For future studies it would be valuable to compare proximal muscles in either the leg or arm of both DMD and BMD patients.

In conclusion, we show that skeletal muscle T2 relaxation times are significantly increased in DMD patients, which is indicative of the presence of inflammation/oedema. We also show no such increase is present in the generally less severely affected BMD patients. Therefore we believe that quantitative T2 mapping, while taking the lipid signal into account can be a useful method for evaluation of oedema/inflammation of DMD patients and could be an outcome parameter in treatment trials aiming to ameliorate DMD to a BMD phenotype.

Chapter

6

Muscle spectroscopy detects elevated PDE/ATP ratios prior to fatty infiltration in Becker muscular dystrophy patients

B.H. Wokke, M.H. Hooijmans, J.C. van den Bergen,
A.G. Webb, J.J. Verschuuren, H.E. Kan

ABSTRACT

Becker muscular dystrophy is characterized by progressive muscle weakness. Muscles show structural changes (fatty infiltration, fibrosis) and metabolic changes, both of which can be assessed using MRI and MRS. It is unknown at what stage of the disease process metabolic changes arise and how this might vary for different metabolites. In this study we assessed metabolic changes in skeletal muscles of Becker patients, both with and without fatty infiltration, quantified via Dixon MRI and ^{31}P MRS. MRI and ^{31}P MRS scans were obtained from twenty-five Becker patients and fourteen healthy controls using a 7T MR scanner. Five lower leg muscles were individually assessed for fat and muscle metabolite levels. In the peroneus, soleus and anterior tibialis muscles with non-increased fat levels PDE/ATP ratios were higher (p<0.02) compared to controls, whereas in all muscles with increased fat levels PDE/ATP ratios were higher compared to healthy controls (p≤0.05). The Pi/ATP ratio in the peroneus muscles was higher in muscles with increased fat fractions (p=0.005) and the PCr/ATP ratio was lower in the anterior tibialis muscles with increased fat fractions (p=0.005). There were no other significant changes in metabolites, but an increase in tissue pH was found in all muscles of the total group of BMD patients in comparison with healthy controls (p<0.05). These findings suggest that ^{31}P MRS can be used to detect early changes in individual muscles of Becker muscular dystrophy patients, which are present before the onset of fatty infiltration.

INTRODUCTION

Becker muscular dystrophy (BMD) is an X-linked disease caused by mutations in the *DMD* gene, which codes for the dystrophin protein, an important factor for muscle membrane stability [10]. In BMD patients the dystrophin protein is only partially functional, resulting in continuous muscle fiber damage. There is inflammation and oedema in the muscle and eventually the muscle cells' regenerative capacity becomes exhausted and muscle tissue is replaced by adipose and fibrotic tissue [38, 54]. The main feature of the disease is progressive muscle weakness with a limb-girdle distribution, but symptoms can be highly variable in age of onset, severity of symptoms and rate of progression [159, 160]. The underlying mechanisms causing the variability are not fully understood and are thought to include factors like the regenerative capacity of the muscle, quantity of the remaining dystrophin protein and the specific mutation [154-157, 198].

Skeletal muscles of BMD patients show a distinct pattern of fatty infiltration, which can be assessed with magnetic resonance imaging (MRI) [199]. With the progression of the disease the amount of adipose tissue in the muscle increases, and muscles of clinically asymptomatic patients can already show fatty infiltration in some muscles, while others still appear to be normal [199]. In addition to these structural changes in the muscle, several phosphorus MR spectroscopy (^{31}P-MRS) studies have reported changes in BMD patients suggestive of an altered energy metabolism [92, 95, 200, 201]. However, the results of these studies have been inconsistent; both unchanged and decreased phosphocreatine (PCr) to adenosine triphosphate (ATP) ratios, increased, unchanged and decreased inorganic phosphate (Pi)/ATP ratios and an unchanged and increased intracellular pH and possibly increased phosphodiesters (PDE)/ATP ratios have been reported [92, 94, 95, 200, 201]. Mitochondrial function is believed to be normal in these patients and it has been suggested that there is reduced glycolytic activity in the skeletal muscles [95, 200]. While structural changes like fatty infiltration and fibrosis are predominantly present in muscles that are in a more advanced stage of the dystrophic process, metabolic changes are thought to occur earlier [202]. However, it is unknown if and how metabolic changes contribute to the muscle degeneration and to what extend these changes are present before the occurrence of fatty infiltration. Previous studies in BMD patients have focused on the more severely affected gastrocnemic muscles using surface coil localization only, without the combination of imaging data and patients with variable disease severity. Therefore it is unknown if the reported changes in phosphorous metabolism in BMD patients are already present in muscles without fatty infiltration, i.e. a less advanced stage of the disease before signs of the dystrophic process are visible with MRI. Since metabolic processes are more likely to be reversible than structural changes like fatty infiltration they could

be valuable as an early marker to evaluate disease progression and possibly effects of future therapeutic interventions [110, 203-205].

In this study, we used high magnetic field quantitative MRI and MRS in BMD patients and healthy controls to assess phosphorous metabolism in five individual lower leg muscles, and correlated the findings to the level of fatty infiltration obtained from the same muscles to assess if metabolic changes vary in different stages of the dystrophic process.

MATERIALS AND METHODS

Subjects

All patients were recruited from the Dutch Dystrophinopathy Database. Controls were recruited from the Leiden University Medical Center Radiology database for healthy controls. The diagnosis BMD was confirmed by a mutation in the *DMD* gene or reduced dystrophin expression in a muscle biopsy. BMD patients were classified into four groups according to their clinical functioning: no motor symptoms, mildly affected (patients with difficulty walking and/or difficulty climbing stairs, but not using a walking aid), moderately affected (patients using a walking aid: stick, frame or intermittent wheelchair use), and severely affected patients (completely wheelchair dependent).

The local medical ethics committee approved the study and all study participants gave written informed consent.

MR examination

Data were acquired on a 7T Philips Achieva MRI (Philips Healthcare, The Netherlands). A custom-built volume birdcage coil (diameter 17.5 cm, length 12 cm) tuned for both proton (^{1}H) imaging (higher order mode) and phosphorous (^{31}P) spectroscopy (homogeneous quadrature mode) was positioned around the left lower leg directly distal of the patella [206]. Patients were positioned in supine position, feet first, in the scanner. The imaging protocol consisted of an anatomical gradient echo sequence (15 slices; slice thickness 7mm; interslice gap 0.5 mm; repetition time (TR) 10 ms; echo time (TE) 3.0 ms; flip angle (FA) 30°; FOV 180x200 mm) a three-point gradient echo Dixon sequence (12 slices; slice thickness 10 mm; interslice gap 0.5 mm; TR/TE/ΔTE 300/2.4/0.33 ms; FA 30°; FOV 180x204 mm) and a B0 map (14 slices; slice thickness 8 mm, no slice gap; TR/TE 30/3.11ms; FA 20°; FOV 160x180 mm). A 2D phosphorous MRS chemical shift imaging (CSI) dataset was acquired based on the T1-weighted images (FOV 160x200 mm; matrix size 8 x 10; TR 2000 ms; samples 2048; voxel size 20x20 mm; FA 45°; Hamming weighted acquisition with 14 signal averages at

the central k-lines, voxel size after hamming weighing 3.42x3.42 x12 cm^3). Second order shimming was performed using an image based shimming routine [207]. As the diameter of the lower leg and the boundaries between the different muscle groups change along the length of the leg, the 2D-CSI sequence was planned in such a way that within the volume of the coil a specific voxel was located within one individual lower leg muscle (Figure 1). The total scan duration was approximately 50 minutes. For quality control of the 7T Dixon data the 7T values were compared to Dixon MRI data acquired from the same patients on a 3T Philips Achieva scanner in a subgroup of 9 patients previously described by Van den Bergen et al. [198]. Data of these patients was obtained on the same day, from the same leg using a 14-cm diameter two-element coil with body coil excitation position directly distal of the patella.
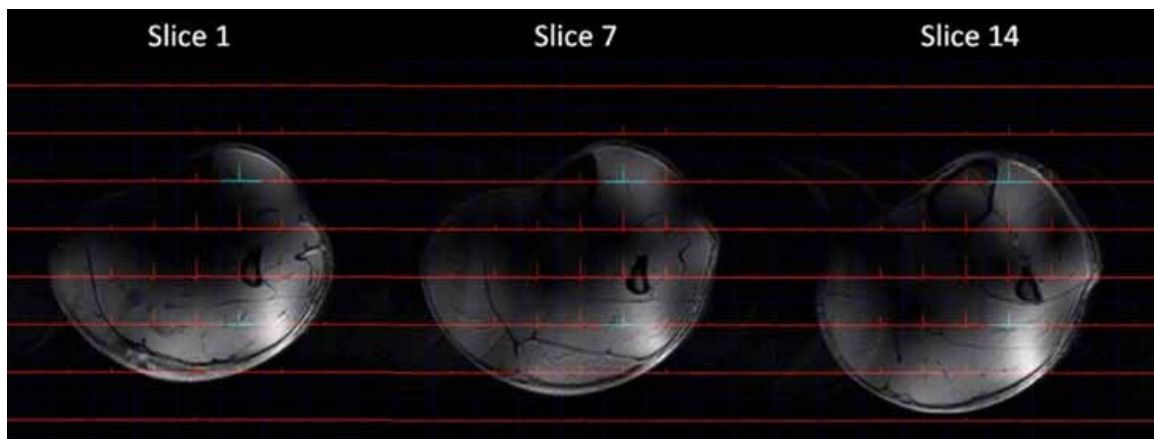
Figure 1. Example of the planning of the ^{31}P 2D-CSI dataset superimposed on an axial T1 weighted image.
The spectroscopy grid was positioned so that specific voxel was located within one individual lower leg muscle over the entire length of the coil: in the first (a.), middle (b.) and last slice (c.) of the T1-weighted image the voxel in the tibialis anterior muscle as well as the voxel in the soleus muscle lies within the same muscle over the length of the coil.

Data analysis

^{31}P Data sets were visualized using the 3D Chemical Shift Imaging package (3DiCSI) and spectra were identified in the tibialis anterior (TA), peronei (PER), soleus (SOL), lateral head of the gastrocnemius (GCL) and medial head of the gastrocnemius (GCM) muscles using a grid overlay on the T1-weighted image (Figure 2). Voxels were carefully positioned to avoid overlap with adjoining muscles.

The free induction decays were exported and fitted using AMARES in jMRUI software package (version 4, http://sermn02.uab.es/mrui). In some patients high amounts of fatty infiltration within the muscle resulted in a low signal-to-noise in the phosphorous spectra due to the very low amount of muscle tissue in the voxel. Consequently only
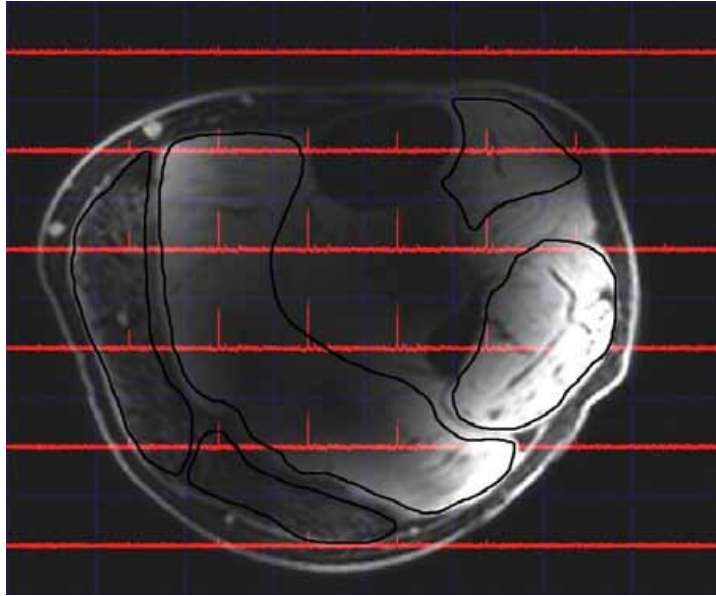
Figure 2. Grid overlay on an axial Dixon water-image of the lower leg of a BMD patient.
Spectra were analysed in the anterior tibialis, peroneus, soleus and medial and lateral head of the gastrocnemic muscle for which the ROIs are drawn on the image. Voxels of the CSI-grid were carefully positioned to avoid overlap with adjoining muscles. Note that the coil used for this image is a single tuned birdcage coil, with the primary homogeneous mode being at the phosphorus frequency and a higher mode at the proton frequency, resulting in a loss of sensitivity in the center of the coil for proton, but not for phosphorous.

the muscles with an acceptable quality spectrum (i.e. SNR greater than 10 for the PCr peak in combination with the ability to identify all other metabolite signals and with percentage Cramér-Rao Lower Bound (CRLB) values for all fitted metabolites below 20%) were included in the analysis. Signals of Pi, PDE, PCr and γ-, α- and β-ATP were fitted with Gaussian line shapes (Figure 3). For the PDE and β-ATP peak prior knowledge on the line width was used. The line width for PDE was set at 1.3* the line width of PCr and the β-ATP line width was set at 1.6* the line width of α-ATP, this prior knowledge was based on the mean line widths of 10 patients with high SNR. Metabolite ratios were obtained from Pi, PDE and PCr relative to the γ- ATP signal and corrected for ^1H relaxation effects measured in human calf muscle at 7T assuming the same relaxation parameters for all muscles [208]. Intracellular tissue pH was calculated from the shift in resonance position (S) of the Pi peak compared to PCr: pH=6.75 + log ((3.27-S)/(S-5.69)) [209].

Quantitative fat fractions of the muscles were calculated from the Dixon MR images using Medical Image Processing, Analysis and Visualization (MIPAV) software (http:// mipav.cit.nih.gov). Regions of interest (ROIs) were drawn on all slices, on the same muscles as used for the spectroscopy analysis. Fat fractions were calculated as signal intensity (SI) fat/ (SI fat+ SI water))*100. 3T values were corrected for relaxation effects as described before [143]. For the comparison of 3T and 7T data, fat fractions

obtained from the TA, PER, SOL, GCL and GCM muscles from a similar number of slices from both scanners were compared on a muscle-by-muscle basis.

All individual muscles of the Becker patients were classified into two groups according to the level of fatty infiltration compared to healthy controls; BMD with non-increased fat levels (NIFL)), and BMD with increased levels of fatty infiltration (IFL). Cut-off values were calculated for the five individual lower leg muscles using mean+2 standard deviations (SD) of the fat fraction of the corresponding lower leg muscle of healthy controls.
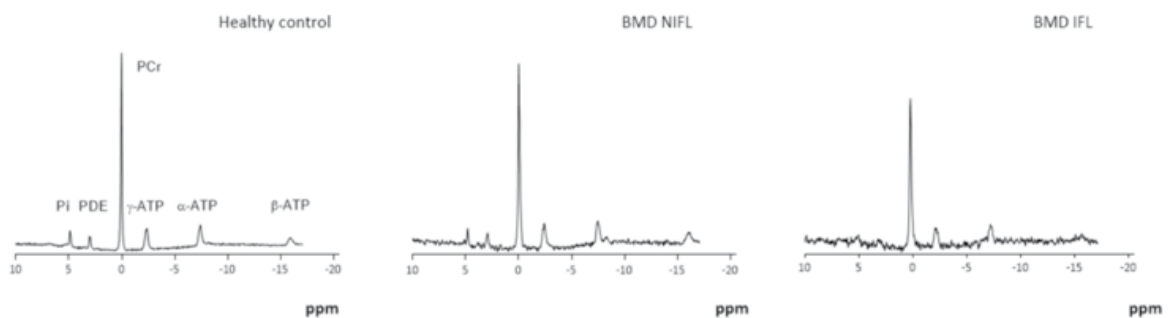
Figure 3. Representative phosphorous 7T spectra of the peroneus muscle in a healthy control, BMD patient with non-increased fat fractions (BMD NIFL) and BMD patient with increased fat fractions (BMD IFL).

Spectra are scaled to the ATP levels. The signal to noise ratio of the 31P signal clearly decreases in the BMD patient with increased fat levels. Peak assignments Pi = inorganic phosphate, PDE = phosphodiester, PCr = phosphocreatine, γ-, α- and β-ATP = three resonances of adenosine triphosphate.

Statistics

For the comparison of the metabolite ratios Pi/ATP, PCr/ATP, PDE/ATP, Pi/PCr and pH between the groups for the five lower leg muscles two general linear models were used, one for the comparison of healthy controls with the whole group of BMD patients and one for the comparison of healthy controls with the NIFL BMD and IFL BMD groups. Age was entered as a covariate and disease as a fixed factor. A Fischer LSD model was used to correct for multiple comparisons. Pearson correlation was used for the comparison of the Dixon scan data acquired at 3T and 7T to explore the relation between fat fractions and the PDE/ATP ratio in both healthy controls and BMD patients. The level of significance was set at $P \leq 0.05$. Statistical analysis was performed using SPSS version 20 for Windows (SPSS Inc., Chicago).

Chapter 6

RESULTS

Patient characteristics

Twenty-five male BMD patients (age 39.6 ± 13 years, range 20-66, BMI 25.04 ± 3.65, range 20-33) and fourteen age-matched healthy male controls (age 35.7 ± 15 years, range 22-65, BMI 22.64 ± 3.37 range: 20-32.4) participated in the study. All subjects completed the scanning protocol. Of the 25 BMD patients five patients had no motor symptoms, eleven were mildly affected, seven moderately affected and two severely affected (Table 1). Four of the patients with no motor symptoms showed normal fat levels on Dixon MRI and one patient with no motor symptoms showed a slightly increased fat fraction in the GCM and GCL. The GCM and GCL showed increased fat levels in all moderately affected patients and fat fractions were increased in all investigated muscles of severely affected patients (Table 1).

Fatty infiltration

The mean fat level in healthy controls was 2.9 ± 1.1% and in patients 16.0 ± 18.6%. Overall the GCM showed the highest mean fat fractions and the SOL the lowest. Muscles with fat fractions lower than the mean fat fraction plus 2 SD in the corresponding muscle of healthy controls were defined as muscles with no significant increase in fatty infiltration and classified in the non-increased fat levels (NIFL) group. The other muscles were classified in the group with increased levels of fatty infiltration (IFL), as compared to healthy controls (Table 1). The fat fractions calculated from five muscles of nine BMD patients acquired at 3T and 7T showed a high correlation (R=0.97).

^{31}P data

All metabolite ratios of the healthy controls and BMD patients are shown in Table 2. For the analysed muscles the NIFL/IFL subgroups were divided as follows; GCL NIFL n=5/IFL n=13 (cut-off fat fraction 3.4%), GCM NIFL n=5/IFL n=9 (cut-off 4.5%), PER NIFL n=10/IFL n=15 (cut-off 6.8%), SOL NIFL n=10/IFL n=15 (cut-off 4.9%), TA NIFL n=18/IFL n=7 (cut-off 8.1%). Due to the high number of patients with increased fat levels in the GCL and GCM muscles, the number of included spectra in the NIFL was lower compared to the other muscles. In addition, for the GCM muscle 11 spectra and seven spectra for the GCL muscle did not meet our quality control criteria and therefore were not included in the analysis. In healthy controls all the acquired spectra were included in the analysis.

For the whole group of BMD patients PDE/ATP ratios were significantly increased compared to healthy controls in all five lower leg muscles. In the NIFL BMD group PDE/ATP ratios were significantly increased compared to healthy controls in the PER, SOL and TA muscles, except for a trend in the GCL (p=0.071) and no significant change

Table 1. Patient parameters.

Patient	Age (years)	Mutation	Age of first symptoms	Disability	Non-increased fat levels muscles
1	56	Unknown*	35	Mild	PER, TA
2	48	Del45-48	14	Moderate	None
3	49	Del45-48	10	Moderate	None
4	29	Exon 19 c.2380+3A>C **	4	Severe	None
5	51	Del45-55	6	Mild	PER, SOL, TA
6	63	Del45-55	40	Mild	TA
7	30	p1172X	4	Mild	TA
8	26	Del45-47	9	No motor symptoms	GCL, GCM, PER, SOL, TA
9	38	Exon 29 p.Arg131>X ***	None	No motor symptoms	GCL, GCM, PER, SOL, TA
10	24	Del30-44	12	Mild	TA
11	63	Del45-47	10	Severe	None
12	33	Del03-05	None	Mild	TA
13	66	Dup14-42	6	Moderate	None
14	39	Del45-47	6	Mild	None
15	37	Del45-47	3	Moderate	SOL, TA
16	20	Del45-47	None	No motor symptoms	GCL, GCM, PER, SOL, TA
17	29	Del45-47	12	Mild	PER, TA
18	39	Del45-47	15	Mild	TA
19	31	Del03-04	18	Moderate	PER, SOL, TA
20	25	Del48-49	Floppy infant	No motor symptoms	GCL, GCM, PER, SOL, TA
21	37	Del03-04	3	Moderate	TA
22	33	Del45-47	3	Mild	GCL, SOL, TA
23	42	Del48-49	6	No motor symptoms	PER, SOL, TA
24	43	Del45-47	4	Moderate	None
25	31	Del45-47	2	Mild	GCL, GCM, PER, SOL, TA

Disability is scored as no motor symptoms, mild (difficulty walking without the use of walking aid), moderate (use of walking aid) or severe (wheelchair dependent). The muscles with non-increased fat fractions as compared to healthy controls are shown for each patient (medial and lateral head of gastrocnemic muscle (GCL and GCM), soleus (SOL), peroneus (PER) and anterior tibialis (TA)).(*No mutation could be found, patient had been found to have 62% dystrophin. **As a result of this mutation a large part of exon 19 is skipped. ***As a result of this mutation exon 29 is skipped)

in the GCM (p=0.404) (Figure 4). The IFL BMD subgroup showed significantly increased PDE/ATP ratios compared to healthy controls in all lower leg muscles. Values of Pi/ATP, Pi/PCr and PCr/ATP showed no significant differences between the whole group of BMD patients and healthy controls, except for an increase in the Pi/ATP ratio in the PER muscle of BMD patients.

|	Controls	BMD total	BMD NIFL	BMD IFL
GCL	n=14	n=18	n=5	n=13
Pi/ATP	0.34±0.02	0.40±0.02	0.37±0.04	0.41±0.03
Pi/PCR	0.10±0.01	0.10±0.01	0.09±0.016	0.11±0.01
PDE/ATP	0.19±0.03	0.34±0.03* (p=0.001)	0.288±0.051	0.36±0.03* (p=0.001)
PCr/ATP	3.59±0.12	3.54±0.11	3.842±0.204	3.4±0.13
pH	7.02±0.01	7.05±0.01*(p=0.017)	7.05±0.014	7.06±0.01*(p=0.017)
GCM	n=14	n=14	n=5	n=9
Pi/ATP	0.38±0.03	0.44±0.03	0.42±0.04	0.45±0.03
Pi/PCR	0.10±0.05	0.18±0.05	0.11±0.08	0.22±0.06
PDE/ATP	0.25±0.04	0.34±0.04*(p=0.046)	0.27±0.06	0.38±0.05*(p=0.036)
PCr/ATP	3.82±0.16	3.77±0.16	3.81±0.27	3.76±0.20
pH	7.02±0.01	7.05±0.01*(p=0.025)	7.04±0.01	7.05±0.01*(p=0.033)
PER	n=14	n=25	n=10	n=15
Pi/ATP	0.32±0.03	0.40±0.02*(p=0.016)	0.36±0.03	0.43±0.03*(p=0.005)
Pi/PCR	0.09±0.01	0.11±0.006	0.11±0.01	0.12±0.01*(p=0.035)
PDE/ATP	0.16±0.03	0.33±0.02*(p<0.001)	0.30±0.032*(p=0.003)	0.35±0.03*(p<0.001)
PCr/ATP	3.48±0.1	3.61±0.07	3.53±0.11	3.66±0.09
pH	7.01±0.01	7.02±0.01*(p=0.047)	7.02±0.01	7.02±0.01
SOL	n=14	n=25	n=10	n=15
Pi/ATP	0.38±0.02	0.40±0.02	0.40±0.03	0.40±0.024
Pi/PCR	0.11±0.01	0.12±0.01	0.13±0.011	0.11±0.01
PDE/ATP	0.21±0.03	0.34±0.02*(p=0.003)	0.33±0.04*(p=0.017)	0.34±0.03*(p=0.006)
PCr/ATP	3.57±0.11	3.65±0.08	3.52±0.13	3.73±0.10
pH	7.02±0.01	7.04±0.004*(p=0.006)	7.04±0.01	7.04±0.01*(p=0.006)
TA	n=14	n=25	n=18	n=7
Pi/ATP	0.35±0.03	0.37±0.02	0.40±0.02	0.29±0.036
Pi/PCR	0.10±0.01	0.10±0.01	0.11±0.01	0.09±0.01
PDE/ATP	0.17±0.04	0.30±0.03*(p=0.01)	0.30±0.03*(p=0.019)	0.30±0.05* (p=0.05)
PCr/ATP	3.66±0.12	3.53±0.1	3.71±0.102	3.06±0.16(p=0.005)
pH	7.00±0.01	7.02±0.01*(p=0.039)	7.01±0.01	7.02±0.01

Table 2. Mean values ±SD for the different metabolites in healthy controls, the overall BMD group, BMD patients with non-increased fat levels (NIFL) and BMD patients with increased fat levels (IFL). Significant differences between patients and controls are marked with an asterisk (*) and for these p values are shown. (Pi = inorganic phosphate, PDE = phosphodiester, PCr = phosphocreatine, ATP=adenosine triphosphate. GCL/GCM= lateral and medial head gastrocnemius, PER= peroneus, SOL=soleus, TA=anterior tibialis).
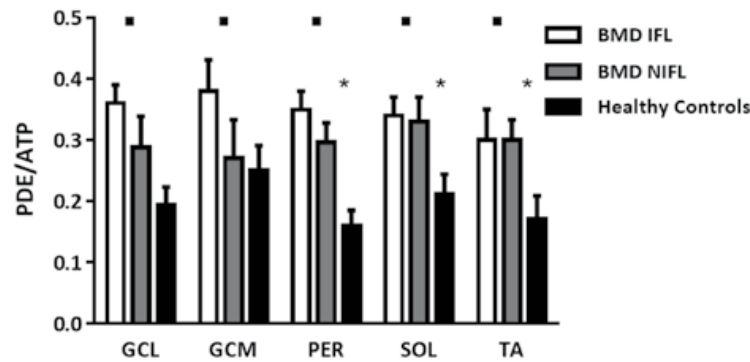
Figure 4. Mean phosphodiester (PDE) in medial and lateral gastrocnemic muscle (GCL and GCM), peroneus (PER), soleus and anterior tibialis (TA) in healthy controls (black), BMD patients with non-increased fat levels (NIFL) (white) and BMD patients with increased fat levels (IFL) (grey).
Ratios significantly higher in BMD NIFL compared to controls are shown with an asterix (*) and significantly higher in BMD IFL compared to control with a square (•). P values are as follows: for the NIFL BMD group (GCL p= 0.071, GCM p= 0.404, PER p= 0.003, SOL p=0.017 and TA p=0.019) and in the IFL BMD group (GCL p=0.001, GCM p=0.036, PER p<0.001, SOL p=0.006 and TA p=0.05).

In the NIFL BMD group no significant differences were found for any of these metabolites (Table 2). Therefore, the increase in Pi/ATP ratio in the PER of the overall BMD group is due to the IFL BMD group in which significant increases in the Pi/ATP (p=0.005) and Pi/PCr (p=0.035) were found for the PER. There was a significant increase in tissue pH in the GCM, GCL and SOL muscle in the IFL group, as well as in all muscles of the whole BMD group. Additionally there was a significant correlation between the fat fraction and PDE/ATP ratio in the BMD patients (R=0.20, p=0.04), but not in healthy controls (R=-0.02, p=0.9) (Figure 5).
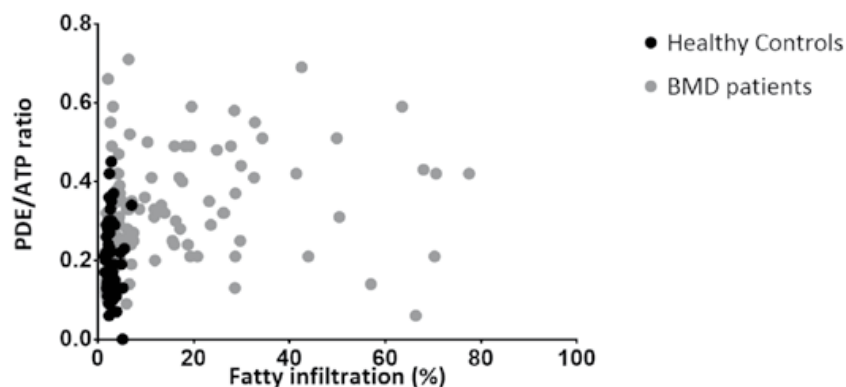
Figure 5. Correlation between PDE/ATP ratios and fatty infiltration in BMD patients (grey dots) and healthy controls (black dots).
For BMD patients there is a low, but significant correlation (R=0.20, p=0.04), however in the higher fat fractions PDE/ATP ratios show great variability.

DISCUSSION

In this study we used a combination of quantitative proton MRI and localized ^{31}P MR spectroscopy to evaluate high-energy phosphate levels in five lower leg muscles of BMD patients. In BMD patients the SOL, PER and TA with non-increased fat fractions and all muscles with increased fat fractions showed increased PDE/ATP ratios. This suggests that ^{31}P MRS can be used to detect changes muscles of BMD patients before the onset of potentially irreversible changes like fatty infiltration.

The PDE signal in the MR spectrum is derived from glycerol 3-phosphocholine (GPC) and glycerol 3-phosphoethanolamine (GPE) which are thought to be membrane phospholipids breakdown products [210, 211]. Slow-twitch, oxidative type 1 fibers have been shown to have higher PDE/ATP ratios and PDE has also been shown to increase with age [212, 213]. In addition, GPCs have been suggested to have some regulatory effects [214-217]. In muscular dystrophies increased PDE/ATP ratios have been found in Golden Retriever muscular dystrophy (GRMD) dogs, in Duchenne muscular dystrophy (DMD) patients, and in moderately affected BMD patients [95, 96, 112, 201, 218]. Our results are in agreement with these studies, although we did not find an increase in PDE/ATP ratio in the GCM and a trend in the GCL muscle. However, as we only had five data points in the NIFL group in these muscles, this could have resulted from a failure to reach statistical significance for these muscles. On the other hand, the SOL, PER and TA have a higher percentage of type 1 muscle fibers, and it could be that they are in some way affected differently by the ongoing membrane damage [210, 219]. As dysfunctional or absent dystrophin results in muscle membrane instability the elevated PDE/ATP ratios may also directly reflect membrane damage [220]. This is supported by the fact that in facioscapular muscular dystrophy (FSHD), a muscular dystrophy with no primary membrane damage, increased PDE/ATP ratios were only found in patients with increased fat levels [221]. However, the finding that in DMD patients fast, glycolytic type 2 fibres are preferentially affected could give some support the theory of a more regulatory role of PDE [112, 214, 217].

In previous studies where ^{31}P MRS was applied in BMD patients only the (posterior) calf muscles of mild to moderately affected patients were scanned, without direct comparison with imaging data. As a result, no data were available on muscles without fatty infiltration and it was not clear if changes in phosphorous signals were already present before the onset of fatty infiltration. This is important, as PDE/ATP ratios have been shown to be adaptable in some conditions, whereas substitution of adipose tissue by muscle fibers has to our knowledge never been reported [110, 203-205, 222]. As it is likely that increased PDE/ATP ratios are to some extend related to muscle membrane damage, they could potentially be a marker for therapy efficacy if therapies preventing the membrane damage become available.

The GCM, GCL and SOL with IFL showed a more alkaline pH than controls, which is in accordance with results of mild to moderately affected BMD patients from previous studies [92, 200, 201]. When evaluating the whole BMD group an increased pH was found for all investigated muscles. The cause for the increased pH, although frequently observed in BMD and DMD patients, is unclear. Possibly factors related to mitogenesis or an altered sarcolemmal proton efflux mechanisms ion transport are involved [95, 223].

We found no consistent changes in Pi/ATP or PCr/ATP ratios in the investigated muscles. The fact that we did not find an increased Pi/ATP ratio and decreased PCr/ATP ratio in gastrocnemic muscles as reported in some previous studies could be related to the fact that we had to discard some of the spectra of severely affected patients, as they were of insufficient quality to analyse [92, 224]. This may have somewhat biased our results with regards to these muscles.

Our study has some limitations, as mentioned above we had to discard some of the spectra of the gastrocnemic muscles of BMD patients as they were of insufficient quality to be used for the analysis. This could have resulted in a bias with regards to the findings in the more severely fatty infiltrated gastrocnemic muscles and possibly be an explanation why no significant abnormalities were found in Pi/ATP and PCr/ATP ratios in these muscles. Secondly the NIFL groups for the gastrocnemic muscles were relatively small compared to the control group. As these muscles are the most severely affected in the lower leg of BMD patients this is not unexpected, however, it might have influenced the findings in terms of PDE levels and possibly the other metabolites in these muscles. Thirdly, the use of a 2D-CSI sequence instead of 3D could potentially result in a voxel spanning different muscles along the length of the leg. To circumvent this problem the 2D-CSI spectroscopy grid was carefully planned so that one voxel of each of the analysed muscles was located within the specific muscle, as demonstrated in Figure 1. If it was not possible to allocate the voxel solely to a specific muscle, due to the muscle being too small, the voxel was positioned in such a way that either air or bone (tissue from which no phosphor signal could be obtained) was included. Finally, the 7T fat fractions were not corrected for relaxation effects, which could have affected the exact fat percentage. However, as fat percentages were calculated using the exact same procedure for patients and age-matched controls, values of healthy controls were used for a muscle specific cut-off value and 3T and 7T values showed a high correlation, this is not likely to have significantly influenced our results.

In conclusion, our results show that MR spectroscopy can detect increased PDE/ATP ratios in lower leg muscles of BMD patients prior to fatty infiltration. Therefore, PDE/ATP ratios could be a useful parameter in the follow-up of muscle membrane damage in early stages of the disease, before more structural changes become apparent.

Chapter 7

Conclusion and general discussion

CONCLUSION AND GENERAL DISCUSSION

In the last decade the interest in MRI and MRS studies in DMD patients, and to a lesser extent in BMD patients, has increased substantially. The ability to quantitatively assess various aspects of the affected muscle makes MRI and MRS potentially useful tools in the assessment of disease severity and progression. The development of future therapies for DMD patients has made such tools of increasing importance. So far the focus of many studies has been on the pattern in which the muscles are affected, the quantification of the fatty infiltration in the muscle and its relation with muscle strength and function and the relation with age [98, 101, 102, 104-106, 109, 140, 225]. Additionally some studies have described techniques to evaluate oedema in muscle and others applied proton and phosphorous MRS to study muscle metabolites [103, 108, 111-115, 225]. As DMD and BMD are the most common muscle diseases with a limb-girdle pattern of weakness, and genetic testing is readily available, MRI and MRS are generally not necessary to reach a diagnosis. However, MR techniques could contribute to the evaluation of disease progression and future therapies.

In terms of disease progression, a striking feature in dystrophinopathy patients is the progressive decline of muscle function and muscle tissue. The muscles show increasing amounts of fatty infiltration, although not all muscles become affected at the same moment or at the same rate. Our studies, and those of others, have shown that MRI can be used to quantify the fatty infiltration in multiple muscles and that these values are compatible with clinical features. We have shown that quantification of the fatty infiltration is more sensitive to subtle changes and shows less variability than semi-quantitative, visual scoring methods. Additionally we have shown that in DMD patients and in a homogeneous group of BMD patients, fatty infiltration increases with age and correlates with muscle function. A drawback of the use of fatty infiltration as outcome parameter is that fat is often regarded as an 'end-point' of the disease process and has so far not been shown to be reversible. Additionally, therapies currently under development aim to slow disease progression, rather than reverse pathology. Therefore evaluating the rate at which muscles become fat infiltrated could be a useful outcome parameter. If strength of muscle tissue were to improve, even with unchanged amounts of fatty infiltrated muscle, parameters such as the specific strength, described in chapter 2 would be useful to evaluate such effects.

As outcome parameter the muscle T2 relaxation time as indicator of oedema/inflammation in the muscle is more likely to be reversible in DMD patients than parameters such as the fatty infiltration [226]. In this thesis we described that the muscle T2 relaxation times in DMD patients were increased, while no such increase was found in BMD patients. This suggests that increased muscle T2 relaxation times as indicator of inflammation/oedema are associated with the severity of the muscle damage. If so, the

Chapter 7

T2 relaxation time could be a valuable outcome parameter. Unfortunately, increased levels of fatty infiltration complicate consistent measurement of T2 relaxation times in dystrophic muscle, as the T2 relaxation time of lipids is much longer than the skeletal muscle water T2 relaxation time. A possible method to overcome this problem is by using fat suppression. However, complete fat saturation is technically very complicated to achieve [227]. Separate assessment of the water and lipid signal would be another method to overcome this problem. This remains technically challenging in the whole muscle, but the recently described tri-exponential model, which can be used to asses both the T2 relaxation time independent of the fatty infiltration and to quantify the fat fraction is a promising alternative [183, 228]. As previous studies have suggested changes of the muscle energy metabolism we studied the phosphorous metabolism in muscles of BMD patients. We established that in BMD patients there was an increase in PDE/ATP ratio, before an increase in fat levels became apparent. As such the PDE/ATP ratio could also be a useful parameter to assess muscle damage in early stages of the disease in BMD patients, but possibly also in DMD patients.

Other, so far not yet implemented in DMD or BMD patients, MR techniques could potentially also be of value as outcome parameters. Such techniques include diffusion tensor imaging for the assessment of the muscle fibre architecture and arterial-spin labelling for the evaluation of the tissue perfusion [229].

So far little is known of the value of the discussed methods in terms of therapy assessment, since it is uncertain to what extent there will be changes in the muscle with appropriate therapy and how this will vary between differently affected muscles. Nevertheless, as MR techniques can be used to assess different properties of the muscle it is likely that MRI and MRS can contribute in the evaluation of disease progression. Currently clinical trials use outcome measures such as the 6-minute walking test as outcome parameter. Although the relation between muscle strength and muscle tissue obtained with MRI has been shown to be significantly lower in DMD patients only one study so far has shown a relation between the mean fat fraction and ambulation in these patients [230]. However, it is likely that functional benefits of therapeutic approaches take longer to become apparent than subtle changes such as a decreased inflammatory response or increase in strength of the muscle tissue. Therefore finding a method which can be used to quantify both the fatty infiltration and muscle T2 relaxation time while accounting for the fat, especially when combined with the quantitative strength measurements, could provide a detailed overview of ongoing damage and muscle regeneration in the various stages of follow-up and as such could be a promising outcome parameter.

Chapter 8

Summary

SUMMARY

Muscle MRI and MRS are increasingly being implemented as diagnostic tool, parameter of disease severity and in the follow-up of neuromuscular disorders. Over the years several MR techniques have become available that could be of use in the assessment of various characteristic parameters such as increased levels of fatty infiltration) of these disorders Muscles of both DMD and BMD patients show signs of oedema, fatty infiltration and fibrosis and possibly an altered muscle energy metabolism. The aim of this thesis was to evaluate several MR methods that could serve as potential outcome parameters in the assessment of muscle pathology in DMD and BMD patients. In **Chapter 2** we compared the visually scored (semi-quantitative) amount of fatty infiltration with quantitative values obtained using 3-point Dixon MRI, a chemical shift-based water-fat separation method. We showed that in muscle with low fat fractions visually scored values correlated well with their quantitative equivalents, but overall overestimated the amount of fatty infiltration. The quantitatively obtained fat fractions also showed less variability, especially in the more severely affected muscles and as such are more sensitive to subtle changes. Additionally we demonstrated that implementation of a multipeak model to account for the multiple peaks of the lipid spectrum in the 3-point Dixon method provided an even more accurate measurement of the fat fraction. We used the 3-point Dixon technique to evaluate the non-contractile and contractile (muscle without fatty infiltration) cross-sectional area in two upper and two lower leg muscle groups of DMD patients in **Chapter 3** and combined these values with quantitative strength measurements. We demonstrated that the process of muscle hypertrophy and increasing levels of fatty infiltration appear to be two distinct processes, as the rate of progression differed between the investigated muscle groups. Additionally, we showed that a combination of quantitative MRI and strength measurements could give an indication of muscle quality. As such, we demonstrated that the muscle strength in relation to the amount of contractile tissue is severely reduced in DMD patients. Thus, DMD patients need more muscle tissue to generate the same force. In **Chapter 4** we applied the 3-point Dixon technique amongst other methods to explore the relation between dystrophin levels and fatty infiltration in the lower leg muscles (as indicator of disease severity) of a group of BMD patients. No such relation could be found, but there was a clear correlation between levels of fatty infiltration and age in a subgroup of patients with an exon 45-47 mutation. This indicated that the location of the mutation, and not the amount of dystrophin, is a major determinant of disease severity in these BMD patients. In **Chapter 5** we measured the T2 relaxation times of muscle as marker of oedema/inflammation in DMD and BMD patients compared to healthy controls, after adjustment for the fatty infiltration obtained with Dixon MRI. We showed that the T2 relaxation times were increased in DMD patients, but not

in BMD patients and as such could be useful as outcome parameter in trials aiming to ameliorate the DMD to a BMD phenotype. In addition to MRI, MRS methods like phosphorous MRS can be used to investigate energy metabolism in the muscle. In **Chapter 6** we used a combination of ^{31}P MRS and Dixon MRI at high magnetic field to show that PDE/ATP ratios were increased in lower leg muscles of BMD patients prior to the onset of fatty infiltration. The other metabolites showed no consistent changes in the investigated muscles, although there was an increase in tissue pH in the more severely affected muscles, with increased fat levels. These findings suggest that ^{31}P MRS can be valuable to detect changes in early stages of the disease process.

NEDERLANDSE SAMENVATTING

Spier MRI en MRS worden in toenemende mate geïmplementeerd in de diagnostiek, als parameter van ziekte ernst en in het vervolgen van neuromusculaire ziekten. De afgelopen jaren zijn verschillende MR technieken beschikbaar gekomen welke zouden kunnen worden gebruikt in de evaluatie van verschillende karakteristieke parameters van de verschillende neuromusculaire ziekten zoals een toename van de vervetting in de skelet spieren. Zowel in DMD als in BMD worden er tekenen van oedeem, vervetting, fibrose en mogelijk veranderingen in het energie metabolisme in de spieren van patiënten geobserveerd. Het doel van dit onderzoek was om verschillende MR technieken te evalueren die mogelijk als uitkomstmaat gebruikt kunnen worden in de evaluatie van spieren van DMD en BMD patiënten. In **hoofdstuk 2** hebben we een visueel gescoorde (semikwantitatieve) schaal gebruikt om de vervetting in spieren van DMD patiënten te scoren en de vet waarden verkregen met deze schaal vergeleken met een kwantitatieve 3-punts Dixon MRI techniek. We hebben aangetoond dat in spieren met weinig vervetting de visuele score goed overeenkwam met de kwantitatief verkregen waarde. Echter, in het algemeen werd met de visuele scoringsmethode de vetfractie overschat in vergelijking met de kwantitatief gescoorde vetfracties. Tevens waren de kwantitatieve waarden minder variabel, voornamelijk in de meer ernstig aangedane spieren, en meer sensitief voor subtiele veranderingen. Aanvullend hebben we aangetoond dat met implementatie van een multipeak model, om te corrigeren voor de verschillende pieken van het vetsignaal bij het gebruiken van de 3-punts Dixon techniek, het vetsignaal meer nauwkeurig kon worden bepaald. In **hoofdstuk 3** hebben we de 3-punts Dixon techniek gebruikt om het contractiele (niet vervette spier) en niet-contractiele cross-sectionele oppervlakte van de spier te berekenen in 2 spiergroepen in zowel het boven- als onderbeen. Deze waarden hebben we gecombineerd met de kracht per spiergroep die kwantitatief is gemeten. Hierbij hebben we aangetoond dat het proces van spierhypertrofie en toename van vervetting in de spier 2 verschillende processen zijn, aangezien de snelheid waarmee de veranderingen optreden in de spiergroepen per proces verschillend zijn. Aanvullend hebben we aangetoond dat een combinatie van kwantitatieve MRI en krachtmetingen een indicatie kan geven van de spierkwaliteit. Door deze twee technieken te combineren konden we demonstreren dat de kracht die gerelateerd is aan de hoeveelheid contractiel weefsel per spiergroep ernstig is afgenomen in DMD patiënten, en dat deze patiënten meer spierweefsel nodig hebben om dezelfde hoeveelheid kracht te leveren. In **hoofdstuk 4** hebben we de 3-punts Dixon techniek in combinatie met andere methoden gebruikt om de relatie tussen dystrofine en vervetting in spieren in het onderbeen (als maat van de ernst van de ziekte) te bepalen in BMD patiënten. We konden geen relatie aantonen tussen de vervetting in de spieren en de hoeveelheid dystrofine maar er was wel een significante

relatie tussen de leeftijd van patiënten met dezelfde mutatie (exon 45-47 mutatie) en de hoeveelheid vervetting. Deze bevinding is een indicator dat de plek van de mutatie, en niet zozeer de hoeveelheid dystrofine, een belangrijke determinant is van de ernst van de ziekte van patiënten met de ziekte van Becker. In **hoofdstuk 5** hebben we de T2 relaxatie tijd, als parameter voor ontsteking in de spier, in DMD en BMD patiënten gemeten en vergleken met gezonde controles, nadat de waarden zijn 'gecorrigeerd' voor de vervetting in de spieren, welke de T2 waarden beïnvloed. We hebben in dit hoofdstuk aangetoond dat de T2 relaxatie tijd in spieren van DMD patiënten is verhoogd, maar dat dit niet zo is in de spieren van BMD patiënten. Dit zou erop kunnen wijzen dat de T2 relaxatie tijd als uitkomstmaat gebruikt zou kunnen worden in trials waar het doel is het DMD fenotype te veranderen in het BMD fenotype. In aanvulling op de verschillende MRI methoden die gebruikt zijn kan MR spectroscopie (MRS) worden gebruikt om het energie metabolisme in de spier te onderzoeken. In **hoofdstuk 6** hebben we een combinatie van fosfor (^{31}P) MRS en Dixon MRI gebruikt op hoge veldsterkte en aangetoond dat PDE/ATP ratio's verhoogd zijn in onderbeen spieren van BMD patiënten en dat deze verandering al aanwezig is voordat er vervetting optreedt in de spieren. Voor de andere onderzochte metabolieten konden geen consistente veranderingen worden gevonden in de spieren die onderzocht zijn. In spieren met ernstige vervetting werd wel een verhoging van de pH in de spier gevonden. Deze bevindingen suggereren dat ^{31}P MRS een waardevolle aanvulling kan zijn om veranderingen vroeg in het ziekte proces van patiënten op te sporen.

Appendices

References

List of abbreviations

List of publications

Curriculum vitae

REFERENCES

[1]   Meryon E. On Granular and Fatty Degeneration of the Voluntary Muscles. Medico-chirurgical transactions 1852;35:73-84 1.

[2]   Meryon E. Practical and Pathological Researches on the Various Forms of Paralysis. London. Churchill 1864:200-215.

[3]   Duchenne G. L'électrisation locatisée et son application a la pathologie et a la thérapeutique. Paris: Bailliere et Fils 1864:354-356.

[4]   Duchenne G. Recherches sur la paralysie musculaire pseudohypertrophique ou paralysie myoscléro-sique Archives Génerales de Médicine 1886;2:5-25, 179-209, 305-321, 421-443, 552-588.

[5]   Gowers W. Pseudohypertrophic Muscular Paralysis: a Clinical Lecture. J&A Churchill 1879.

[6]   Becker PE, Kiener F. [A new x-chromosomal muscular dystrophy]. Archiv fur Psychiatrie und Ner-venkrankheiten, vereinigt mit Zeitschrift fur die gesamte Neurologie und Psychiatrie 1955;193:427-48.

[7]   Kingston HM, Harper PS, Pearson PL, Davies KE, Williamson R, Page D. Localisation of gene for Becker muscular dystrophy. Lancet 1983;2:1200.

[8]   Lindenbaum RH, Clarke G, Patel C, Moncrieff M, Hughes JT. Muscular dystrophy in an X; 1 trans-location female suggests that Duchenne locus is on X chromosome short arm. Journal of medical genetics 1979;16:389-92.

[9]   Koenig M, Hoffman EP, Bertelson CJ, Monaco AP, Feener C, Kunkel LM. Complete cloning of the Duchenne muscular dystrophy (DMD) cDNA and preliminary genomic organization of the DMD gene in normal and affected individuals. Cell 1987;50:509-17.

[10]   Hoffman EP, Brown RH, Jr., Kunkel LM. Dystrophin: the protein product of the Duchenne muscular dystrophy locus. Cell 1987;51:919-28.

[11]   Zubrzycka-Gaarn EE, Bulman DE, Karpati G, et al. The Duchenne muscular dystrophy gene product is localized in sarcolemma of human skeletal muscle. Nature 1988;333:466-9.

[12]   Koenig M, Beggs AH, Moyer M, et al. The molecular basis for Duchenne versus Becker muscu-lar dystrophy: correlation of severity with type of deletion. American journal of human genetics 1989;45:498-506.

[13]   Bushby KM, Thambyayah M, Gardner-Medwin D. Prevalence and incidence of Becker muscular dystrophy. Lancet 1991;337:1022-4.

[14]   Helderman-van den Enden AT, Madan K, Breuning MH, et al. An urgent need for a change in policy revealed by a study on prenatal testing for Duchenne muscular dystrophy. European journal of hu-man genetics : EJHG 2013;21:21-6.

[15]   Jennekens FG, ten Kate LP, de Visser M, Wintzen AR. Diagnostic criteria for Duchenne and Becker muscular dystrophy and myotonic dystrophy. Neuromuscular disorders : NMD 1991;1:389-91.

[16]   Dubowitz V. Muscle disorders in childhood. Major problems in clinical pediatrics 1978;16:iii-xiii, 1-282.

[17]   Emery A, Muntoni, F. Duchenne muscular dystrophy. Oxford University Press 2003.

[18]   Kinali M, Messina S, Mercuri E, et al. Management of scoliosis in Duchenne muscular dystrophy: a large 10-year retrospective study. Developmental medicine and child neurology 2006;48:513-8.

[19]   Bach J, Alba A, Pilkington LA, Lee M. Long-term rehabilitation in advanced stage of childhood onset, rapidly progressive muscular dystrophy. Archives of physical medicine and rehabilitation 1981;62:328-31.

[20]   Ishikawa Y, Miura T, Ishikawa Y, et al. Duchenne muscular dystrophy: survival by cardio-respiratory interventions. Neuromuscular disorders : NMD 2011;21:47-51.

[21] Eagle M, Baudouin SV, Chandler C, Giddings DR, Bullock R, Bushby K. Survival in Duchenne muscular dystrophy: improvements in life expectancy since 1967 and the impact of home nocturnal ventilation. Neuromuscular disorders : NMD 2002;12:926-9.

[22] Nigro G, Comi LI, Politano L, Bain RJ. The incidence and evolution of cardiomyopathy in Duchenne muscular dystrophy. International journal of cardiology 1990;26:271-7.

[23] Cotton SM, Voudouris NJ, Greenwood KM. Association between intellectual functioning and age in children and young adults with Duchenne muscular dystrophy: further results from a meta-analysis. Developmental medicine and child neurology 2005;47:257-65.

[24] Mehler MF. Brain dystrophin, neurogenetics and mental retardation. Brain research. Brain research reviews 2000;32:277-307.

[25] Cyrulnik SE, Fee RJ, De Vivo DC, Goldstein E, Hinton VJ. Delayed developmental language milestones in children with Duchenne's muscular dystrophy. The Journal of pediatrics 2007;150:474-8.

[26] Kieny P, Chollet S, Delalande P, et al. Evolution of life expectancy of patients with Duchenne muscular dystrophy at AFM Yolaine de Kepper centre between 1981 and 2011. Annals of physical and rehabilitation medicine 2013;56:443-54.

[27] Emery AE. Population frequencies of inherited neuromuscular diseases—a world survey. Neuromuscular disorders : NMD 1991;1:19-29.

[28] Bushby KM, Gardner-Medwin D. The clinical, genetic and dystrophin characteristics of Becker muscular dystrophy. I. Natural history. Journal of neurology 1993;240:98-104.

[29] Emery AE, Skinner R. Clinical studies in benign (Becker type) X-linked muscular dystrophy. Clinical genetics 1976;10:189-201.

[30] Bradley WG, Jones MZ, Mussini JM, Fawcett PR. Becker-type muscular dystrophy. Muscle & nerve 1978;1:111-32.

[31] Bushby K, Muntoni F, Bourke JP. 107th ENMC international workshop: the management of cardiac involvement in muscular dystrophy and myotonic dystrophy. 7th-9th June 2002, Naarden, the Netherlands. Neuromuscular disorders : NMD 2003;13:166-72.

[32] Nigro G, Comi LI, Politano L, et al. Evaluation of the cardiomyopathy in Becker muscular dystrophy. Muscle & nerve 1995;18:283-91.

[33] Pardo JV, Siliciano JD, Craig SW. A vinculin-containing cortical lattice in skeletal muscle: transverse lattice elements ("costameres") mark sites of attachment between myofibrils and sarcolemma. Proceedings of the National Academy of Sciences of the United States of America 1983;80:1008-12.

[34] Campbell KP. Three muscular dystrophies: loss of cytoskeleton-extracellular matrix linkage. Cell 1995;80:675-9.

[35] Rybakova IN, Patel JR, Ervasti JM. The dystrophin complex forms a mechanically strong link between the sarcolemma and costameric actin. The Journal of cell biology 2000;150:1209-14.

[36] Ervasti JM, Ohlendieck K, Kahl SD, Gaver MG, Campbell KP. Deficiency of a glycoprotein component of the dystrophin complex in dystrophic muscle. Nature 1990;345:315-9.

[37] Williams MW, Bloch RJ. Extensive but coordinated reorganization of the membrane skeleton in myofibers of dystrophic (mdx) mice. The Journal of cell biology 1999;144:1259-70.

[38] Petrof BJ, Shrager JB, Stedman HH, Kelly AM, Sweeney HL. Dystrophin protects the sarcolemma from stresses developed during muscle contraction. Proceedings of the National Academy of Sciences of the United States of America 1993;90:3710-4.

[39] Monaco AP, Bertelson CJ, Liechti-Gallati S, Moser H, Kunkel LM. An explanation for the phenotypic differences between patients bearing partial deletions of the DMD locus. Genomics 1988;2:90-5.

[40] Whitehead NP, Yeung EW, Allen DG. Muscle damage in mdx (dystrophic) mice: role of calcium and reactive oxygen species. Clinical and experimental pharmacology & physiology 2006;33:657-62.

[41] Alderton JM, Steinhardt RA. Calcium influx through calcium leak channels is responsible for the elevated levels of calcium-dependent proteolysis in dystrophic myotubes. The Journal of biological chemistry 2000;275:9452-60.

[42] Goll DE, Thompson VF, Li H, Wei W, Cong J. The calpain system. Physiological reviews 2003;83:731-801.

[43] Robert V, Massimino ML, Tosello V, et al. Alteration in calcium handling at the subcellular level in mdx myotubes. The Journal of biological chemistry 2001;276:4647-51.

[44] Brenman JE, Chao DS, Xia H, Aldape K, Bredt DS. Nitric oxide synthase complexed with dystrophin and absent from skeletal muscle sarcolemma in Duchenne muscular dystrophy. Cell 1995;82:743-52.

[45] Chang WJ, Iannaccone ST, Lau KS, et al. Neuronal nitric oxide synthase and dystrophin-deficient muscular dystrophy. Proceedings of the National Academy of Sciences of the United States of America 1996;93:9142-7.

[46] Sander M, Chavoshan B, Harris SA, et al. Functional muscle ischemia in neuronal nitric oxide synthase-deficient skeletal muscle of children with Duchenne muscular dystrophy. Proceedings of the National Academy of Sciences of the United States of America 2000;97:13818-23.

[47] Chao DS, Gorospe JR, Brenman JE, et al. Selective loss of sarcolemmal nitric oxide synthase in Becker muscular dystrophy. The Journal of experimental medicine 1996;184:609-18.

[48] Torelli S, Brown SC, Jimenez-Mallebrera C, Feng L, Muntoni F, Sewry CA. Absence of neuronal nitric oxide synthase (nNOS) as a pathological marker for the diagnosis of Becker muscular dystrophy with rod domain deletions. Neuropathology and applied neurobiology 2004;30:540-5.

[49] Thomas GD, Sander M, Lau KS, Huang PL, Stull JT, Victor RG. Impaired metabolic modulation of alpha-adrenergic vasoconstriction in dystrophin-deficient skeletal muscle. Proceedings of the National Academy of Sciences of the United States of America 1998;95:15090-5.

[50] Martin EA, Barresi R, Byrne BJ, et al. Tadalafil alleviates muscle ischemia in patients with Becker muscular dystrophy. Science translational medicine 2012;4:162ra155.

[51] Tidball JG, Wehling-Henricks M. The role of free radicals in the pathophysiology of muscular dystrophy. Journal of applied physiology 2007;102:1677-86.

[52] Li D, Yue Y, Lai Y, Hakim CH, Duan D. Nitrosative stress elicited by nNOSmicro delocalization inhibits muscle force in dystrophin-null mice. The Journal of pathology 2011;223:88-98.

[53] Buyse GM, Van der Mieren G, Erb M, et al. Long-term blinded placebo-controlled study of SNT-MC17/idebenone in the dystrophin deficient mdx mouse: cardiac protection and improved exercise performance. European heart journal 2009;30:116-24.

[54] McDouall RM, Dunn MJ, Dubowitz V. Nature of the mononuclear infiltrate and the mechanism of muscle damage in juvenile dermatomyositis and Duchenne muscular dystrophy. Journal of the neurological sciences 1990;99:199-217.

[55] Arahata K, Engel AG. Monoclonal antibody analysis of mononuclear cells in myopathies. I: Quantitation of subsets according to diagnosis and sites of accumulation and demonstration and counts of muscle fibers invaded by T cells. Annals of neurology 1984;16:193-208.

[56] Wehling M, Spencer MJ, Tidball JG. A nitric oxide synthase transgene ameliorates muscular dystrophy in mdx mice. The Journal of cell biology 2001;155:123-31.

[57] Morrison J, Lu QL, Pastoret C, Partridge T, Bou-Gharios G. T-cell-dependent fibrosis in the mdx dystrophic mouse. Laboratory investigation; a journal of technical methods and pathology 2000;80:881-91.

[58]   Engel AG, Arahata K. Mononuclear cells in myopathies: quantitation of functionally distinct subsets, recognition of antigen-specific cell-mediated cytotoxicity in some diseases, and implications for the pathogenesis of the different inflammatory myopathies. Human pathology 1986;17:704-21.

[59]   Mantegazza R, Andreetta F, Bernasconi P, et al. Analysis of T cell receptor repertoire of muscle-infiltrating T lymphocytes in polymyositis. Restricted V alpha/beta rearrangements may indicate antigen-driven selection. The Journal of clinical investigation 1993;91:2880-6.

[60]   Gorospe JR, Tharp M, Demitsu T, Hoffman EP. Dystrophin-deficient myofibers are vulnerable to mast cell granule-induced necrosis. Neuromuscular disorders : NMD 1994;4:325-33.

[61]   Gussoni E, Pavlath GK, Miller RG, et al. Specific T cell receptor gene rearrangements at the site of muscle degeneration in Duchenne muscular dystrophy. Journal of immunology 1994;153:4798-805.

[62]   Chen YW, Nagaraju K, Bakay M, et al. Early onset of inflammation and later involvement of TGF-beta in Duchenne muscular dystrophy. Neurology 2005;65:826-34.

[63]   Spencer MJ, Tidball JG. Do immune cells promote the pathology of dystrophin-deficient myopathies? Neuromuscular disorders : NMD 2001;11:556-64.

[64]   Schmalbruch H. Regenerated muscle fibers in Duchenne muscular dystrophy: a serial section study. Neurology 1984;34:60-5.

[65]   Deconinck N, Dan B. Pathophysiology of duchenne muscular dystrophy: current hypotheses. Pediatric neurology 2007;36:1-7.

[66]   Mendell JR, Moxley RT, Griggs RC, et al. Randomized, double-blind six-month trial of prednisone in Duchenne's muscular dystrophy. The New England journal of medicine 1989;320:1592-7.

[67]   Henricson EK, Abresch RT, Cnaan A, et al. The cooperative international neuromuscular research group Duchenne natural history study: glucocorticoid treatment preserves clinically meaningful functional milestones and reduces rate of disease progression as measured by manual muscle testing and other commonly used clinical trial outcome measures. Muscle & nerve 2013;48:55-67.

[68]   Schram G, Fournier A, Leduc H, et al. All-cause mortality and cardiovascular outcomes with prophylactic steroid therapy in Duchenne muscular dystrophy. Journal of the American College of Cardiology 2013;61:948-54.

[69]   Biggar WD, Gingras M, Fehlings DL, Harris VA, Steele CA. Deflazacort treatment of Duchenne muscular dystrophy. The Journal of pediatrics 2001;138:45-50.

[70]   Drachman DB, Toyka KV, Myer E. Prednisone in Duchenne muscular dystrophy. Lancet 1974;2:1409-12.

[71]   Fenichel GM, Florence JM, Pestronk A, et al. Long-term benefit from prednisone therapy in Duchenne muscular dystrophy. Neurology 1991;41:1874-7.

[72]   Fisher I, Abraham D, Bouri K, Hoffman EP, Muntoni F, Morgan J. Prednisolone-induced changes in dystrophic skeletal muscle. FASEB journal : official publication of the Federation of American Societies for Experimental Biology 2005;19:834-6.

[73]   Bushby K, Finkel R, Birnkrant DJ, et al. Diagnosis and management of Duchenne muscular dystrophy, part 2: implementation of multidisciplinary care. Lancet neurology 2010;9:177-89.

[74]   Finder JD, Birnkrant D, Carl J, et al. Respiratory care of the patient with Duchenne muscular dystrophy: ATS consensus statement. American journal of respiratory and critical care medicine 2004;170:456-65.

[75]   Beytia Mde L, Vry J, Kirschner J. Drug treatment of Duchenne muscular dystrophy: available evidence and perspectives. Acta myologica : myopathies and cardiomyopathies : official journal of the Mediterranean Society of Myology / edited by the Gaetano Conte Academy for the study of striated muscle diseases 2012;31:4-8.

[76]   Pichavant C, Aartsma-Rus A, Clemens PR, et al. Current status of pharmaceutical and genetic thera-peutic approaches to treat DMD. Molecular therapy : the journal of the American Society of Gene Therapy 2011;19:830-40.

[77]   Goemans NM, Tulinius M, van den Akker JT, et al. Systemic administration of PRO051 in Duch-enne's muscular dystrophy. The New England journal of medicine 2011;364:1513-22.

[78]   van Deutekom JC, Janson AA, Ginjaar IB, et al. Local dystrophin restoration with antisense oligo-nucleotide PRO051. The New England journal of medicine 2007;357:2677-86.

[79]   Cirak S, Arechavala-Gomeza V, Guglieri M, et al. Exon skipping and dystrophin restoration in pa-tients with Duchenne muscular dystrophy after systemic phosphorodiamidate morpholino oligomer treatment: an open-label, phase 2, dose-escalation study. Lancet 2011;378:595-605.

[80]   Witting N, Kruuse C, Nyhuus B, et al. Effect of sildenafil on skeletal and cardiac muscle in Becker muscular dystrophy. Annals of neurology 2014.

[81]   Heckmatt J, Rodillo E, Doherty M, Willson K, Leeman S. Quantitative sonography of muscle. Journal of child neurology 1989;4 Suppl:S101-6.

[82]   Jiddane M, Gastaut JL, Pellissier JF, Pouget J, Serratrice G, Salamon G. CT of primary muscle diseases. AJNR. American journal of neuroradiology 1983;4:773-6.

[83]   Jones DA, Round JM, Edwards RH, Grindwood SR, Tofts PS. Size and composition of the calf and quadriceps muscles in Duchenne muscular dystrophy. A tomographic and histochemical study. Journal of the neurological sciences 1983;60:307-22.

[84]   Rott HD, Breimesser FH, Rodl W. Imaging technics in muscular dystrophies. Journal de genetique humaine 1985;33:397-403.

[85]   Liu M, Chino N, Ishihara T. Muscle damage progression in Duchenne muscular dystrophy evaluated by a new quantitative computed tomography method. Archives of physical medicine and rehabilita-tion 1993;74:507-14.

[86]   Arai Y, Osawa M, Fukuyama Y. Muscle CT scans in preclinical cases of Duchenne and Becker muscular dystrophy. Brain & development 1995;17:95-103.

[87]   Schreiber A, Smith WL, Ionasescu V, et al. Magnetic resonance imaging of children with Duchenne muscular dystrophy. Pediatric radiology 1987;17:495-7.

[88]   Matsumura K, Nakano I, Fukuda N, Ikehira H, Tateno Y, Aoki Y. Proton spin-lattice relaxation time of Duchenne dystrophy skeletal muscle by magnetic resonance imaging. Muscle & nerve 1988;11:97-102.

[89]   Murphy WA, Totty WG, Carroll JE. MRI of normal and pathologic skeletal muscle. AJR. American journal of roentgenology 1986;146:565-74.

[90]   Huang Y, Majumdar S, Genant HK, et al. Quantitative MR relaxometry study of muscle composi-tion and function in Duchenne muscular dystrophy. Journal of magnetic resonance imaging : JMRI 1994;4:59-64.

[91]   Liu GC, Jong YJ, Chiang CH, Jaw TS. Duchenne muscular dystrophy: MR grading system with functional correlation. Radiology 1993;186:475-80.

[92]   Barbiroli B, Funicello R, Iotti S, Montagna P, Ferlini A, Zaniol P. 31P-NMR spectroscopy of skeletal muscle in Becker dystrophy and DMD/BMD carriers. Altered rate of phosphate transport. Journal of the neurological sciences 1992;109:188-95.

[93]   Newman RJ, Bore PJ, Chan L, et al. Nuclear magnetic resonance studies of forearm muscle in Duchenne dystrophy. British medical journal 1982;284:1072-4.

[94]   Newman RJ. An in vivo study of muscle phosphate metabolism in Becker's dystrophy by 31P NMR spectroscopy. Metabolism: clinical and experimental 1985;34:737-40.

[95] Kemp GJ, Taylor DJ, Dunn JF, Frostick SP, Radda GK. Cellular energetics of dystrophic muscle. Journal of the neurological sciences 1993;116:201-6.

[96] Younkin DP, Berman P, Sladky J, Chee C, Bank W, Chance B. 31P NMR studies in Duchenne muscular dystrophy: age-related metabolic changes. Neurology 1987;37:165-9.

[97] Griffiths RD, Cady EB, Edwards RH, Wilkie DR. Muscle energy metabolism in Duchenne dystrophy studied by 31P-NMR: controlled trials show no effect of allopurinol or ribose. Muscle & nerve 1985;8:760-7.

[98] Wren TA, Bluml S, Tseng-Ong L, Gilsanz V. Three-point technique of fat quantification of muscle tissue as a marker of disease progression in Duchenne muscular dystrophy: preliminary study. AJR. American journal of roentgenology 2008;190:W8-12.

[99] Kim HK, Laor T, Horn PS, Racadio JM, Wong B, Dardzinski BJ. T2 mapping in Duchenne muscular dystrophy: distribution of disease activity and correlation with clinical assessments. Radiology 2010;255:899-908.

[100] Mathur S, Lott DJ, Senesac C, et al. Age-related differences in lower-limb muscle cross-sectional area and torque production in boys with Duchenne muscular dystrophy. Archives of physical medicine and rehabilitation 2010;91:1051-8.

[101] Kinali M, Arechavala-Gomeza V, Cirak S, et al. Muscle histology vs MRI in Duchenne muscular dystrophy. Neurology 2011;76:346-53.

[102] Fischmann A, Hafner P, Fasler S, et al. Quantitative MRI can detect subclinical disease progression in muscular dystrophy. Journal of neurology 2012;259:1648-54.

[103] Arpan I, Forbes SC, Lott DJ, et al. T(2) mapping provides multiple approaches for the characterization of muscle involvement in neuromuscular diseases: a cross-sectional study of lower leg muscles in 5-15-year-old boys with Duchenne muscular dystrophy. NMR in biomedicine 2013;26:320-8.

[104] Fischmann A, Hafner P, Gloor M, et al. Quantitative MRI and loss of free ambulation in Duchenne muscular dystrophy. Journal of neurology 2013;260:969-74.

[105] Forbes SC, Walter GA, Rooney WD, et al. Skeletal muscles of ambulant children with Duchenne muscular dystrophy: validation of multicenter study of evaluation with MR imaging and MR spectroscopy. Radiology 2013;269:198-207.

[106] Hollingsworth KG, Garrood P, Eagle M, Bushby K, Straub V. Magnetic resonance imaging in Duchenne muscular dystrophy: longitudinal assessment of natural history over 18 months. Muscle & nerve 2013;48:586-8.

[107] Triplett WT, Baligand C, Forbes SC, et al. Chemical shift-based MRI to measure fat fractions in dystrophic skeletal muscle. Magnetic resonance in medicine : official journal of the Society of Magnetic Resonance in Medicine / Society of Magnetic Resonance in Medicine 2013.

[108] Willcocks RJ, Arpan ,I.A., Forbes, S.C., Lott, D.J., Senesac, C.R., Senesac ,E., Deol J., Triplett , W.T., Baligand, C., Daniels, M.J., Sweeney, H.L., Walter, G.A., Vandenborde, K. Longitudinal measurements of MRI-T2 in boys with Duchenne muscular dystrophy: Effects of age and disease progression. Neuromuscular disorders : NMD 2014.

[109] Garrood P, Hollingsworth KG, Eagle M, et al. MR imaging in Duchenne muscular dystrophy: quantification of T1-weighted signal, contrast uptake, and the effects of exercise. Journal of magnetic resonance imaging : JMRI 2009;30:1130-8.

[110] Banerjee B, Sharma U, Balasubramanian K, Kalaivani M, Kalra V, Jagannathan NR. Effect of creatine monohydrate in improving cellular energetics and muscle strength in ambulatory Duchenne muscular dystrophy patients: a randomized, placebo-controlled 31P MRS study. Magnetic resonance imaging 2010;28:698-707.

[111] Torriani M, Townsend E, Thomas BJ, Bredella MA, Ghomi RH, Tseng BS. Lower leg muscle involvement in Duchenne muscular dystrophy: an MR imaging and spectroscopy study. Skeletal radiology 2012;41:437-45.

[112] Wary C, Naulet T, Thibaud JL, Monnet A, Blot S, Carlier PG. Splitting of Pi and other (3)(1)P NMR anomalies of skeletal muscle metabolites in canine muscular dystrophy. NMR in biomedicine 2012;25:1160-9.

[113] Marden FA, Connolly AM, Siegel MJ, Rubin DA. Compositional analysis of muscle in boys with Duchenne muscular dystrophy using MR imaging. Skeletal radiology 2005;34:140-8.

[114] Kim HK, Laor T, Horn PS, Wong B. Quantitative assessment of the T2 relaxation time of the gluteus muscles in children with Duchenne muscular dystrophy: a comparative study before and after steroid treatment. Korean journal of radiology : official journal of the Korean Radiological Society 2010;11:304-11.

[115] Rooney WD, Forbes SC, Triplett W, et al. Soleus muscle water T2 values in Duchenne muscular dystrophy: Associations with age and corticosteroid treatment. Proc Intl Soc Mag Reson Med 2013;21:(Abstract 689).

[116] Pichiecchio A, Uggetti C, Egitto MG, et al. Quantitative MR evaluation of body composition in patients with Duchenne muscular dystrophy. European radiology 2002;12:2704-9.

[117] Kinali M, Arechavala-Gomeza V, Feng L, et al. Local restoration of dystrophin expression with the morpholino oligomer AVI-4658 in Duchenne muscular dystrophy: a single-blind, placebo-controlled, dose-escalation, proof-of-concept study. Lancet neurology 2009;8:918-28.

[118] Dixon WT. Simple proton spectroscopic imaging. Radiology 1984;153:189-94.

[119] Hernando D, Liang ZP, Kellman P. Chemical shift-based water/fat separation: a comparison of signal models. Magnetic resonance in medicine : official journal of the Society of Magnetic Resonance in Medicine / Society of Magnetic Resonance in Medicine 2010;64:811-22.

[120] Kovanlikaya A, Mittelman SD, Ward A, Geffner ME, Dorey F, Gilsanz V. Obesity and fat quantification in lean tissues using three-point Dixon MR imaging. Pediatric radiology 2005;35:601-7.

[121] Glover GH, Schneider E. Three-point Dixon technique for true water/fat decomposition with B0 inhomogeneity correction. Magnetic resonance in medicine : official journal of the Society of Magnetic Resonance in Medicine / Society of Magnetic Resonance in Medicine 1991;18:371-83.

[122] Yu H, Shimakawa A, McKenzie CA, Brodsky E, Brittain JH, Reeder SB. Multiecho water-fat separation and simultaneous R2* estimation with multifrequency fat spectrum modeling. Magnetic resonance in medicine : official journal of the Society of Magnetic Resonance in Medicine / Society of Magnetic Resonance in Medicine 2008;60:1122-34.

[123] Mercuri E, Pichiecchio A, Allsop J, Messina S, Pane M, Muntoni F. Muscle MRI in inherited neuromuscular disorders: past, present, and future. Journal of magnetic resonance imaging : JMRI 2007;25:433-40.

[124] Fischer D, Walter MC, Kesper K, et al. Diagnostic value of muscle MRI in differentiating LGMD2I from other LGMDs. Journal of neurology 2005;252:538-47.

[125] Goutallier D, Postel JM, Bernageau J, Lavau L, Voisin MC. Fatty muscle degeneration in cuff ruptures. Pre- and postoperative evaluation by CT scan. Clinical orthopaedics and related research 1994:78-83.

[126] Fuchs B, Weishaupt D, Zanetti M, Hodler J, Gerber C. Fatty degeneration of the muscles of the rotator cuff: assessment by computed tomography versus magnetic resonance imaging. Journal of shoulder and elbow surgery / American Shoulder and Elbow Surgeons 1999;8:599-605.

Appendices

[127] Alizai H, Nardo L, Karampinos DC, et al. Comparison of clinical semi-quantitative assessment of muscle fat infiltration with quantitative assessment using chemical shift-based water/fat separation in MR studies of the calf of post-menopausal women. European radiology 2012;22:1592-600.

[128] Jonker J, Wida R, Hammer S. 1.5T and 7T MR spectroscopy of tissue specific changes in ectopic fat content in response to exercise training in type 2 diabetes mellitus patients; the ATLAS-study. Proc Intl Soc Mag Reson Med 2011;19th Annual Meeting Montreal:(abstract 872).

[129] Karampinos DC, Yu H, Shimakawa A, Link TM, Majumdar S. Chemical shift-based water/fat separation in the presence of susceptibility-induced fat resonance shift. Magnetic resonance in medicine: official journal of the Society of Magnetic Resonance in Medicine / Society of Magnetic Resonance in Medicine 2012;68:1495-505.

[130] Liu CY, McKenzie CA, Yu H, Brittain JH, Reeder SB. Fat quantification with IDEAL gradient echo imaging: correction of bias from T(1) and noise. Magnetic resonance in medicine : official journal of the Society of Magnetic Resonance in Medicine / Society of Magnetic Resonance in Medicine 2007;58:354-64.

[131] Boesch C, Machann J, Vermathen P, Schick F. Role of proton MR for the study of muscle lipid metabolism. NMR in biomedicine 2006;19:968-88.

[132] Gloor M, Fasler S, Fischmann A, et al. Quantification of fat infiltration in oculopharyngeal muscular dystrophy: comparison of three MR imaging methods. Journal of magnetic resonance imaging : JMRI 2011;33:203-10.

[133] Hollingsworth KG, Garrood P, Aribisala BS. Progression of fat infiltration in calf, thigh and pelvic muscles in Duchenne muscular dystrophy: quantification by MRI over an 18 month period. Proc Intl Soc Mag Reson Med 2009;17th Annual Meeting:(abstract 1916).

[134] Gaeta M, Scribano E, Mileto A, et al. Muscle fat fraction in neuromuscular disorders: dual-echo dual-flip-angle spoiled gradient-recalled MR imaging technique for quantification—a feasibility study. Radiology 2011;259:487-94.

[135] Reeder SB, Robson PM, Yu H, et al. Quantification of hepatic steatosis with MRI: the effects of accurate fat spectral modeling. Journal of magnetic resonance imaging : JMRI 2009;29:1332-9.

[136] Boland BJ, Silbert PL, Groover RV, Wollan PC, Silverstein MD. Skeletal, cardiac, and smooth muscle failure in Duchenne muscular dystrophy. Pediatric neurology 1996;14:7-12.

[137] Bowles DE, McPhee SW, Li C, et al. Phase 1 gene therapy for Duchenne muscular dystrophy using a translational optimized AAV vector. Molecular therapy : the journal of the American Society of Gene Therapy 2012;20:443-55.

[138] Cirak S, Feng L, Anthony K, et al. Restoration of the dystrophin-associated glycoprotein complex after exon skipping therapy in Duchenne muscular dystrophy. Molecular therapy : the journal of the American Society of Gene Therapy 2012;20:462-7.

[139] Malik V, Rodino-Klapac LR, Viollet L, et al. Gentamicin-induced readthrough of stop codons in Duchenne muscular dystrophy. Annals of neurology 2010;67:771-80.

[140] Akima H, Lott D, Senesac C, et al. Relationships of thigh muscle contractile and non-contractile tissue with function, strength, and age in boys with Duchenne muscular dystrophy. Neuromuscular disorders : NMD 2012;22:16-25.

[141] Mercuri E, Jungbluth H, Muntoni F. Muscle imaging in clinical practice: diagnostic value of muscle magnetic resonance imaging in inherited neuromuscular disorders. Current opinion in neurology 2005;18:526-37.

[142] Kovanlikaya A, Guclu C, Desai C, Becerra R, Gilsanz V. Fat quantification using three-point dixon technique: in vitro validation. Academic radiology 2005;12:636-9.

[143] Wokke BH, Bos C, Reijnierse M, et al. Comparison of dixon and T1-weighted MR methods to assess the degree of fat infiltration in duchenne muscular dystrophy patients. Journal of magnetic resonance imaging : JMRI 2013;38:619-24.

[144] Yu H, McKenzie CA, Shimakawa A, et al. Multiecho reconstruction for simultaneous water-fat decomposition and T2* estimation. Journal of magnetic resonance imaging : JMRI 2007;26:1153-61.

[145] Kan HE, Scheenen TW, Wohlgemuth M, et al. Quantitative MR imaging of individual muscle involvement in facioscapulohumeral muscular dystrophy. Neuromuscular disorders : NMD 2009;19:357-62.

[146] Hogrel JY, Payan CA, Ollivier G, et al. Development of a French isometric strength normative database for adults using quantitative muscle testing. Archives of physical medicine and rehabilitation 2007;88:1289-97.

[147] Cros D, Harnden P, Pellissier JF, Serratrice G. Muscle hypertrophy in Duchenne muscular dystrophy. A pathological and morphometric study. Journal of neurology 1989;236:43-7.

[148] Chan S, Head SI, Morley JW. Branched fibers in dystrophic mdx muscle are associated with a loss of force following lengthening contractions. American journal of physiology. Cell physiology 2007;293:C985-92.

[149] Coulton GR, Curtin NA, Morgan JE, Partridge TA. The mdx mouse skeletal muscle myopathy: II. Contractile properties. Neuropathology and applied neurobiology 1988;14:299-314.

[150] Angelini C, Fanin M, Pegoraro E, Freda MP, Cadaldini M, Martinello F. Clinical-molecular correlation in 104 mild X-linked muscular dystrophy patients: characterization of sub-clinical phenotypes. Neuromuscular disorders : NMD 1994;4:349-58.

[151] Eagle M, Bourke J, Bullock R, et al. Managing Duchenne muscular dystrophy—the additive effect of spinal surgery and home nocturnal ventilation in improving survival. Neuromuscular disorders : NMD 2007;17:470-5.

[152] Kohler M, Clarenbach CF, Bahler C, Brack T, Russi EW, Bloch KE. Disability and survival in Duchenne muscular dystrophy. Journal of neurology, neurosurgery, and psychiatry 2009;80:320-5.

[153] Nicholson LV, Johnson MA, Bushby KM, et al. Integrated study of 100 patients with Xp21 linked muscular dystrophy using clinical, genetic, immunochemical, and histopathological data. Part 1. Trends across the clinical groups. Journal of medical genetics 1993;30:728-36.

[154] Anthony K, Cirak S, Torelli S, et al. Dystrophin quantification and clinical correlations in Becker muscular dystrophy: implications for clinical trials. Brain : a journal of neurology 2011;134:3547-59.

[155] Bushby KM, Gardner-Medwin D, Nicholson LV, et al. The clinical, genetic and dystrophin characteristics of Becker muscular dystrophy. II. Correlation of phenotype with genetic and protein abnormalities. Journal of neurology 1993;240:105-12.

[156] Nicholson LV, Johnson MA, Bushby KM, et al. Integrated study of 100 patients with Xp21 linked muscular dystrophy using clinical, genetic, immunochemical, and histopathological data. Part 2. Correlations within individual patients. Journal of medical genetics 1993;30:737-44.

[157] Pegoraro E, Hoffman EP, Piva L, et al. SPP1 genotype is a determinant of disease severity in Duchenne muscular dystrophy. Neurology 2011;76:219-26.

[158] Ruszczak C, Mirza A, Menhart N. Differential stabilities of alternative exon-skipped rod motifs of dystrophin. Biochim Biophys Acta 2009;1794:921-8.

[159] Comi GP, Prelle A, Bresolin N, et al. Clinical variability in Becker muscular dystrophy. Genetic, biochemical and immunohistochemical correlates. Brain : a journal of neurology 1994;117 (Pt 1):1-14.

Appendices

[160] Beggs AH, Hoffman EP, Snyder JR, et al. Exploring the molecular basis for variability among patients with Becker muscular dystrophy: dystrophin gene and protein studies. American journal of human genetics 1991;49:54-67.

[161] Bushby KM. Genetic and clinical correlations of Xp21 muscular dystrophy. Journal of inherited metabolic disease 1992;15:551-64.

[162] Hoffman EP, Kunkel LM, Angelini C, Clarke A, Johnson M, Harris JB. Improved diagnosis of Becker muscular dystrophy by dystrophin testing. Neurology 1989;39:1011-7.

[163] Magri F, Govoni A, D'Angelo MG, et al. Genotype and phenotype characterization in a large dystrophinopathic cohort with extended follow-up. Journal of neurology 2011;258:1610-23.

[164] Neri M, Torelli S, Brown S, et al. Dystrophin levels as low as 30% are sufficient to avoid muscular dystrophy in the human. Neuromuscular disorders : NMD 2007;17:913-8.

[165] Aartsma-Rus A, Fokkema I, Verschuuren J, et al. Theoretic applicability of antisense-mediated exon skipping for Duchenne muscular dystrophy mutations. Human mutation 2009;30:293-9.

[166] van Ommen GJ, van Deutekom J, Aartsma-Rus A. The therapeutic potential of antisense-mediated exon skipping. Current opinion in molecular therapeutics 2008;10:140-9.

[167] Aartsma-Rus A, Van Deutekom JC, Fokkema IF, Van Ommen GJ, Den Dunnen JT. Entries in the Leiden Duchenne muscular dystrophy mutation database: an overview of mutation types and paradoxical cases that confirm the reading-frame rule. Muscle & nerve 2006;34:135-44.

[168] Kaspar RW, Allen HD, Ray WC, et al. Analysis of dystrophin deletion mutations predicts age of cardiomyopathy onset in becker muscular dystrophy. Circulation. Cardiovascular genetics 2009;2:544-51.

[169] van Putten M, Hulsker M, Young C, et al. Low dystrophin levels increase survival and improve muscle pathology and function in dystrophin/utrophin double-knockout mice. FASEB journal : official publication of the Federation of American Societies for Experimental Biology 2013;27:2484-95.

[170] van Putten M, Hulsker M, Nadarajah VD, et al. The effects of low levels of dystrophin on mouse muscle function and pathology. PloS one 2012;7:e31937.

[171] Li D, Yue Y, Duan D. Preservation of muscle force in Mdx3cv mice correlates with low-level expression of a near full-length dystrophin protein. The American journal of pathology 2008;172:1332-41.

[172] Li D, Yue Y, Duan D. Marginal level dystrophin expression improves clinical outcome in a s train of dystrophin/utrophin double knockout mice. PloS one 2010;5:e15286.

[173] Lai Y, Thomas GD, Yue Y, et al. Dystrophins carrying spectrin-like repeats 16 and 17 anchor nNOS to the sarcolemma and enhance exercise performance in a mouse model of muscular dystrophy. The Journal of clinical investigation 2009;119:624-35.

[174] Lai Y, Zhao J, Yue Y, Duan D. alpha2 and alpha3 helices of dystrophin R16 and R17 frame a microdomain in the alpha1 helix of dystrophin R17 for neuronal NOS binding. Proceedings of the National Academy of Sciences of the United States of America 2013;110:525-30.

[175] England SB, Nicholson LV, Johnson MA, et al. Very mild muscular dystrophy associated with the deletion of 46% of dystrophin. Nature 1990;343:180-2.

[176] Arechavala-Gomeza V, Kinali M, Feng L, et al. Immunohistological intensity measurements as a tool to assess sarcolemma-associated protein expression. Neuropathology and applied neurobiology 2010;36:265-74.

[177] Spitali P, van den Bergen JC, Verhaart IE, et al. DMD transcript imbalance determines dystrophin levels. FASEB journal : official publication of the Federation of American Societies for Experimental Biology 2013;27:4909-16.

[178] Petrof BJ. Molecular pathophysiology of myofiber injury in deficiencies of the dystrophin-glyco-protein complex. American journal of physical medicine & rehabilitation / Association of Academic Physiatrists 2002;81:S162-74.

[179] Wokke BH, van den Bergen JC, Versluis MJ, et al. Quantitative MRI and strength measurements in the assessment of muscle quality in Duchenne muscular dystrophy. Neuromuscular disorders : NMD 2014.

[180] Hollingsworth KG, de Sousa PL, Straub V, Carlier PG. Towards harmonization of protocols for MRI outcome measures in skeletal muscle studies: consensus recommendations from two TREAT-NMD NMR workshops, 2 May 2010, Stockholm, Sweden, 1-2 October 2009, Paris, France. Neuromuscular disorders : NMD 2012;22 Suppl 2:S54-67.

[181] Dennett X, Shield LK, Clingan LJ, Woolley DA. Becker and Duchenne muscular dystrophy: a comparative morphological study. Australian paediatric journal 1988;24 Suppl 1:15-20.

[182] Fullerton GD, Cameron IL, Hunter K, Fullerton HJ. Proton magnetic resonance relaxation behavior of whole muscle with fatty inclusions. Radiology 1985;155:727-30.

[183] Carlier PG. Global T2 versus water T2 in NMR imaging of fatty infiltrated muscles: Different methodology, different information and different implications. Neuromuscular disorders : NMD 2014.

[184] Hatakenaka M, Ueda M, Ishigami K, Otsuka M, Masuda K. Effects of aging on muscle T2 r elaxation time: difference between fast- and slow-twitch muscles. Investigative radiology 2001;36:692-8.

[185] Spencer MJ, Montecino-Rodriguez E, Dorshkind K, Tidball JG. Helper (CD4(+)) and cytotoxic (CD8(+)) T cells promote the pathology of dystrophin-deficient muscle. Clinical immunology 2001;98:235-43.

[186] Bernasconi P, Torchiana E, Confalonieri P, et al. Expression of transforming growth factor-beta 1 in dystrophic patient muscles correlates with fibrosis. Pathogenetic role of a fibrogenic cytokine. The Journal of clinical investigation 1995;96:1137-44.

[187] Weber MA, Nagel AM, Wolf MB, et al. Permanent muscular sodium overload and persistent muscle edema in Duchenne muscular dystrophy: a possible contributor of progressive muscle degeneration. Journal of neurology 2012;259:2385-92.

[188] Hernando D, Karampinos DC, King KF, et al. Removal of olefinic fat chemical shift artifact in diffusion MRI. Magnetic resonance in medicine : official journal of the Society of Magnetic Resonance in Medicine / Society of Magnetic Resonance in Medicine 2011;65:692-701.

[189] Williams SE, Heemskerk AM, Welch EB, Li K, Damon BM, Park JH. Quantitative effects of inclusion of fat on muscle diffusion tensor MRI measurements. Journal of magnetic resonance imaging : JMRI 2013;38:1292-7.

[190] Janiczek RL, Gambarota G, Sinclair CD, et al. Simultaneous T(2) and lipid quantitation using IDEAL-CPMG. Magnetic resonance in medicine : official journal of the Society of Magnetic Resonance in Medicine / Society of Magnetic Resonance in Medicine 2011;66:1293-302.

[191] Friedman SD, Poliachik SL, Carter GT, Budech CB, Bird TD, Shaw DW. The magnetic resonance imaging spectrum of facioscapulohumeral muscular dystrophy. Muscle & nerve 2012;45:500-6.

[192] Yao L, Gai N. Fat-corrected T2 measurement as a marker of active muscle disease in inflammatory myopathy. AJR. American journal of roentgenology 2012;198:W475-81.

[193] Azzabou N, Loureiro de Sousa, P., Caldas, E., Carlier, P.G. Validation of a generic approach to muscle water T2 determination at 3T in fat-infiltrated skeletal muscle. Journal of magnetic resonance imaging 2014;DOI 10.1002/jmri.24613

[194] Kim HK, Merrow AC, Shiraj S, Wong BL, Horn PS, Laor T. Analysis of fatty infiltration and inflammation of the pelvic and thigh muscles in boys with Duchenne muscular dystrophy (DMD):

grading of disease involvement on MR imaging and correlation with clinical assessments. Pediatric radiology 2013;43:1327-35.

[195]   Wary C, Azzabou N, Giraudeau C, et al. Quantitative NMRI and NMRS indices identify augmented disease progression after loss of ambulation in forearms of boys with Duchenne Muscle Dystrophy. Proc Intl Soc Mag Reson Med 2014;22.

[196]   Forbes SC, Willcocks RJ, Triplett WT, et al. Magnetic resonance imaging and spectroscopy assessment of lower extremity skeletal muscles in boys with Duchenne muscular dystrophy: a multicenter cross sectional study. PloS one 2014;9:e106435.

[197]   Arpan I, Willcocks RJ, Forbes SC, et al. MR supports therapeutic effects of corticosteroids in 5-7 year old boys with DMD. Proc Intl Soc Mag Reson Med 2014;22.

[198]   van den Bergen JC, Wokke BH, Janson AA, et al. Dystrophin levels and clinical severity in Becker muscular dystrophy patients. Journal of neurology, neurosurgery, and psychiatry 2013.

[199]   Tasca G, Iannaccone E, Monforte M, et al. Muscle MRI in Becker muscular dystrophy. Neuromuscular disorders : NMD 2012;22 Suppl 2:S100-6.

[200]   Lodi R, Kemp GJ, Muntoni F, et al. Reduced cytosolic acidification during exercise suggests defective glycolytic activity in skeletal muscle of patients with Becker muscular dystrophy. An in vivo 31P magnetic resonance spectroscopy study. Brain : a journal of neurology 1999;122 (Pt 1):121-30.

[201]   Tosetti M, Linsalata S, Battini R, et al. Muscle metabolic alterations assessed by 31-phosphorus magnetic resonance spectroscopy in mild Becker muscular dystrophy. Muscle & nerve 2011;44:816-9.

[202]   Crilley JG, Boehm EA, Rajagopalan B, et al. Magnetic resonance spectroscopy evidence of abnormal cardiac energetics in Xp21 muscular dystrophy. Journal of the American College of Cardiology 2000;36:1953-8.

[203]   Gladstone JN, Bishop JY, Lo IK, Flatow EL. Fatty infiltration and atrophy of the rotator cuff do not improve after rotator cuff repair and correlate with poor functional outcome. The American journal of sports medicine 2007;35:719-28.

[204]   Di Marzo L. MA, Sapienza P., Tedesco M., Mingoli A., Capuani G., Aureli T., Giuliani A., Conti F., Cavallaro A. 31Phosphorus magnetic resonance spectroscopy to evaluate medical therapy efficacy in peripheral arterial disease. A pilot study. Panminerva Med 1999;41:283-290.

[205]   Argov Z, Renshaw PF, Boden B, Winokur A, Bank WJ. Effects of thyroid hormones on skeletal muscle bioenergetics. In vivo phosphorus-31 magnetic resonance spectroscopy study of humans and rats. The Journal of clinical investigation 1988;81:1695-701.

[206]   Webb AG, Smith NB, Aussenhofer S, Kan HE. Use of tailored higher modes of a birdcage to design a simple double-tuned proton/phosphorus coil for human calf muscle studies at 7 T. Concepts in Magnetic Resonance Part B: Magnetic Resonance Engineering 2011;39B:89-97.

[207]   Schar M, Kozerke S, Fischer SE, Boesiger P. Cardiac SSFP imaging at 3 Tesla. Magnetic resonance in medicine : official journal of the Society of Magnetic Resonance in Medicine / Society of Magnetic Resonance in Medicine 2004;51:799-806.

[208]   Bogner W, Chmelik M, Schmid AI, Moser E, Trattnig S, Gruber S. Assessment of (31)P relaxation times in the human calf muscle: a comparison between 3 T and 7 T in vivo. Magnetic resonance in medicine : official journal of the Society of Magnetic Resonance in Medicine / Society of Magnetic Resonance in Medicine 2009;62:574-82.

[209]   Taylor DJ, Bore PJ, Styles P, Gadian DG, Radda GK. Bioenergetics of intact human muscle. A 31P nuclear magnetic resonance study. Molecular biology & medicine 1983;1:77-94.

[210]   Burt CT. GT, Barany M. Phosphorus-31 nuclear magnetic resonance detection of unexpected phoshpodiesters in muscle. Biochemistry 1976;15:4850-4853.

[211] Ruiz-Cabello J, Cohen JS. Phospholipid metabolites as indicators of cancer cell function. NMR in biomedicine 1992;5:226-33.

[212] Satrustegui J, Berkowitz H, Boden B, et al. An in vivo phosphorus nuclear magnetic resonance study of the variations with age in the phosphodiester content of human muscle. Mechanisms of ageing and development 1988;42:105-14.

[213] Szendroedi J, Schmid AI, Chmelik M, et al. Skeletal muscle phosphodiester content relates to body mass and glycemic control. PloS one 2011;6:e21846.

[214] Burt CT. Phosphodiesters and NMR: a tale of rabbits and chickens. TIBS 1985;10:404-406.

[215] Fallbrook A, Turenne SD, Mamalias N, Kish SJ, Ross BM. Phosphatidylcholine and phosphatidyl-ethanolamine metabolites may regulate brain phospholipid catabolism via inhibition of lysophospholipase activity. Brain research 1999;834:207-10.

[216] Sterin M, Cohen JS, Mardor Y, Berman E, Ringel I. Levels of phospholipid metabolites in breast cancer cells treated with antimitotic drugs: a 31P-magnetic resonance spectroscopy study. Cancer research 2001;61:7536-43.

[217] Webster C, Silberstein L, Hays AP, Blau HM. Fast muscle fibers are preferentially affected in Duchenne muscular dystrophy. Cell 1988;52:503-13.

[218] Barbiroli B, Funicello R, Ferlini A, Montagna P, Zaniol P. Muscle energy metabolism in female DMD/BMD carriers: a 31P-MR spectroscopy study. Muscle & nerve 1992;15:344-8.

[219] Johnson MA, Polgar, J., Weightman, D., Appleton, D. Data on the distribution of fibre types in thirty-six human muscles. An autopsy study. Journal of neurological Sciences 1973;18:111-129.

[220] Taylor DJ, Kemp GJ, Thompson CH, Radda GK. Ageing: effects on oxidative function of skeletal muscle in vivo. Molecular and cellular biochemistry 1997;174:321-4.

[221] Kan HE, Klomp DW, Wohlgemuth M, et al. Only fat infiltrated muscles in resting lower leg of FSHD patients show disturbed energy metabolism. NMR in biomedicine 2010;23:563-8.

[222] Bernus G, Gonzalez de Suso JM, Alonso J, Martin PA, Prat JA, Arus C. 31P-MRS of quadriceps reveals quantitative differences between sprinters and long-distance runners. Medicine and science in sports and exercise 1993;25:479-84.

[223] Argov Z, Lofberg M, Arnold DL. Insights into muscle diseases gained by phosphorus magnetic resonance spectroscopy. Muscle & nerve 2000;23:1316-34.

[224] Kemp GJ, Manners DN, Clark JF, Bastin ME, Radda GK. A theoretical model of some spatial and temporal aspects of the mitochondrion creatine kinase myofibril system in muscle. Molecular and cellular biochemistry 1997;174:29-32.

[225] Forbes SC, Walter G, Rooney WD, et al. T2 mapping and single voxel 1H-MRS detect skeletal muscle invovement in young boys with Duchenne muscular dystrophy. Proc Intl Soc Mag Reson Med 2014;22.

[226] Arpan I, Willcocks RJ, Forbes SC, et al. Examination of effects of corticosteroids on skeletal muscles of boys with DMD using MRI and MRS. Neurology 2014.

[227] Bley TA, Wieben O, Francois CJ, Brittain JH, Reeder SB. Fat and water magnetic resonance imaging. Journal of magnetic resonance imaging : JMRI 2010;31:4-18.

[228] Azzabou N, Loureiro de Sousa P, Caldas E, Carlier PG. Validation of a generic approach to muscle water T2 determination at 3T in fat-infiltrated skeletal muscle. Journal of magnetic resonance imaging : JMRI 2014.

[229] Noseworthy MD, Davis AD, Elzibak AH. Advanced MR imaging techniques for skeletal muscle evaluation. Seminars in musculoskeletal radiology 2010;14:257-68.

Appendices

[230] Kukita A, Chenu C, McManus LM, Mundy GR, Roodman GD. Atypical multinucleated cells form in long-term marrow cultures from patients with Paget's disease. The Journal of clinical investigation 1990;85:1280-6.

LIST OF ABBREVIATIONS

ANCOVA	Analysis of covariance
ATP	Adenosine triphosphate
BMD	Becker muscular dystrophy
CRLB	Cramér-Rao Lower Bound
CSA	Cross sectional area
CT	Computed tomography
DGC	Dystrophin-glycoprotein complex
DMD	Duchenne muscular dystrophy
EDL	Extensor digitorum longus muscle
FIB	Fibularis muscle
FOV	Field of view
GCL	Lateral gastrocnemius muscle
GCM	Medial gastrocnemius muscle
GPC	Glycerol 3-phosphocholine
GPE	Glycerol 3-phosphoethanolamine
IFL	Increased fat levels
MRI	Magnetic resonance imaging
MRS	Magnetic resonance spectroscopy
MVIC	Maximal voluntary isometric contraction
NIFL	Non-increased fat levels
nNOS	Neuronal nitric oxide synthase
NO	Nitric oxide
TA	Anterior tibialis muscle
TE	Echo time
TP	Posterior tibialis muscle
TSE	Turbo spin-echo
TR	Repetition time
PCr	Phosphocreatine
PDE	Phosphodiesterase
PER	Peroneus muscle
Pi	Inorganic phosphate
S	Sartorius muscle
SD	Standard deviation
SE	Spin echo
SOL	Soleus muscle
SPAIR	Spectral pre-saturation with inversion recovery
ROI	Region of interest
QMA	Quantitative muscle assessment
QMT	Quantitative muscle testing

Appendices

LIST OF PUBLICATIONS

Brockington A, **Wokke BH**, Nixon H, Hartley J, Shaw PJ. Screening of the transcriptional regulatory regions of vascular endothelial growth factor receptor 2 (VEGFR2) in amytrophic lateral sclerosis. *BMC Med Genet* 2007 Apr 24;8:23

Wokke BH, Bos C, Reijnierse M, van Rijswijk CS, Eggers H, Webb A, Verschuuren JJ, Kan HE. Comparison of Dixon and T1-weighted MR methods to assess the degree of fat infiltration in Duchenne muscular dystrophy patients. *J Magn Reson Imaging* 2013 Sep;38(3):619-24

Spitali P, van den Bergen JC, Verhaart IE, **Wokke BH**, Janson AA, van den Eijnde R, den Dunnen JT, Laros JF, Verschuuren JJ, 't Hoen PA, Aartsma-Rus A. DMD transcript imbalance determines dystrophin levels. *FASEB J* 2013 Dec;27(12):4909-16

Van den Bergen JC, Schade van Westrum SM, Dekker L, van der Kooi AJ, de Visser M, **Wokke BH**, Straathof CS, Hulsker MA, Aartsma-Rus A, Verschuuren JJ, Ginjaar HB. Clinical characterisation of Becker muscular dystrophy patients predicts favourable outcome in exon-skipping therapy. *J Neurol Neurosurg Psychiatry* 2014 Jan;85(1):92-8

Wokke BH, van den Bergen JC, Versluis MJ, Niks EH, Milles J, Webb AG, van Zwet EW, Aartsma-Rus A, Verschuuren JJ, Kan HE. Quantitative MRI and strength measurements in the assessment of muscle quality in Duchenne muscular dystrophy. *Neuromuscul Disord* 2014 May;24(5):409-16

Van den Bergen JC, **Wokke BH**, Janson AA, van Duinen SG, Hulsker MA, Ginjaar HB, van Deutekom JC, Aartsma-Rus A, Kan HE, Verschuuren JJ. Dystrophin levels and clinical severity in Becker muscular dystrophy patients. *J Neurol Neurosurg Psychiatry* 2014 Jul;85(7):747-53

Nowak VA, Bremner F, Massey L, **Wokke BH**, Moosavi R, Kara E, Houlden H. Kjellin syndrome: hereditary spastic paraplegia with pathognomonic macular appearance. *Pract Neurol* 2014 Aug;14(4):278-9

Doorenweerd N, Straathof CS, Dumas EM, Spitali P, Ginjaar IB, **Wokke BH**, Schrans DG, van den Bergen JC, van Zwet EW, Webb A, van Buchem MA, Verschuuren JJ, Hendriksen JG, Niks EH, Kan HE.
Reduced cerebral gray matter and altered white matter in boys with Duchenne muscular dystrophy. *Ann Neurol* 2014 Sep;76(3):403-11

Straathof CS, Doorenweerd N, **Wokke BH**, Dumas EM, van den Bergen JC, van Buchem MA, Hendriksen JG, Verschuuren JJ, Kan HE. Temporalis muscle hypertrophy and reduced skull eccentricity in duchenne muscular dystrophy. *J Child Neurol* 2014 Oct;29(10):1344-8

Wokke BH, Hooijmans MT, van den Bergen JC, Webb AG, Verschuuren JJ, Kan HE. Muscle MRS detects elevated PDE/ATP ratios prior to fatty infiltration in Becker muscular dystrophy. *NMR Biomed* 2014 Nov;27(11):1371-7

Van den Bergen JC, **Wokke BH**, Hulsker MA, Verschuuren JJ, Aartsma-Rus AM. Studying the role of dystrophin-associated proteins in influencing Becker muscular dystrophy disease severity. *Neuromuscul Disord* 2015 Mar;25(3):231-7

Wokke BH, van den Bergen JC, Hooijmans MT, Verschuuren JJ, Niks EH, Kan HE. T2 relaxation times are increased in skeletal muscle of DMD but not BMD patients. *Muscle Nerve* 2015 Apr 6 doi:10.1002/mus.24679

CURRICULUM VITAE

Beatrijs Wokke werd op 16 augustus 1983 geboren in Haarlem. In 2001 haalde ze haar gymnasium diploma aan het Nieuwe Lyceum in Bilthoven. Ze startte in 2001 haar studie geneeskunde aan de Universiteit Leiden. In 2005 deed ze tijdens haar wetenschappelijke stage aan de Universiteit van Sheffield (Verenigd Koninkrijk) onderzoek naar 'vasculair endothelial growth factor receptor 2 in amyotrophic lateral sclerosis' onder begeleiding van prof. dr. P. Shaw. Als ondertdeel van haar co-schappen liep ze in 2007 stage op de afdeling neurologie in Tygerberg ziekenhuis, Stellenbosch (Zuid Afrika). Ze begon in 2008 aan haar opleiding tot neuroloog aan het Leids Universitair Medisch Centrum (opleiders prof. dr. R.A.C. Roos en prof. dr. J.J. van Hilten). In juli 2009 startte ze haar promotie onderzoek naar "Spier MRI in Duchenne en Becker spierdystrofie", zoals beschreven in dit proefschrift, onder leiding van prof.dr. J.J.G.M. Verschuuren. Van 2010 tot 2013 was ze actief als bestuurslid bij de Jonge Orde, met de portefeuille "Opleidingen" en nam vanuit deze functie plaats in verschillende commissies gericht op de modernisering van de medische vervolgopleidingen. Van juli 2013 tot juni 2014 was ze werkzaam als 'Specialist Registrar Neurology' in The National Hospital for Neurology and Neurosurgery, Queen Square, Londen (Verenigd Koninkrijk). Ze hoopt haar opleiding tot neuroloog in 2016 af te ronden. Beatrijs woont in Leiden met haar man Alexander en hun zoon Sweder.